Physical and Mathematical Modelling of Inert Gas Shrouded Ladle Nozzles, and Their Role on Fluid Flow Patterns and Slag Behaviour in a Four Strand Billet Caster Tundish

Kinnor Chattopadhyay

Mining and Materials Engineering

McGill University, Montreal

May 2009

A thesis submitted to McGill University in partial fulfilment of the requirements of the degree of Master of engineering

ABSTRACT

In the present study inert gas shrouding practices were simulated using a full scale, four strand, water model of a 12 tonne delta shaped tundish. Compressed air was aspirated into the ladle shroud, so as to model volumetric flow rates ranging between 2% and 10% of steel entry flows. Bubble trajectories, slag layer movements, and flow fields, were visualized. Flow fields were visualised using Particle Image Velocimetry (PIV). A numerical model was also developed using Discrete Phase Modelling (DPM), along with the standard K-ε turbulence model with two way turbulence coupling. Predicted flow fields and bubble trajectories were in good agreement with the water model experiments. From both the physical and mathematical modelling results it was evident that reversed flows were generated within the tundish in the vicinity of the ladle shroud which swept away the protective layer of slag and thereby created an exposed 'eye' of steel. The area of this exposed 'eye' increased with increasing amount of shroud gas.

RÉSUMÉ

Dans la présente étude, la technologie d'injection de gaz inerte fut simulée à l'aide d'un modèle pleine grandeur de panier répartiteur d'une capacité de 12 tonnes, en forme delta et possédant quatre drains de coulée. De l'air comprimé fut aspiré dans le jet de coulée du creuset de façon à modéliser des débits volumiques de gaz variant entre 2% et 6% du volume d'acier entrant. Les trajectoires des bulles, les mouvements du laitier, et les champs vectoriels des écoulements furent observés. Les champs d'écoulement furent rendu visibles à l'aide d'un « Particle Image Velocimeter (PIV). Un modèle numérique fut aussi développé en utilisant la modélisation biphasée (Discrete Phase Modelling, DPM) et le modèle standard K-ε de turbulence avec couplage bidirectionnel (des bulles au fluide et du fluide aux bulles). Les champs d'écoulement et les trajectoires des bulles prévues concordent bien avec les expérimentations sur le modèle réelle utilisant l'eau. À partir des résultats obtenus des deux modèles, mathématique et physique, il est évident que des écoulements inverses sont formés dans le panier répartiteur autour du jet principal par le gaz injecté. Ces écoulements inverses dispersent la couche protectrice de laitier créant ainsi une zone en forme d'œil exposé à l'air. La surface de cet œil augmente avec le débit de gaz.

ACKNOWLEDGEMENTS

I deeply acknowledge the encouragement, academic advice and financial support given by my thesis supervisors, Professor R.I.L. Guthrie and Dr M. Isac during my studies here. I would like to thank Shamik Kumar Ray and Dr Luis Calzado for their valuable knowledge of water modelling that I learned from them. I would also like to thank Prof Mainul Hasan for offering us his course MIME 653 from which I learnt a lot about fluid flow and turbulence.

My sincere thanks to all the members of the machine shop, and specially Csaba Szalacsi for fabricating various components of the experimental setup and also for his great suggestions which made the design better.

I would like to thank Patrick Lemieux for his efforts in translating the abstract into French and also for helping me in making a logic circuit in my setup.

I will cherish the warm memories of time well spent with friends and colleagues here at McGill University.

Lastly, but most importantly, I would like to express my gratitude to my loving parents for their constant encouragement and support.

NOMENCLATURE

Bo, Bond Number

ρ, Density of the fluid, Kg m^{-3}

g, Acceleration due to gravity, m s^{-2}

L, Characteristic length, m

σ, Surface tension, N m^{-1}

We, Weber Number

Re, Reynolds number

Fr, Froude number

U, Fluid velocity, m s^{-1}

Gr, Grasshoffs Number

β, Coefficient of thermal expansion of the fluid,K^{-1}

ΔT_0, Change in temperature in a fluid due to mixing with a hot fluid, K

m , p, Subscripts indicate model and prototype respectively

V_f , V_r , fluid and Stokes rise velocities respectively, m s^{-1}

k, Kinetic energy of turbulence per unit mass,m^2 s^{-2}

ε, Rate of dissipation of k, m^2 s^{-3}

ω, Specific rate of dissipation, m^2 s^{-3}

G_K, Rate of production of k, Kg $m^{-1}s^{-3}$

C_1, C_2, C_μ, σ_k *and* σ_ε, Empirical Constants

μ, Viscosity of the fluid, Kg $m^{-1}s^{-1}$

μ_t, Turbulent viscosity, Kg $m^{-1}s^{-1}$

μ_{eff}, Effective viscosity, Kg $m^{-1}s^{-1}$

l_m, Mixing length, m

l_0, Length scale of turbulence, m

v_0, Velocity scale, m s^{-1}

d, Distance from nearest wall, m

y^+, Dimensionless wall distance

f, Constant determined by the shape of the tundish

u, X component of velocity, m s^{-1}

v, Y component of velocity, m s^{-1}

w, Z component of velocity, m s^{-1}

c_i, Concentration of the i^{th} species

u_T, Terminal rise velocity, m s^{-1}

S_i, Source term indicating

Γ_{eff}, Effective diffusivity, m^2s^{-1}

u_p, Particle velocity, m s^{-1}

ρ_p, Density of the particle, Kg m^{-3}

F_D, A defined drag force (strictly not a force), s^{-1}

F_p, Force of excess pressure differential per unit mass, m s^{-2}

F_x, Additional acceleration term per unit mass, m s^{-2}

g_x, acceleration in x direction, m s^{-2}

$\bar{u}_i$, Time averaged velocity, m s^{-1}

ζ_i, random number, normally distributed between -1 and 1

C_D, Drag coefficient

d_p, Particle diameter, m

a_1, a_2, a_3, Constants

PIV, Particle Image Velocimetry

FCD, Flow Control Devices

SLS, Swirling Ladle Shroud

VOF, Volume of Fluid

1.0 INTRODUCTION

Continuous casting has now become the standard choice for all steel makers around the world for casting the liquid steel into slabs, blooms and billets. The problem lies in transferring the liquid steel from the ladle to the tundish where there are chances of re-oxidation of the melt stream by ambient air. The steel is usually transferred through a refractory ladle shroud, but it is not always possible to secure an effective seal at the joint of the ladle and the shroud. This is because of the negative static pressure at the joint causing ambient air from the atmosphere to be sucked in. One of the ways of preventing air aspiration is to inject inert argon gas at the ladle-shroud joint. Argon there acts as a protective shield and thereby prevents the steel from re-oxidation.

Inert gas shrouding is already practised in the steel industry and its benefits are numerous. There is a definite reduction in the oxygen content in the bath, a lesser number of oxide inclusions, a decrease in nozzle clogging frequency, an improvement in surface quality of slabs and billets, and a reduction of melt temperature loss from ladle to tundish. Despite these benefits, argon gas in excess should be avoided as it forms an exposed 'eye' of steel around the ladle shroud by sweeping off the protective layer of tundish slag. The amount of shroud gas that should be used is still a matter of debate and a scientific explanation of the phenomena is very much required.

Physical and mathematical modelling of steel making tundish operations has been a vast area for research over the past three decades. The purpose of this research was to understand the physical phenomena and to improve operational processes and procedures. Mazumdar and Guthrie[1] in a comprehensive review article of ISIJ summarized research done up to 1999. However, a lot more work has been done in the last decade (1999-2008) as well.

The objective of the present thesis was to carry out an extensive review of research done in the field of modelling of steel making tundish operations in the last decade (1999-2008) and to apply physical and mathematical modelling simultaneously for simulating the inert gas shrouding phenomena and see its effect on fluid flow patterns and slag behaviour within the tundish. In the present work, a full scale water model of a 12 tonne delta shaped tundish was used and compressed air was aspirated into the shroud to physically model volumetric flow rates of inert argon ranging between 2% and10% of steel entry flows. The FLUENT code was used to develop a mathematical model for simulating the same phenomena. The numerical predictions were in good agreement with corresponding physical modelling results.

A general literature review on physical and mathematical modelling of continuous casting tundish operations, details of the experimental setup and experimental procedure and theory involved in mathematical modelling are given prior to the analysis and discussion of the results.

2.0 LITERATURE REVIEW

2.1 Introduction

In the continuous casting of steel, the tundish is basically an intermediate vessel placed between the ladle and the mould. It distributes and supplies liquid steel to different moulds at an approximately constant rate. In recent years, with continuing emphasis on superior steel quality, the tundish has become more of a continuous reactor than merely a distribution vessel. Thus, a modern day steel making tundish is designed to provide maximum opportunity for carrying out various metallurgical operations such as inclusion separation, inclusion floatation, alloy trimming of steel, and thermal and chemical homogenization. All these have led to the development of a separate area of secondary steelmaking referred to as "tundish metallurgy"[1]. Thus significant efforts have been made by researchers around the globe in the last decade (ie:1999 to 2008) to fully exploit and enhance the potential of the continuous casting tundish as a molten steel refining vessel. Research activities concerning the associated theoretical and applied aspects have naturally led to a large number of publications. Mazumdar and Guthrie[1] in 1999 concluded that numerous experimental and theoretical studies had been carried out using both aqueous models and industrial units to investigate various transport phenomena of relevance to continuous casting tundish systems. A wide range of tundish geometries along with numerous designs of flow modifiers were applied and studied, primarily to investigate the floatation of inclusions from tundishes as a function of operating variables. In addition to these, the roles of increased throughput rate, electromagnetic stirring and auxiliary heating on tundish performance were also investigated. Flow conditions suitable to facilitate inclusion separation by floatation can be created by insertion of flow modifiers. However, the optimal design of such flow modifiers and their location within the tundish is highly dependent on the tundish geometry, operating conditions and the size range of inclusions present within the molten steel. Mixing, both thermal and material, on the other hand, require significantly different flow conditions. Useful inferences on industrial tundish performance can be made from observations derived from reduced scale water models. Extensive mathematical modelling of fluid flow and transport phenomena and the concurrent validation of mathematical model predictions against laboratory, as well as plant scale experimental data, indicate that a reasonably accurate mathematical framework now exists for effective tundish design and process analysis. For simplicity and lucidity, this whole review has been divided into three parts i.e. physical modelling, mathematical modelling, and tundish research in the last decade.

2.2 Physical modelling

Physical modelling involves the use of a low temperature aqueous analogue, generally water, to represent molten metal in the tundish. Water flow in a transparent model tundish can be used to observe the melt flow physically. Models can be either reduced scale or full scale. There are certain advantages to using a full scale model over a reduced scale model and these are mentioned by Guthrie and Isac[2]. For a faithful representation of flow in the model tundish, there should be constant ratios between corresponding quantities in the model and the actual tundish. For melt flow in tundishes, the states of similarity normally include geometric, kinematic, dynamic and thermal similarities. Here, the industrial vessel is known as the prototype, and its laboratory-scale counterpart is known as the model. Laboratory-scale modelling of various secondary steelmaking operations has most frequently used water as the modelling medium to represent molten steel. The most important single property in this context, apart from its ubiquity, is that its kinematic viscosity (that is, molecular viscosity/density) is essentially equivalent to that of molten steel at 1600°C (i.e., within 10%). Flow visualization experiments in aqueous systems using dyes or other tracers have therefore proved to be very helpful in developing a qualitative understanding of various flows in real liquid steel systems. Similarly, more detailed information on flow characteristics has also been possible by measuring velocity fields by tracking the motion of neutrally buoyant particles or by using hot wire or hot film anemometry, or by laser Doppler anemometry, and, lately, by PIV (Particle Image Velocimetry). In addition, measurements of residence time distributions to characterize mixing in water model experiments using dye, acids, or KCl salt solution, have proved very popular and efficient. Having realized the advantages of using water as the representative fluid, it is now appropriate to discuss the general problem of how to physically model or characterize metallurgical processes. It is important to note here that, if the same forms of dimensionless differential equations and boundary conditions apply to two or more such metallurgical operations, and if an equivalence of dimensionless velocity, temperature, pressure or concentration fields, etc. also exist between the two, then one of them becomes a faithful representation of the other; i.e., one can be termed as a model of the other. This is a general statement of the need for similarity between a model and a prototype, which requires that there be constant ratios between corresponding quantities. The state of similarity between a model and a full-scale system includes geometric, mechanical, thermal, and chemical similarity. Mechanical similarity is further subdivided into static, kinematic, and dynamic similarity. The various states of similarity are discussed in standard texts in great detail[3].

Recently a new dimensionless number has gained important recognition in the modelling of steel/slag systems, and that is the Bond number. The Bond number, notated Bo, is a dimensionless number expressing the ratio of body forces (often gravitational or buoyancy) to surface tension forces .

$$Bo = \frac{\rho g L^2}{\sigma} \qquad \text{[Eq: 2.2.1]}$$

The Bond number is a measure of the importance of surface tension forces compared to body forces. A high Bond number indicates that the system is relatively unaffected by surface tension effects; a low number (typically less than one is the requirement) indicates that surface tension dominates. Intermediate values indicate a non-trivial balance between the two effects.

Both the We and Bo similarity criteria become very important when we simulate the slag phase with oils or emulsions. Different liquids like Benzene, Toluene, CCl_4, oils, paraffin oil[4], etc., have been used to simulate the slag phase. G. A. Irons[5] reported that paraffin oil is the best liquid for simulating the slag phase in water models.

If we use reduced scale models we cannot simultaneously achieve Reynolds number similarity and Froude number similarity as only one of them can be respected. Since the flows in the tundish are naturally associated with high Reynolds numbers, inertial forces far exceed laminar viscous forces and correspond to the Newtonian range which are insensitive to Re. By contrast, inertial to gravitational forces are similar in magnitude. As such, flows in the tundish are Froude dominated and hence Froude number similarity is maintained between the model and the prototype. However in full scale modelling, both Re and Fr similarities can be achieved simultaneously.

The above mentioned similarity criteria are alright when there are no temperature changes and no effect of buoyancy forces. However, for non isothermal modelling, we have the modified Froude Number which is the ratio of inertial forces to buoyancy forces caused by thermally induced density variations within the liquid.

$$Fr_{modified} = \frac{\rho U^2}{(\rho_l - \rho) g L} \qquad \text{[Eq: 2.2.2]}$$

Damle and Sahai[6] called the inverse of this, the Tundish Richardson Number (Tu). Tu denotes the ratio of buoyancy force to the inertial force and is expressed as

$$Tu = \frac{Gr}{Re^2} = \frac{gL\beta\Delta T_0}{U^2} = \frac{(\rho_l - \rho)gL}{\rho U^2} \qquad \text{[Eq: 2.2.3]}$$

If inclusion removal modelling is done then another essential modelling requirement is that

$$\frac{V_{f,m}}{V_{f,p}} = \frac{V_{r,m}}{V_{r,p}} \qquad \text{[Eq: 2.2.4]}$$

is to be maintained where V_f and V_r are fluid and Stokes rise velocities respectively.[7] However, the inclusions rise velocities may not always be in the Stoke's regime. So it is essential to keep them in the same flow regimes.

In modelling heat transfer operations, thermally similar systems are those in which corresponding temperature differences bear a constant ratio to one another at corresponding positions. When the systems are moving, kinematic similarity is a prerequisite to any thermal similarity. Thus, the heat transfer ratio by conduction, convection, and/or radiation to a certain location in the model must bear a fixed ratio to the corresponding rates in the prototype.[8] Finally, for chemical similarity between a model and a full scale system, the dynamic and thermal similarity first must be satisfied. The former, since mass transfer and chemical reaction usually occur by convective and diffusive processes during motion of reacting material through the system, and the latter since chemical kinetics are normally temperature dependent.

2.3 Mathematical modelling

Mathematical modelling represents an alternative approach for visualising flow fields inside a tundish. In mathematical modelling, the turbulent Navier-Stokes equation is solved in a boundary fitted coordinate system, so as to predict the velocity distributions. Analytical solutions to the 3D Navier-Stokes equation are not normally possible in most cases. In practice, therefore, we have to go for numerical methods, and for numerical solutions of these equations, in recent years a lot of commercial software packages such as FLUENT, CFX, FLOW-3D, PHOENICS, FIDAP, COMSOL, etc. have been marketed, and have allowed CFD to become an increasingly common tool for the non- experts. Various turbulence models are available such as the $k-\varepsilon$, RNG k- ε , Realizable k- ε etc. An extensive review of the published literature shows that the basic framework of the mathematical modelling used in tundish research can be divided in three sub divisions, namely defining the problem, which is done by expressing the process in terms of some physical variables using partial differential equations, with appropriate operating and boundary conditions, then 'grid generation of the flow domain and discretization' of those partial differential equations into algebraic form, using different schemes and the third part is, 'solution to those discretized equations' using numerical techniques. The main physical variables related to any flow field is the velocity. Since other properties follow directly from the velocity field, determination of the velocity is the prime step in solving a flow problem. For this reason, velocity was chosen as the primary physical variable for all mathematical modelling studies. Realizing the fact that liquid steel flows within a tundish are three dimensional and turbulent in nature, almost all of the mathematical modelling works published in literature in the recent past, assume the flow to be three dimensional and turbulent. As the equation of continuity and equation of "Conservation of momentum" describe the fluid flow in mathematical terms, they are, along with treatment of turbulence and boundary conditions, used as the starting point of all mathematical modelling studies for the tundish. In addition to using the above equations, different researchers used different equations, to model different parameters. Some included the energy equation to predict temperature distributions under non isothermal conditions.[9,10,11] Other researchers included additional differential equations to describe inclusion trajectories and inclusion number density distributions.[12,13] Modelling has also been used to predict parameters such as 'Residence Time Distributions'[11] (RTD), distribution of top surface slag layer[12] etc.. It is practically impossible to solve these equations numerically by Direct Numerical Simulation (DNS) because of its requirement of unrealistically high computational memory, power and time. So for 99% of the CFD problems without going for solving the turbulent Navier-Stokes equation in its original form, turbulence modelling is incorporated to capture the critical effects of turbulent flow without having to resolve the actual small length and time scales of turbulent motion. One of the most popular practices is of first averaging the 'Continuity' and 'Navier-Stokes' equations, and then devising means for solving the resulting system of equations for mean quantities of velocity and pressure. The approach along this line was first proposed by Reynolds and is called as **Reynolds Averaged Navier-Stokes (RANS)** equation. Here the equations are averaged over a time scale, which is long compared with the time scale of the turbulent motions, but small compared with the unsteady mean flow. In this approach, instantaneous velocity and pressure are decomposed into the mean and fluctuating part and incorporated in the continuity and Navier-Stokes equations.

(a) Turbulence Models

Among the different methods, the most widely used concepts in the present day turbulence models for practical engineering applications is the " Eddy viscosity" concept. In analogy to the viscous stresses in laminar flows, Boussinesq suggested that the turbulent stresses are proportional to the mean- gradients of velocity. Of the different turbulence models available in literature, only a few have been used in tundish modelling. Prandtl's 'Mixing Length Model', is one of the early turbulence models used for tundish modelling. In this model, Prandtl defined the mixing length, l_m, as the distance travelled by a fluid lump in the transverse direction before the mean velocity changes by an amount equal to the transverse fluctuation velocity. This momentum transport is equivalent to generating a turbulent shear stress. Prandtl also postulated that: the turbulence length scale l_0 , is equal to the mixing length l_m, and the velocity scale v_0, is equal to the mean velocity gradient times the mixing length ($l_m \frac{\partial \overline{u_x}}{\partial y}$). In very early modelling attempt, Debroy and Sychterz[14], used this turbulence model for their numerical studies of flow pattern in a tundish and specified a mixing length $l_m = 0.4d$, where d is the distance from nearest wall. But later investigations had shown that the mixing length, l_m, which according to the Prandtl's postulate equals to the turbulent length scale, varies within the turbulent boundary layer itself. So assignment of a single value for l_m throughout the flow field is questionable and is one of the weaknesses of this approach. Though this model was not used in any further tundish modelling work in later years, the 'Law of the Wall', which is used for boundary conditions for more sophisticated turbulence models, uses this concept and is used frequently.

To date, the most popular approach using the eddy viscosity concept have been the two equation models. In these models, two separate transport equations are solved to determine the length and velocity scales for eddy viscosity. Review of the literature on mathematical modelling in tundish reveals that most of the researchers have used the standard k- ε model of Launder & Spalding[15] to calculate eddy viscosity. Later on, variants of this model were introduced, such as the RNG k- ε model of Yakhot and Orszag[16] and the Realizable k-ε model of Shih et al[17]. Schwarze et al[18,19] used different turbulence models in their prediction of flow field and dispersed phase behaviour. Though their predicted velocity field using standard k- ε vs. the RNG k- ε models does not seem to vary much, the mean turbulent quantities do differ significantly. Comparing the results with the available experimental data, they concluded, that the RNG model approximates the turbulence in flow situations with a high curvature of streamlines better than other models. Though the literature survey shows, that most of the simulation works were done using the standard k- ε turbulence model, they[20] argued that this model, over predicts k values, because it does not take into account the fact that the strain rate of the flow field influences turbulence. Hou & Zou[20] came to the same type of conclusion. They compared the standard k- ε turbulence model with the RNG k- ε turbulence model, while numerically simulating swirling flows in a tundish. They also obtained converged results more easily using the RNG k- ε turbulence model and concluded that this model is more appropriate for swirling motions. By far the most elaborate computational study on tundish performance prediction was done by Jha et al.[21]They studied the effect of different turbulence models on residence time distribution predictions. Apart from these, they also applied LES (large eddy simulation) in tundish modelling. Models such as the standard k- ε, RNG k- ε, Chen – Kim k- ε, LES, etc. predict gross flow properties fairly well. While others like Lam- Bremhorst low Reynolds number k- ε model, predicts initial variation better than the others.

The most widely used model of turbulence is the standard k- ε. In general, as stated earlier, the standard k- ε model tends to overestimate mixing situations where highly turbulent and essentially laminar regions coexist such as in tundish. To adequately predict such situations the model must be able to represent the existence probability of the turbulent fluid at a particular location. Realizing this fact, Ilegbusi et al.[22] used a two fluid model of turbulence to predict the flow behaviour in a tundish. This model essentially considers the system to be composed of two interpenetrating fluids (a turbulent and a non turbulent fluid). These fluids are allowed to exchange mass, momentum and energy at the interface. At any location, transport equations would be solved for the characteristics of each fluid, including velocity components, temperature, and volume fractions. The volume fraction of the turbulent fluid provides a measure of the intermittency or turbulence. The model is therefore well suited to represent the whole tundish domain, the intermittency factor being high in the turbulent inlet region and low in the quiescent region.

In wall-bounded turbulent flows, as in a tundish, the presence of solid walls has a strong effect on flow characteristics. So all the researchers who tried to model the flows within the tundish, had to use special treatments like the wall function approach or the low Reynolds number model approach to tackle the boundaries. However, when there are strong reattaching and separating flows, the wall function approach is not recommended.

Only a few researchers [23,24]have used the Low Reynolds number method. In this approach computations are carried out all the way to the walls and hence a very fine grid is required near the wall. Some researchers[24] used low Reynolds number model of Launder & Jones to study the residence time distribution in a 6-strand tundish, and found better agreement with experimental results. The low Reynolds number models like the model of Lam & Bremhorst (used by ref.[23,24]) and the Chen-Kim low Reynolds number (with and without Yap correction) (used by ref. [21]) were used only for comparison purposes.

The capabilities of RANS models are limited. Under certain conditions these models can be very accurate, but these are not suitable for transient flows, because the averaging process wipes out most of the important characteristics of a time-dependent solution. On the other hand, ' **Direct Numerical Simulation** '(**DNS**), which is direct solution of turbulent Navier-Stokes equation, is not practical for 99.9% of CFD problems because of its requirement of unrealistically high computational power and time. As a result a new simulation technique, called **'Large eddy simulation' (LES)** also became very popular. In **LES,** the contribution of the large scale eddies to the momentum and energy transfer is computed exactly as DNS and the effect of the small eddies are modeled. The distinction between the large and small eddies is done by a filtering operation. But an exhaustive survey of literature shows only Jha et al [21] applied the LES technique during their modelling of tundish flows.

(b) Solution of the PDE's

Due to the complex nature of the governing equations and geometries of the tundishes, analytical solutions for the equations are not possible in a practical sense. So different numerical techniques have been developed to solve these transport equations. The numerical solution aims to provide the values of the variables at some discrete number of points in the domain of interest. These points are called grid points, nodes or cell centroids, depending on the scheme it follows. The conversion of differential equations into a set of discrete algebraic equations requires the discretization of domain. This is called mesh generation or meshing.

The different techniques are:

1. Finite Difference Method (FDM)
2. Finite Element Method (FEM)
3. Spectral Methods.
4. Hybrid Methods (like Control Volume Finite Element Method, Control volume Finite Difference Method etc.)

All the techniques perform three basic steps i.e. approximation of unknown flow variables by means of simple functions followed by discretization by substitution of the approximations into the governing flow equations and subsequent mathematical solutions.

Close examination of the three components of the momentum equation and continuity equation shows that they are closely coupled, because all velocity components appear in each momentum and continuity equation. The most complex issue is to know the pressure term in the momentum equations. This is because there is no equation available for pressure for the case of incompressible fluid flows such as the flows in a tundish.

These problems are generally tackled by the use of different iterative solution strategies like SIMPLE, SIMPLER, SIMPLEC, PISO[25,26] etc. All these techniques are iterative methods and use either the Tri Diagonal Matrix Algorithm (TDMA) of Spalding or the Gauss Sidle method for solution. Several other techniques like the Penta Diagonal Matrix Algorithm, the implicit under-relaxation scheme of Patankar, etc. are also used.

2.4 Research in the last decade

Having given a brief description of physical modelling and mathematical modelling in the last section, this section provides a comprehensive review of the work of different researchers in the last decade. The review has been done hereafter in ascending order of chronology. FAN and HWANG[27],in 2000, developed a mathematical model to analyze fluid flow phenomena of liquid steel in the tundish, during its filling stage and subsequent casting operation in the continuous casting process of steel. The ultimate goal was to ensure smooth initial casting operations without nozzle clogging. The mathematical model was developed using a CFD technique, named SOLA-MAC and the famous $K-\varepsilon$ turbulence model. SOLA-MAC (Solution Algorithm Marker And Cell) had the capability to handle transient flow problem with highly distorted free surfaces. The SOLA-MAC technique uses a finite-difference scheme for the mathematical analysis of the fluid flow problems. Like most numerical techniques, it first divides the system, which is the configuration of the tundish under consideration, into a number of volume elements. Then a set of imaginary markers is introduced into the system to represent the location of the fluid at any instant. The velocity field of the moving fluid domain can be calculated by the application of fluid dynamics principles. Next, the markers are moved according to the calculated velocity field in order to represent the new location of the fluid domain. The procedure can be repeated from the beginning when the tundish is empty until it is filled to a predetermined height in the tundish. The mathematical model was first tested on a one fourth scale water model and good consistency was observed when the simulated filling patterns were compared with the water model experiments. Inclusion distribution and the amount of "dirt" exiting through the outlets of the various strands in the tundish were also analyzed by a fluid particle method. The simulated results showed that for the tundish, inclusion contamination was not uniform at the different strands, which was also confirmed by actual experience in the plant.

Odenthal et al[28]. reported results of digital particle image velocimetry (DPIV) on a one fourth scale model of a single strand tundish. It lead to a good interpretation of the dynamic flow phenomena. The flow separated at the bottom of the tundish and a recirculating region was developed. Simultaneously, the jet out of the shroud induced a counter-rotating double vortex and a short circuit flow around the side walls. A two equation model was developed in order to describe turbulence and the results obtained with this model corresponded well with the DPIV data. They concluded that DPIV can be used as an effective tool to determine two dimensional velocity fields and transient velocity fields. They also suggested the use of 3D DPIV and Laser Doppler Anemometry (LDA) for the future. LDA has an advantage is that it can measure turbulent fluctuations.

A transient two fluid model was developed by Sheng and Jonsson[29] to simulate fluid flow and heat transfer in a non isothermal water model of a continuous casting tundish. Thermal stratification in the bath was evident and the results, predicted by the two fluid approach adopted, made the effect of natural convection more clear compared with the generally used single fluid k-ε model. The overvaluation of the conductive heat transfer in the transition region of the system found by using the single fluid approach was eliminated by using the two fluid k-ε model. The two fluid approach was also found to be better in describing the counter gradient diffusion phenomenon caused by the thermal buoyancy force.

J.H. Ann et al.[30]predicted a concentration change during grade transition operations during steel thin slab casting based on computer simulations, a water model, and plant trials. Fluid flow and mixing patterns in various tundish levels and flow rates were analyzed through 3D mathematical modelling. They correlated their results with water model experiments and developed a simple, efficient and accurate computational model which could predict the concentration profile at the outlet of the tundish. Based on the model, mixing in/below the mould was analyzed considering EMBR (electro magnetic breaking). The total amount of mixed grade steel only depended on the mixing in the tundish when EMBR is applied. They also concluded that the optimum tundish operating condition to minimize intermixed slabs greatly depends on tundish geometry.

A systematic study was conducted by S.K.Sinha et al.[31] of the National Metallurgical Laboratory in India on the fluid flow behaviour in a two strand tundish under conditions of submerged entry nozzle (SEN) and open entry nozzle (OEN) with different levels of water in the tundish. Flow was characterized by the profiles of tracer responses at the tundish outlets. Two configurations of entry nozzle (ladle shroud), the straight tube (for SEN and OEN) and the T-shaped (for SEN only) were applied. At 34 mm immersion depth of the straight ladle shroud, the optimal level of mixed flow in the tundish was produced and thus uniformity in composition was obtained. With the OEN configuration, the more was the height of the entry nozzle, the less was the dead volume and the mixing increased. They suggested that tracer response profiles from different outlets should be nearly the same to have unity A-ratio and vessel dispersion number.

Y. Sahai[32] made a summary on modelling of melt flows in continuous casting tundishes at the Brimacombe Memorial Symposium. He emphasized the importance of proper melt flow in tundishes for the production of high quality clean steel and that this can be achieved by good tundish design and optimum volumetric flow rate of liquid metal. In a full scale model, the Reynolds and Froude similarities can be satisfied simultaneously. However, in a reduced scale model, both similarities cannot be satisfied for a water model. Thus, only Froude similarity is sufficient and convenient similarity criterion for water modelling. In non isothermal systems where buoyancy forces become important, the tundish Richardson number is the sufficient and necessary similarity criteria for modelling. Sahai also mentioned that the solution of the turbulent Navier-Stokes equation with an appropriate set of boundary conditions provides detailed information about the velocity and turbulence fields in the tundish. A coupled solution with the heat transfer equation also provides the temperature field existing in the melt.

Robert and Mazumdar[24] developed a steady state, three dimensional, turbulent flow model for analyzing melt flow and RTD in steelmaking tundish systems. They used a control volume based, finite difference procedure and the SIMPLE algorithm. To ensure that their model is consistent and sufficiently robust, they tested the model on several standard systems and obtained satisfactory results. Accordingly, the turbulent model was applied to simulate flow and RTD in four different tundishes. The results were compared with equivalent water model experiments. Except for the single strand tundish system, large differences between measurements and prediction were noted for the other three tundish geometries. Numerical modelling of RTD in the rectangular, six strand tundish system embodying the low Reynolds number $K - \varepsilon$ model of Launder and Jones, was found to produce estimates of RTD parameters that are in reasonable agreement with the corresponding experimental results and superior to those deduced via the high Reynolds number $K - \varepsilon$ model.

Sergio. P. Ferro et al.[33] presented mathematical models for the evaluation of residence time distribution curves for a large variety of vessels. They introduced a new volume called convection diffusion volume to obtain a good representation of RTD curves. Two numerical models for simulation of RTD curves in different vessels were presented. The comparison of measured RTD curves with numerical results from the proposed model shows that these models can successfully represent the general behaviour of a fluid inside a variety of systems. The first of the two models proved to be efficient to describe most of the one-peaked RTD curves, in spite of its simplicity. The second one, slightly more complex, represented successfully all the different RTD curves under consideration including those with double peaks. The key feature of these models was the use of a new type of volume, the convection diffusion volume. In order to find the parameters of the model for a given experimental RTD curve, a numerical algorithm was developed and also some simple mathematical relations were found, that allowed the estimation of the parameters of the model from the characteristic parameters of the RTD curve.

P. Gardin et al.[34] carried out an experimental and numerical CFD study of turbulence in a tundish container. Extensive mean and fluctuating velocity measurements were performed using LDA in order to determine the flow field and these data formed the basis for the numerical model validation. CFD modelling of this problem apparently seems easy but actually it was not. Accurate description of the jet is the most important and requires a localized fine grid, but also a turbulence model that predicts the correct spreading rates of the jet and impinging wall boundary layers. The velocities in the bulk of the tundish are generally much smaller than those of the jet, leading to damping of turbulence, or even laminar flow. They started the work with an objective of applying and validating the $\mathbf{k}-\omega$ model of Wilcox to a tundish flow problem. This model was thought to have advantages over the k- ε model. After initial 2D studies they found that the $\mathbf{k}-\omega$ model was diffusing the wall jet too quickly. Medium grid density 3D computations, confirmed this finding. The authors developed several low- Reynolds number k- ε model variants to compute the flow and compare against measurements. The k- ε modifications proved to be very successful, with the newly developed k- ε D1 model being the best. This indicated there is no need to use more sophisticated differential Reynolds stress models, which are more difficult and take longer to converge. From the grid refinement they concluded that certain turbulence models were more grid-sensitive than others. They also concluded that the LES model might still have certain limitations for practical use.

Guthrie and Isac[2] reported on the importance of the use of full-scale models for studying the fluid flow and transport phenomena in ladle-tundish-mould operations. They mentioned that reduced scale models are convenient to simulate first order simulations of inertially dominated flows, but the finer details are better analyzed in full scale models where Re, Fr and Tu can be simultaneously respected.

Jha and Dash[35] employed different turbulence models to the design of optimum steel flows in a tundish. The Navier-Stokes equation and the species continuity equation were solved numerically in a boundary fitted coordinate system comprising the geometry of a large-scale industrial size tundish. The solution of the species continuity equation predicted the time evolution of the concentration of a tracer at the outlets of a six-strand billet caster tundish. The numerical prediction of the tracer concentration using six different turbulence models' [the standard k- ε, the k- ε RNG, the Low Re number Lam-Bremhorst model, the Chen-Kim high Re number model (CK), the Chen-Kim low Re number model (CKL) and the simplest constant effective viscosity model (CEV)] which compared favourably with that of the experimental observation for a single strand bare tundish. It was found that the overall comparison of the k- ε model, the RNG, the Lam-Bremhorst and the CK model was much better than the CKL model and the CEV model as far as gross quantities like the mean residence time and the ratio of mixed to dead volume were concerned. However, the k- ε model predicted the closest value to the experimental observation compared to all other models. The prediction of the transient behaviour of the tracer was best done by the Lam-Bremhorst model and then by the RNG model, but these models did not predict gross quantities very accurately as did the k- ε model for a single strand bare tundish. With the help of the above six turbulence models, mixing parameters, such as the ratio of mix to dead volume and the mean residence time, were computed for the six strand tundish for different outlet positions, height of advanced pouring box (APB) and shroud immersion depth. It was found that three turbulence models show a peak value in the ratio of mixed to dead volume when the outlets were placed at 200 mm away from the side wall as shown in Figure 2.4.1 below.

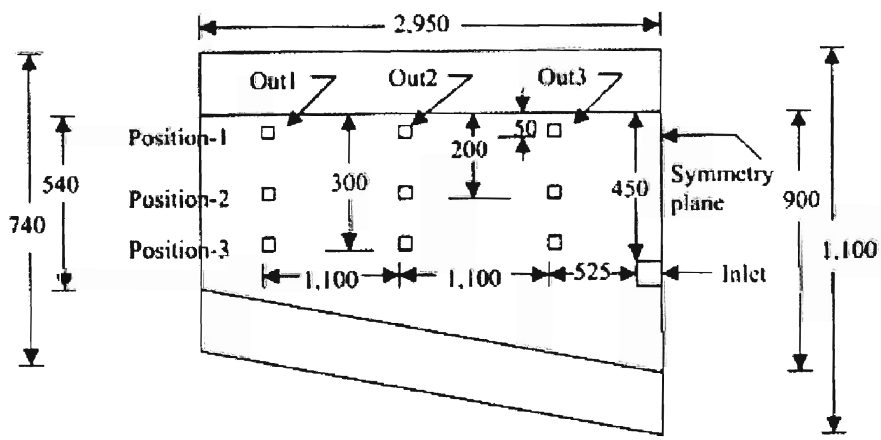

Figure-2.4.1 Top view of the tundish showing outlets on the bottom plane[35]

An advanced pour box (APB) was put on the bottom of the tundish surrounding the inlet jet when the outlets were kept at 200 mm away from the wall. It was also found that there exists an optimum height of the APB where the ratio of mixed to dead volume and the mean residence time attain further peak values signifying better mixing in the tundish. At this optimum height of the APB, the shroud immersion depth was made to change from 0 to 400 mm. It was also observed that there exists an optimum immersion depth of the shroud where the ratio of mixed to dead volume still attains another peak signifying slightly better mixing However, none of the turbulence models predict the same optimum height of the APB and the same shroud immersion depth, as the optimum depth. The optimum height of the APB and the shroud immersion depth were decided when two or more turbulence models predicted the same values.

P. K. Jha et al.[21] also performed large eddy simulation to study mixing in a tundish. They took the solution of the k- ε model as a starting guess for the large eddy simulation (LES). A solution for the LES could be arrived at after adapting a local refinement of the cells (twice), so that the near wall y^+ could be set less than 1. Such a refined grid gave a time independent solution for the LES, which was used to solve the species continuity equation. The LES solution slightly over predicted the mean residence time but could predict fairly well the mixed volume. However the LES was unable to predict both the peaks in the tracer concentration like the k- ε , RNG and Lam-Bremhorst models were able.

S. Lopez. Ramirez et al.[9] studied the influence of input temperature changes on molten steel flow in tundishes by physical and mathematical modelling. In their study, the difference between considering and not considering the thermal influence changed the parameter values in approximately 5% of the relative standard deviation. The thermal response obtained from an input step temperature change reproduced the real behaviour of the molten steel flow in a tundish dominated by buoyancy forces. A comprehensive process model for fluid flow and heat transfer in the tundish was developed by R. Pardeshi et al.[36] which had the capability to capture the transient process dynamics. The model was based on a conjugate thermal analysis of the tundish, accounting for simultaneous heat transfer through the liquid steel, refractory, steel shell and dams. The model was validated by comparing model predictions for laminar and turbulent fluid flow conditions cited in the literature. Plant campaigns were undertaken to collect plant data for tuning and validation of the model.

Kumar, Koria and Mazumdar[37] from their experimental and computational study on flow modelling and RTD, indicated that a sufficiently small grid resolution (control volume of the order of 10^{-6} m^3) is necessary to arrive at a practical grid independent solution. They also reported that the Reynolds Stress model was found to simulate RTD in the system somewhat better to the standard coefficient k- ε model. Their mathematical model was validated with experimental results and proved sufficiently robust and reliable to predict mixing parameters in tundishes with and without flow control devices.

A. V. Zamora et al.[38] studied inertial and buoyancy driven water flows under gas bubbling and thermal stratification conditions in a tundish model. Steel flow dominated by inertial and buoyancy flows under gas bubbling and thermal stratification conditions, in a one-strand tundish, was studied, using a 2/5 scale water model. The use of a turbulence inhibitor yielded plug flow volume fractions well above 40% for a simulated casting rate of 3.12 tons/min under isothermal conditions. Small flow rates of gas injection (246 cm^3/min), through a gas curtain, improved the fluid flow by enhancing the plug flow volume fraction. Higher flow rates caused an increase in back-mixing flow, forming recirculating flows on either side of this curtain. Step inputs of hot water drove streams of this fluid towards the bath surface due to buoyancy forces. A rise in gas flow rate led to thermal homogenization within the two separated cells of flow located on either side of the gas curtain. Step inputs of cold water drove streams of fluid along the tundish bottom. The use of the gas curtain homogenized the lower part of the tundish as well as the upper part of the bath to the left side of the curtain. However, the temperature at the top corner of the tundish, in the outlet box, remained very different than the rest of the temperatures inside this tundish. High gas flow rates (912 cm^3/min) were required to homogenize the bath after times as long as twice the mean residence time of the fluid.

A. Ramos Banderas et al.[39] performed mathematical simulation and physical modelling of unsteady fluid flows in a water model tundish mould. The LES approach used by them was able to predict, qualitatively, the instantaneous upper recirculating flow fields of water in the physical model. Agreement of simulated and measured jet parameters such as the jet angle and the impingement position of the entry jets in the narrow wall of the mould were acceptably good. Thus they suggested that the LES approach is well recommended to estimate jet characteristics. Changes of flow pattern with time were generated as a result of the vertical oscillation motion of the jet core. This motion was promoted by the residual Reynolds stresses that characterize turbulent flow. The fluid flow pattern in the jet root was unaltered by changes of the flow rate of the liquid. The asymmetry of fluid flows caused by these stresses yielded biased flows. Mass transfer in the mould also yielded asymmetric flow patterns as a consequence of the fluid flow characteristics.

Tripathi and Ajmani[40] reported on a numerical investigation of fluid flow phenomena in a curved shape tundish (Fig 2.4.2). A 3D mathematical model was developed by them. The results were compared with a conventional delta shaped tundish. The strong role of curvature in improving fluid flow characteristics and enhancing inclusion floatation was evident from their results. They also reported a considerable increase in the plug volume and mean residence time through the use of contour shaped pouring chambers as compared to those with sharp corners. The mathematical model was validated with experimental results for a single strand bare tundish.

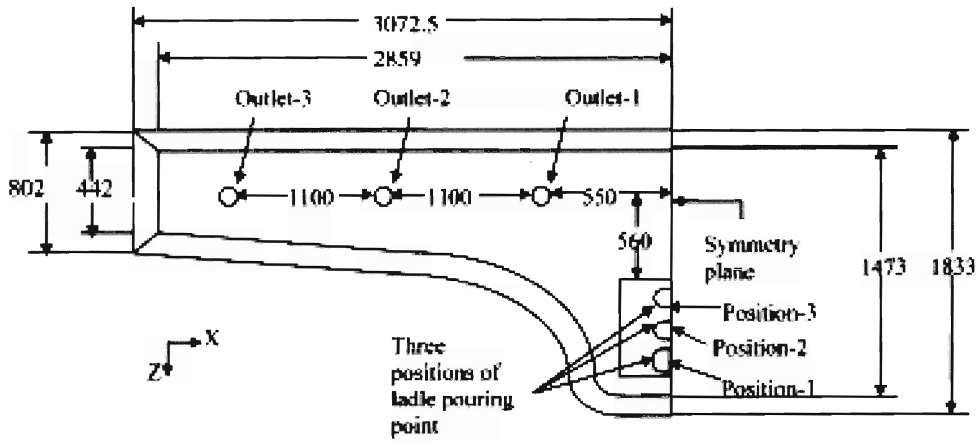

Figure-2.4.2 Curved shaped tundish of Tripathi and Ajmani[40]

A novel tundish mixing model was proposed to predict the outlet concentration of the tundish during a grade transition by Cho and Kim[41]. To enhance the efficiency and replication performance, the present model was designed to minimize the number of parameters to only one that needs to be tuned for easier application to new situations whereas the Huang and Thomas[42] model had six parameters to be tuned. Two types of water model were employed to verify Cho and Kim's model, and the real grade mixed blooms were produced through a grade transition continuous casting. When the present tundish mixing model was applied to the cases of the water models and real bloom casting, the numerical results of the present model were found to be in good agreement with the experimental data, and the constant parameter *f* of the present model was found to be determined according to the tundish shape.

Alkishriwi, Meinke and Schroder[43] carried out large eddy simulations of a continuous casting tundish to investigate the turbulent flow structure and vortex dynamics. The method used an implicit time accurate dual time stepping scheme in conjunction with low Mach number preconditioning and multigrid acceleration. To validate the scheme, large-eddy simulations of turbulent pipe flow at $Re_T = 1280$ and cylinder flow at $Re_D = 3900$ were performed. The results showed the scheme to be efficient and to improve the accuracy at low Mach number flows. The findings from the LES showed the presence of many intricate flow details that have not been observed before by customary RANS approaches. Fluid flow dynamics during ladle drainage operations of steel under isothermal and non-isothermal conditions were studied using the turbulence shear stress transport k- ε model (SST k-ω) and the multiphase volume of fluid (VOF) model by O. Davila et al.[44] At high bath levels, the angular velocity of the melt, close to the ladle nozzle, was small, rotating anticlockwise, while intense vertical-recirculating flows were developed in most of the liquid volume due to descending steel streams along the ladle vertical wall. These streams ascended further downstream driven by buoyancy forces. At low bath levels, the melt, which was close to the nozzle, rotated in a clockwise direction with higher velocities for shorter ladle stand still times (holding time). Figure 2.4.3 to 2.4.6 shows draining operations under isothermal and non-isothermal conditions. These velocities were responsible for the formation and development of a vortex on the bath free surface, which entrained slag into the nozzle by shear-stress mechanisms at the metal-slag interface. The critical bath level or bath height for this phenomenon was 0.35 m (in this particular ladle design) for a ladle standstill time of 15 minutes and decreased with longer ladle stand still times. At these steps, the vertical-recirculating flows were substituted by complex horizontal-rotating flows in most of the liquid volume. Under isothermal conditions, the critical bath level for vortex formation on the melt free surface was 0.20 m, which agrees very well with that determined with a 1/3 scale water model of 0.073 m. It was concluded that buoyancy forces, generated as a result of thermal gradients, as the ladle cools, were responsible for increasing the critical bath level for vortex formation.

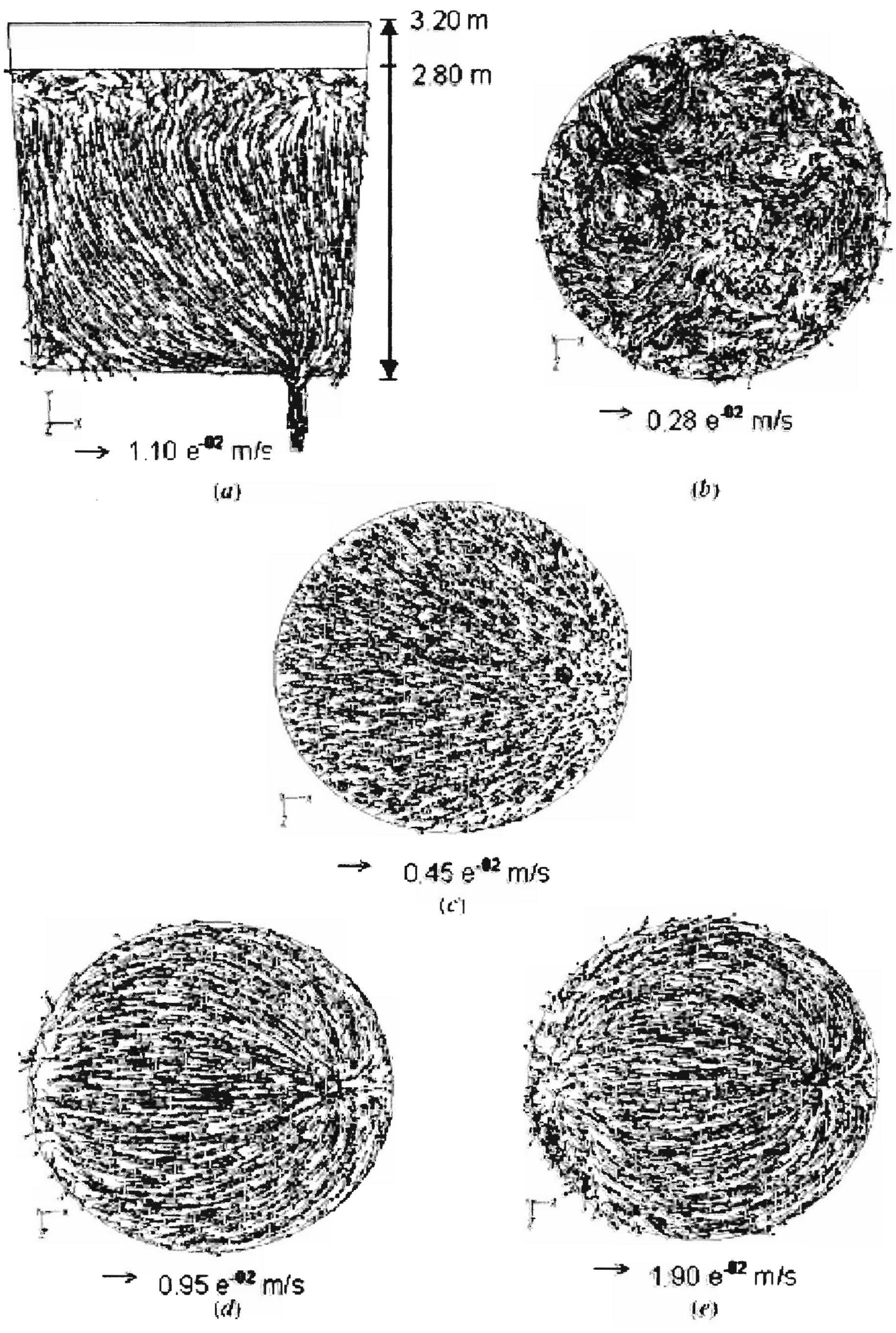

Figure- 2.4.3 Velocity fields in different planes during isothermal drainage of liquid steel from a ladle at a throughput of 2.1 ton/min for a bath level of 2.80 m: (*a*) vertical plane, (*b*) horizontal plane at 2.50 m from the bottom, (*c*) horizontal plane at 1.50 m from the bottom, (*d*) horizontal plane at 0.35 m from the bottom and (*e*) horizontal plane at 0.20 m from the bottom.[44]

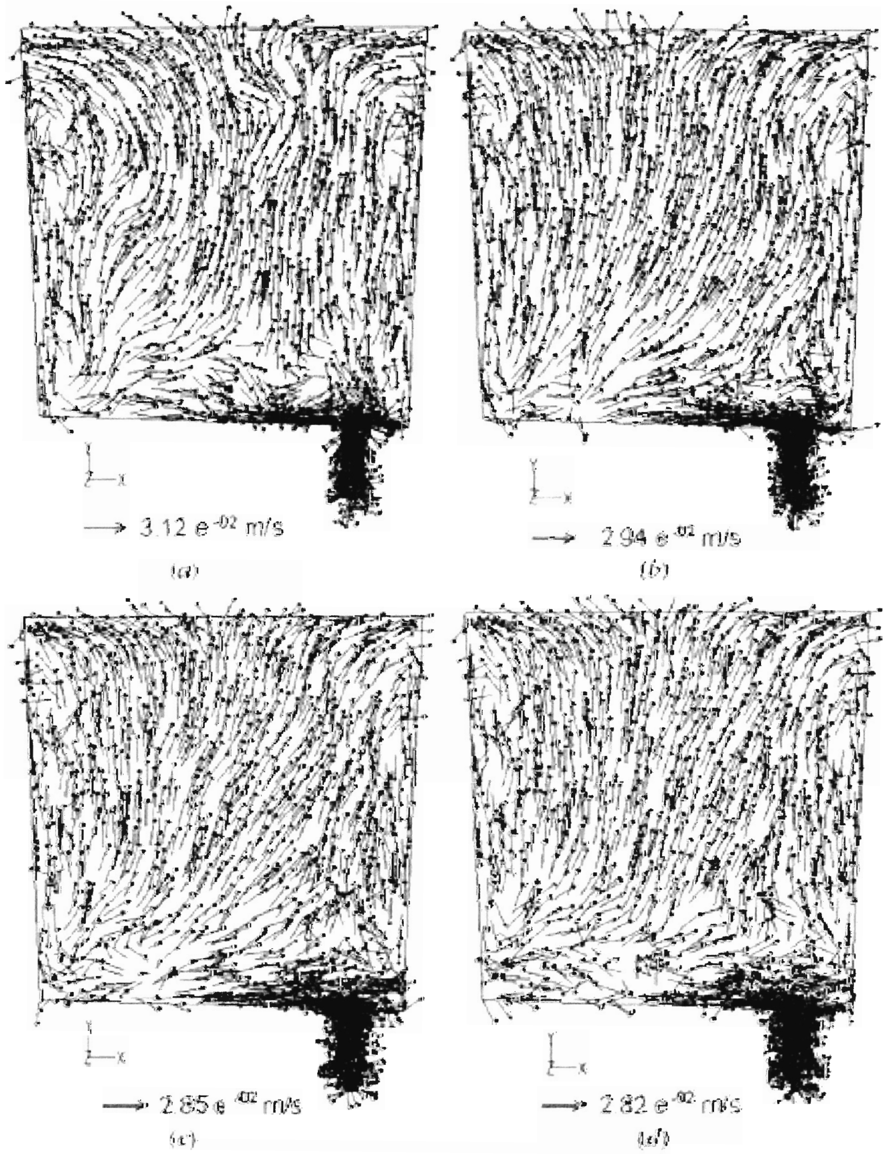

Figure- 2.4.4 Velocity fields developed during thermal stratification of liquid steel at different standstill times of the ladle: (*a*) 15 min, (*b*) 30 min, (*c*) 45 min,and (*d*) 60 min.[44]

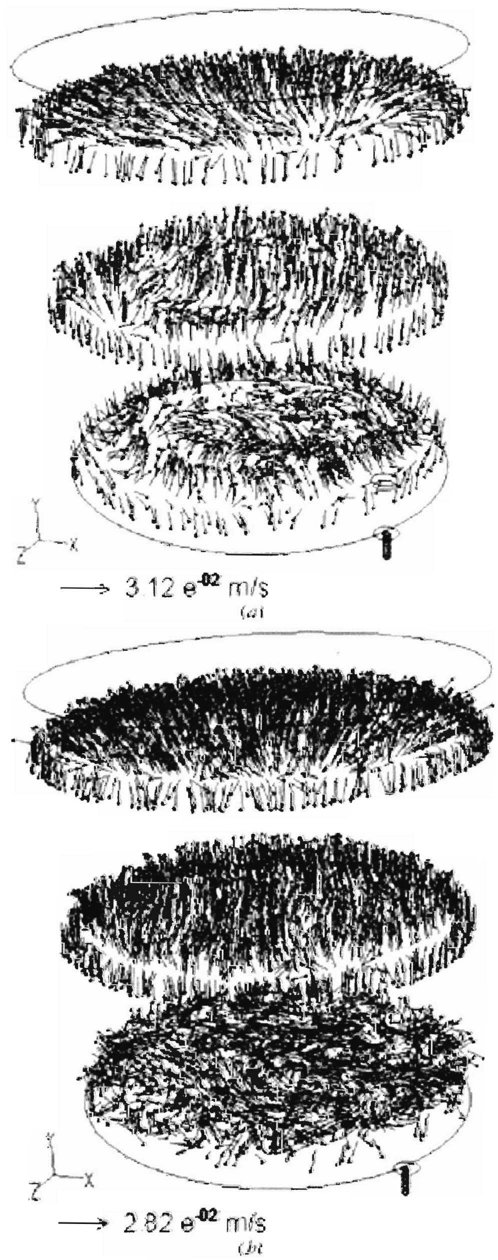

Figure- 2.4.5 Velocity fields at different horizontal planes located at 2.80, 1.50, and 0.30 m from the bottom: (*a*) after a standstill time of 15 min and (*b*) after a standstill time of 60 min.[44]

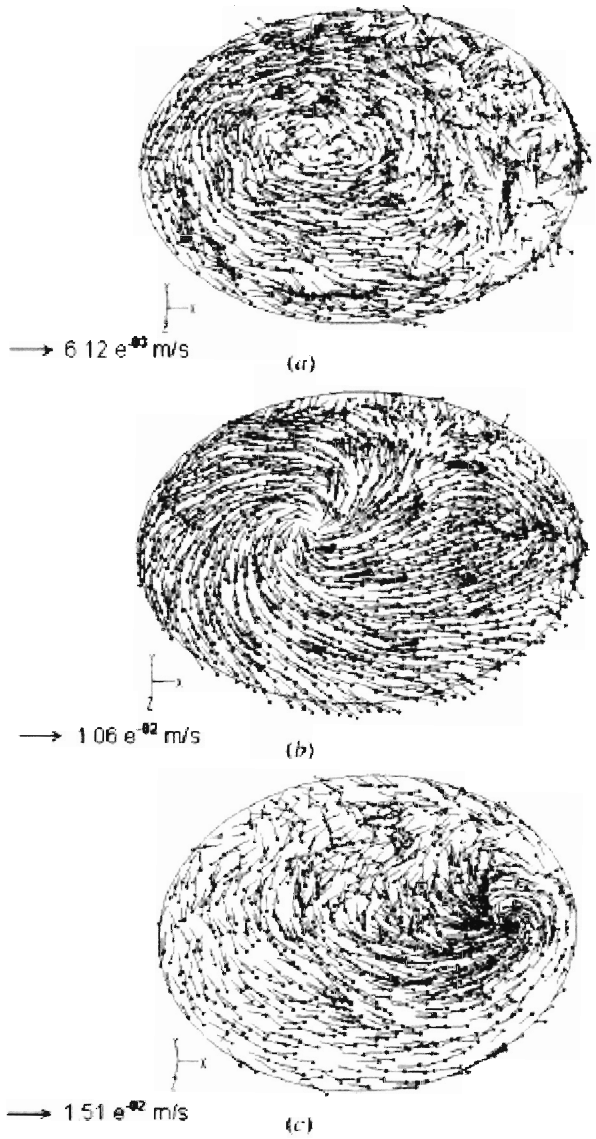

Figure-2.4.6 Velocity fields at horizontal planes during non isothermal drainage of liquid steel from a ladle at different horizontal planes for a bath level of 1.50 m: (*a*) 0.80 m from the bottom, (*b*) 0.40 m from the bottom, and (*c*) 0.20 m from the bottom.[44]

Sankanarayan and Guthrie[45,46] showed that the diameter ratio of the outlet nozzle and the ladle is important and this ratio and the critical height for vortex formation are proportional. For a constant ratio of outlet diameter to ladle diameter, the critical height becomes larger with higher initial bath heights. Understanding vortex mechanisms will be useful to design simple and efficient devices to break down the vortex flow during steel draining even at very low metal residues in the ladle.

P. Vayrynen et al.[47] modeled steady state and transient casting situations. Their work was focused on tuning and validation of a commercial CFD package which will be used to simulate tundish operations. They concluded that the software was not able to simulate the downscaled water model accurately, but on the other hand both temperature and transient casting situation results of the full scaled tundish were satisfactory. They mentioned that one possible reason for this behaviour is that areas of clearly turbulent flow in the water model are much smaller than in actual tundish and this transition of flow type is very difficult for the present turbulence models to calculate accurately.

M. Zorzut et al.[48] developed a mathematical model which could predict steel grade change. The model was set up using dilution interconnecting elementary cells that describe the shroud and each strand. The cells were considered with uniform concentration. Such a model was very useful in the definition of the technological practice for the steel grade change operation.

Fluid flow and mixing of molten steel in a twin-slab-strand continuous casting tundish were investigated using a mixing model under non isothermal conditions by ALIZADEH et al.[49] This model led to a set of ordinary differential equations that were solved with a Runge-Kutta algorithm. Steady state water modelling were carried out under non-isothermal conditions. Experimental data obtained from the water model was used to calibrate the mixing model. As a result of the presence of mixed convection phenomena in the non-isothermal tundish, parts of the primary fluid were mixed with the warm incoming fluid. Due to the density difference between the two fluids, fluid channelling was evident within the tundish. The volume flow rate of the fluid in the channel was found to depend on the ratio of inertial to buoyancy forces inside the tundish. They mentioned that if Re_T and Tu between two tundishes are same the RTD curves would be in absolute accordance with each other. However, the mixing model results showed that the total mixing flow volume fraction in the non-isothermal tundish was lower than that in the isothermal one.

Inclusion removal in the tundish is a very important operation and a lot of work has been in literature till date. Mazumdar & Guthrie[1] had discussed the studies on inclusion separation where Stokes terminal rising velocity of the inclusion particles were vectorially added to the vertical component of the fluid motion in the partial differential equation which is basically convection – diffusion equation for species transfer [Eq:2.4.1]

$$\frac{\partial(\rho c_i)}{\partial t}+\frac{\partial(\rho u c_i)}{\partial x}+\frac{\partial(\rho[v+u_{T,i}]c_i)}{\partial y}+\frac{\partial(\rho w c_i)}{\partial z}=\frac{\partial}{\partial x}\left(\Gamma_{eff}\frac{\partial c_i}{\partial x}\right)+\frac{\partial}{\partial y}\left(\Gamma_{eff}\frac{\partial c_i}{\partial y}\right)+\frac{\partial}{\partial z}\left(\Gamma_{eff}\frac{\partial c_i}{\partial z}\right)+S_i$$

[Eq: 2.4.1]

After obtaining a steady state velocity field, equation 2.4.1 is solved for inclusion concentration. Generally each group of inclusions is characterized by their diameter. They also discussed the source term S_i that represents generation or destruction of a particular size of inclusion by coalescence and the boundary conditions. Details of these are not repeated here. Recent studies showed the use of different models to study inclusion separation phenomenon. Hamill and Lucas[50] used an algebraic slip model (ASM) which basically is a simplified form of a multi-phase model to study inclusion motion and its removal. Assuming that the small particles (40μm-300μm) always move at their slip velocity, which basically comes from a balance between the buoyancy and drag forces, they solved separate scalar volume fraction equation for each particle species along with the basic conservation equations for multiphase (the equations are not given here). They used software CFX to compute the results and compared their results with previously published results of Joo et al[51], who used equation 2.4.1 which is based on single phase modelling approach. Joo et al.[51] used the METFLO 3D software (a code developed in McGill university) to solve those equations. For the flow conditions modelled, they showed that most inclusions greater than 100 microns should float out, independent of flow control devices while all those less than 40 microns would not be helped by flow modifying devices, and be retained in liquid steel exiting to the strands.

More recently Huelstrung et al.[52] studied the influence of tundish volume and Schwarze et al.[18] studied the influence of different weir & dam arrangements on predicting the degree of inclusion separation. Huelstrung et al.[52] used a "discrete phase model" to predict the degree of inclusion separation and used the results as a tool for designing a higher capacity tundish. Better macroscopic cleanliness of steel slabs produced during abnormal casting conditions caused due to the stopping of one of the strand slab caster, led them to design a tundish with a higher volume. They investigated the behaviour of solid alumina particles using an Euler-Lagrangian method. In this method, the particle trajectories were computed in a Lagrangian reference frame. The equations involved in this method are discussed in the later part of the thesis. Schwarze et al.[18], in their isothermal and non isothermal studies of a V-shaped tundish, also considered the effect of added mass (Figure 2.4.7), which should be included when a thin film of liquid surrounds a moving particle. Apart from that, they also included a term for the force of excess pressure differential with acceleration of the fluid motion (equations 2.4.2 and 2.4.3).

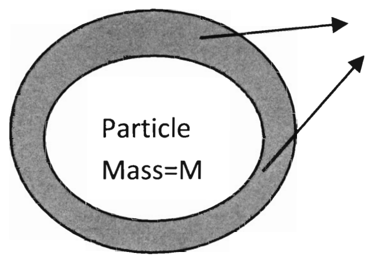

Figure-2.4.7 showing added mass due to thin film of liquid surrounding the particle[18]

$$\frac{du_p}{dt} = F_D\left(u - u_p\right) + \frac{g_x(\rho_p - \rho)}{\rho_p} + F_x + F_p \qquad \text{[Eq: 2.4.2]}$$

$$F_p = \frac{\rho}{\rho_p}\left(u_p \frac{du}{dx}\right) \qquad \text{[Eq: 2.4.3]}$$

To simulate the chaotic effect of the turbulence eddies of the liquid phase on the inclusion trajectories; a discrete random-walk model was applied by S. Diaz et al.[53] In this model, a fluctuant random-velocity vector (u_i') is added to the calculated time-averaged vector ($\overline{u_i}$), in order to obtain the inclusion velocity (u_i) at each time step, as particles travels through the fluid. Each random component of the inclusion velocity is proportional to the local turbulent kinetic energy level(k_p), according to the following equation (2.4.4)

$$u_i' = \zeta_i\sqrt{\overline{u_i'^2}} = \zeta_i\sqrt{\frac{2k}{3}} \qquad \text{[Eq: 2.4.4]}$$

Where ζ_i is a random number, normally distributed between -1 and 1, which changes at each integration step.

Lifeng Zhang et al.[54] proposed three modes of inclusion removal from molten steel in the tundish viz. floatation to the free surface, collision and coalescence of inclusions to form larger ones and adhesion to the lining solid surfaces. They studied the 3D fluid flow with and without flow control devices. The results indicated that flow control devices effectively limit the strong stirring energy to within the inlet zone. Flow control devices were also favourable for inclusion removal. The total removal ratio was 51% without flow control devices where inclusions with radii greater than 72 microns were totally removed. This increased to 79% with flow control devices where inclusions with radii greater than 61 microns were totally removed. Out of this 79%, removal by floatation was 49.5% and removal by adhesion was 29.5%. The collision and coalescence mode was a better way to remove smaller size inclusions as the number of collisions per unit time per unit volume of steel was much higher for smaller inclusions than bigger inclusions.

M. Javurek et al.[55] considered the removal of non metallic inclusions due to buoyancy forces in continuous casting tundishes. They found the reasons why the particle separation is worse than the calculated maximal possible removal rate. The reasons were unfavourable fluid flow pattern and the turbulent particle diffusion. They also concluded that RTD curves are inappropriate to estimate the particle separation in tundishes. The use of direct calculation and CFD simulation was recommended.

R. Schwarze et al.[18] studied the degree of inclusion separation in different (V shaped) tundish configurations by numerical modelling. The numerical model was based on the Euler-Lagrange approach. The flow was described by the Reynolds averaged transport equations for mass, momentum and energy in conjunction with the RNG - $k-\varepsilon$ model. They considered both isothermal and non isothermal flows. Only small differences between the isothermal and non isothermal flows were observed for the conditions modelled. Thermal natural convection was not that significant. The results of the numerical model were in good agreement with corresponding data from water model studies. The highest degree of inclusion separation was reached when a dam was positioned just at the beginning of the tundish arm (Figure 2.4.8).

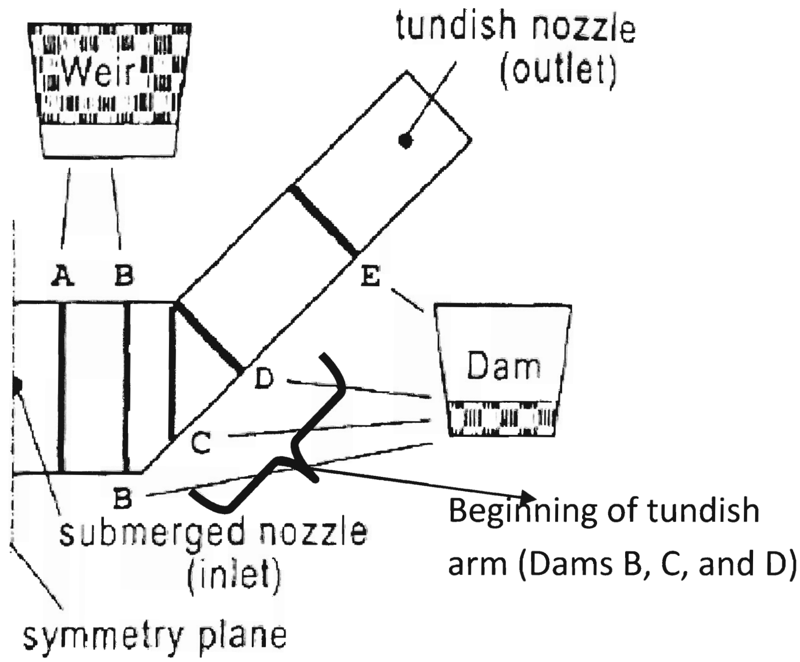

Figure-2.4.8 Showing V shaped tundish with different arrangements of weir and dams[18]

Thomas and Bai[56] summarized the formation mechanisms, detection methods and prevention of tundish nozzle clogging, focusing on the role of computational models in quantifying the non-composition-related aspects. They classified tundish clogging into four main types viz. the transport of oxides present in the steel to the nozzle wall, air aspiration into the nozzle, chemical reaction between the nozzle refractory and the steel and steel solidified in the nozzle. However, in practice, a clog can be a combination of two or more of the above types. They mentioned that clogging can be best detected during casting by simultaneous monitoring of several different parameters like argon back pressure, nitrogen pickup, mould level fluctuations and flow control position relative to casting speed. Solutions to clogging problems were also mentioned by them. They are minimizing inclusions by improved steelmaking practices, optimizing fluid flow and transfer processes, controlling steel alloy additions, slag and refractory compositions, improving nozzle material design and avoiding air aspiration. J. P. Rogler et al.[57] reported the probability of inclusion removal in a tundish by gas bubbling. They developed a simple mathematical model and concluded that the probability of particle/bubble attachment (P_{at}) is the product of the probabilities of three fundamental steps of this process including thinning, rupture and three-phase contact stability[58] (Figure 2.4.9).

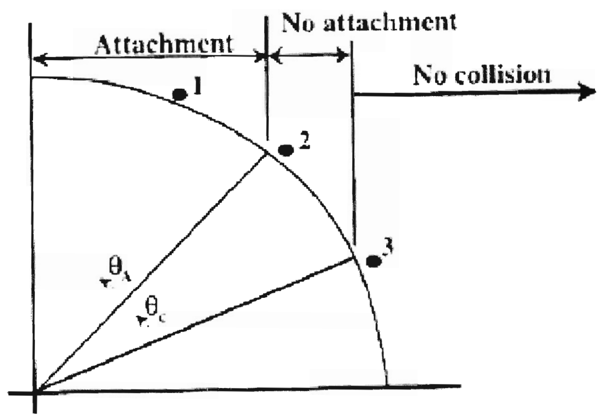

Figure- 2.4.9(a) Schematic diagram of critical angles.[58]

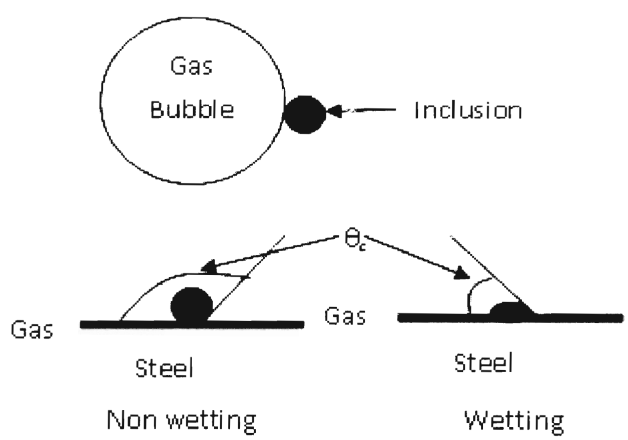

Figure- 2.4.9(b) Schematic diagram of steel gas and inclusion system

However, only the probability of film thinning can be calculated by any known method and they suggested that the probability of the last two steps could be assumed to be unity. P_{at} increases with decreasing particle size and increases with increasing bubble size. But for attachment collision is necessary and hence the particle collection probability (P) is the product of P_{at} and the collision probability P_c. A semi-analytical solution of the Navier-Stokes equation gives a rough estimate of P_c. This analysis shows that the collection probability (P) increases with decreasing bubble size and increases with increasing particle size. The removal of exogenous non-metallic inclusions by optimization of hydrodynamic characteristics was reported by A. V. Kuklev et al.[59] The suggested methods are increasing tundish size to allow more residence time and the use of flow control devices. J. P. Rogler et al.[60] performed physical modelling of inclusion removal in a tundish by gas bubbling. They used water as the analogue of steel and linear low density polyethylene (LLDPE, ρ=0.92) as an analogue of inclusions. They concluded that separation efficiency of inclusion particles within the flowing liquid bath in a tundish is influenced by a number of factors such as the overall fluid flow behaviour, the chemical and physical nature of the inclusion, size of the inclusions, and the rates and mechanisms of particle capture by various potential particle sinks. From their study, they concluded that FCD enhanced particle separation efficiency and properly sized bubbles induced the highest particle separation efficiencies.

An extensive review of the literature shows a large number of modelling efforts covering various aspects, such as fluid flow , RTD, effects of FCD on flow pattern, inclusion removal, thermal energy transport, etc, have been reported. However, most of the modelling did not consider refractories, slag, and fluxes; in their predictions. Henrik Solhed et al.[12] did include these in their modelling effort, and studied slag-steel interactions in continuous-casting tundishes. A model was developed that took into account the steel, slag and refractory phases. The model was also used to determine the optimal location of flow devices, rendering the temperature distribution in the steel more uniform and enhancing the removal of inclusions to the upper slag phase. In that study, the focus was to study the slag/steel interface. Predictions showed that slag is dispersed into the steel close to the interface, as well as close to the ladle shroud. A momentary interfacial solidification sampling (MISS) method was developed to confirm these predictions with plant tests. Analysis of the samples by ultrasonic testing, optical microscopy and SEM confirmed the presence of non metallic particles close to the slag steel interface and close to the ladle shroud. The analyses also showed that the slag steel interface is very irregular despite low velocities. They concluded that the slag/steel interface is unstable and that the liquid steel at the interface can engulf slag and may lead to the formation of inclusions in the final cast product. In another investigation, slag floatation and entrapment was studied by Henrik Solhed et al.[13] using fluid flow simulations, sampling and physical metallurgy. A model of a continuous casting tundish was developed, which considers refractory, slag and flux phases in addition to the steel phase. The model was verified with velocity and temperature measurements in the liquid steel and temperature profiles in the refractory walls.. The agreement between the measured velocities and temperatures and the corresponding predictions were good. From their computational results it was seen that slag concentrations were very low in the regions near the walls, where flows were upwardly directed, but that near to the shroud and the stopper rod, slag concentrations were higher and the downwardly directed velocity components caused the slag to penetrate the steel. It is evident that not much work has been done on slag entrainment. So more work on slag entrainment using both physical and mathematical modelling needs to be done. Here at the MMPC, modelling slag entrainment both physically and numerically is being done by some researchers. In the numerical model the VOF approach is currently used.

The effect of flow control devices have also been extensively studied by a number of researchers[61,62 ,19,63,64,65,66.] The research on FCD has been so vast in the past decade that perhaps it needs a separate review on the effect of FCD on the performance of tundish. However it has been seen that a FCD can have a positive effect on tundish performance if its design is properly optimised and positioning within the tundish is proper. But for inclusion removal FCD have failed to show their efficiency either in physical or mathematical modelling[67,68,69] Also improper positioning of a FCD may result in detrimental flow patterns inside the tundish. Also in large tundishes which allow sufficient residence time for inclusion floatation FCD are not recommended because they are inconvenient to sustain hot cycle tundish practice, which is quite economical. With a large tundish, the deep melt bath does not require a pour pad either.[7]

A swirling ladle shroud may be very useful to reduce turbulent kinetic energy within the inlet zone. A new design of ladle shroud (Figure-2.4.10), obtained through water modelling, that controls turbulence of the entry jet in continuous casting tundishes has been proposed by G. S. Diaz et al.[70] Particle Image Velocimetry (PIV) measurements indicated that this design decreased the impact velocity on the tundish bottom close to 1/3 of that provided by a conventional ladle shroud. This achievement was due to a swirling jet that promoted a recirculatory flow in the horizontal planes of the tundish. The swirling effects helped to dissipate the turbulence energy of the jet before it hit the tundish bottom thereby decreasing fluid velocities impacting the back and front walls of the tundish.

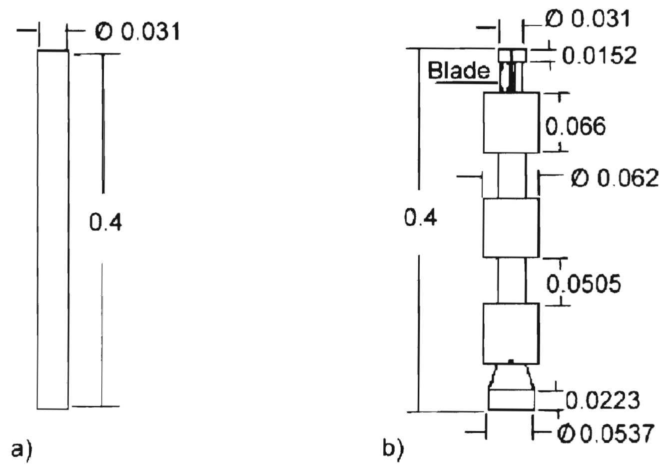

Figure-2.4.10 Geometric dimensions of the experimental shrouds (a) Conventional and (b) Swirling Ladle Shroud (SLS).[70]

Turbulence models such as k- ε , k- ω and RSM were applied to simulate the experimental PIV measurements of velocities in the fluid flow. Only the RSM model yielded predictions that agreed remarkably well with the experimental determinations. These results were sufficiently good as to avoid the employment of flow control devices such as dams, weirs, turbulence inhibitors and the like, in tundishes.

G. S. Diaz et al.[71] in another study concluded that the SLS efficiently avoids the formation of vortexes and recirculating flows either under isothermal and non isothermal conditions. The SLS enhances floatation of inclusion and makes the floatation rate less dependent on particle size. The trajectories of inclusions in the water flow are shown in Figures 2.4.11, 2.4.12 and 2.4.13.

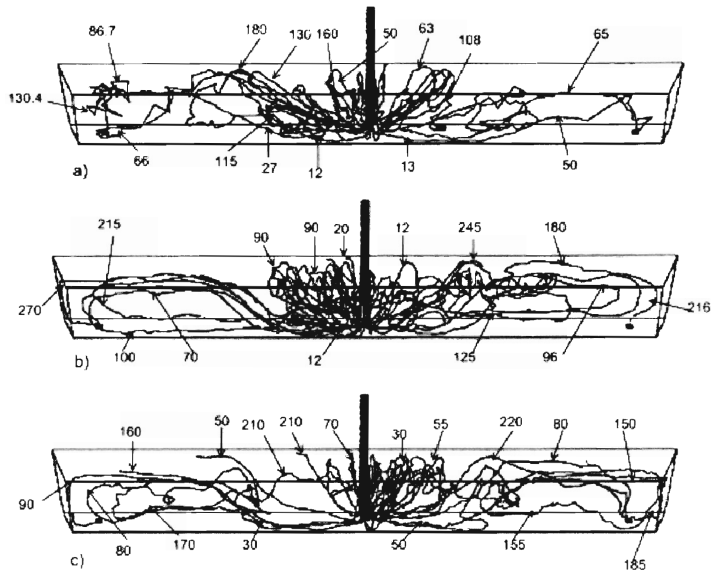

Figure 2.4.11 Trajectories of inclusions in the water flow obtained by mathematical simulation. Isometric view using conventional ladle shroud and particle of 20μm under: (a) 27 s after the thermal step up input, (b) 120 s after the thermal step up input, (c) 240 s after the thermal step up input.[71]

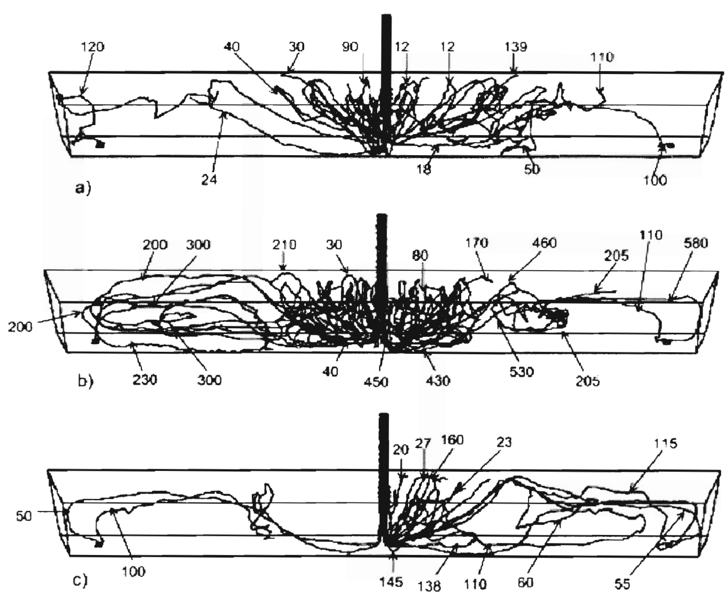

Figure 2.4.12 Trajectories of inclusions in the water flow obtained by mathematical simulation (isometric view) for a conventional ladle shroud and particle of 100μ m under:(a) 27 s after the thermal step up input, (b)

120 s after the thermal step up input, (c) 240 s after the thermal step up input.[71]

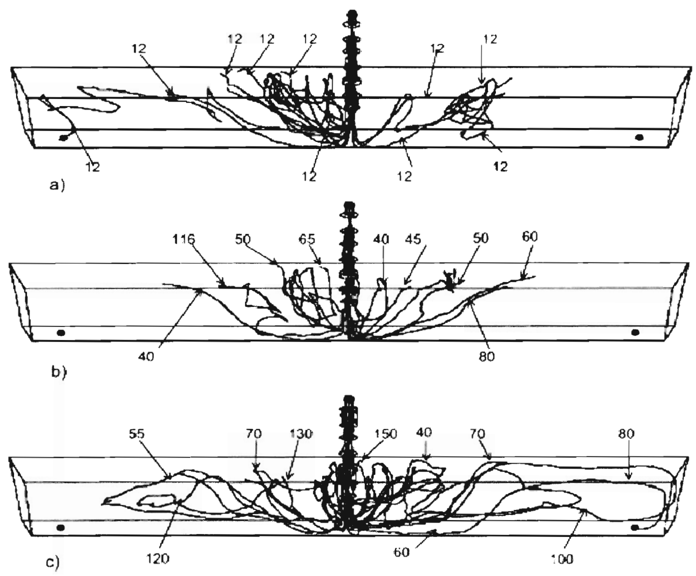

Figure 2.4.13 Trajectories of inclusions in the water flow obtained by mathematical simulation at the isometric view using swirling ladle shroud and particle of 20µm under: (a)27 s after the thermal step up input, (b) 120 s after the thermal step up input, (c) 240 s after the thermal step up input.[71]

Thus the SLS is a good alternative to substitute the FCD available in the market.

The SLS may have many advantages but from the flow fields it appears that the flows are highly complex and certainly cause erosion of refractory inside the shroud which is not economical and detrimental for the steel quality.

In summary, it is seen that a lot of work has been done on the development of mathematical models for studying fluid flow patterns in tundishes, to study the effect of FCDs, to evaluate mean residence times, RTD and inclusion removal ratios. This R&D effort has been possible, thanks to the increase in computational power and the logarithmic decreases in computational costs (MOHR's Law). However, slag entrainment, one of the most important issues in continuous casting, has not gained much attention and only few researchers have reported that in the literature. Also, it is essential to validate these numerical models with actual experiments. The review also shows a recent trend in modelling considering non isothermal conditions. In reality tundish operations are inevitably non-isothermal to some extent,(unless plasma heated tundishes are practised). Hence, there are effects of inlet steel temperatures and buoyant forces. So isothermal modelling predictions may not be sufficiently correct since tundish flows are very sensitive to even minor fluctuations in steel/slag temperature (ie.~5^0C). Many researchers are now advocating against the use of FCDs and are proposing increased tundish volumes for sufficient residence times and better inclusion removal. This practice has already started in Japan some twenty years ago together with the adoption of plasma heating for maintaining isothermal conditions during casting. Although, DNS seems to be impossible, at least one research centre of a Japanese Steel Company is doing this with the aid of parallel processing, with over 300 computers in synergy.

2.5 Review on gas shrouding

The injection of argon gas into the ladle shroud and Submerged Entry Nozzles (SEN's) is a common practice in continuous casting. The primary objective is to prevent the melt stream from re-oxidation due to aspiration of ambient air. H.B. Kim[72] in 1998 is his M. Eng thesis at McGill University, discussed in detail about air aspirations in ladle shrouds. The benefits resulting from shrouding the melt stream are manifold. There is a definite reduction in the oxygen content in the bath, a lesser number of oxide inclusions, a decrease in nozzle clogging frequency, an improvement in surface quality of slabs and billets, and a reduction of melt temperature loss from ladle to tundish[7]. Despite these benefits, too much of argon gas should be avoided, as it forms an exposed eye of steel around the ladle shroud by sweeping off the protective layer of tundish slag. The optimal argon flow rate depends on casting speed, tundish level and nozzle bore diameter[73]. G.M.Evans et al.[74], mentioned that for applications like SEN's, too much gas injection results in a transition from the bubbly flow regime to the churn-turbulent regime, and that is highly undesirable. Thus, it is essential to have a scientific understanding of the gas shrouding phenomenon, so that it becomes easier to optimize the process. Bai and Thomas[75, 76] studied turbulent flow of liquid steel and argon gas bubbles in a slide gate tundish nozzle during the transfer of liquid steel from tundish to mould. They developed an Eulerian multiphase mathematical model using the finite difference program CFX and studied 3D turbulent flow of liquid steel and gas bubbles. The multi-fluid Eulerian multiphase model of CFX[77] was used to simulate the time averaged flow of argon bubbles within the liquid steel. In CFX modelling , each phase has its own set of continuity and momentum equations. Coupling is achieved through an empirical interphase drag between liquid steel and argon bubbles. The model predictions agreed both quantitatively and qualitatively with measurements conducted using PIV on a 0.4-scale water model. G. M. Evans et al[74] studied the flow characteristics of a down flowing gas-liquid column incorporating a submerged entry porous nozzle system. They developed the model based on the one-dimensional drift flux analysis and critical Weber number for stable bubble size. The model was used to predict the bubble size and gas void fraction as a function of the gas and liquid flow velocities within the bubbly flow regime. It could also be used to predict the gas and liquid flow conditions at which the transition from bubbly to churn-turbulent flow occurs. Li Tao et al.[78] developed a mathematical model to study inclusion removal by injecting gas in to the ladle shroud. They reported that the greater the number of bubbles generated, the better this was for maximum removal of inclusions. Koria and Srivastava[79] investigated the residence time distribution of steel melts associated with an argon shrouded stream of water pouring in a water model tundish. In the model, the air shrouded water stream entered the tundish and flow patterns and RTD's were studied using the impulse response technique. They concluded that the mean residence time depends on shroud diameter, air rate and submergence depth of the shroud. From the above discussions, it is clear that many researchers have studied the injection of gas in SENs, inclusion removal by gas shrouding, and RTD due to argon shrouded stream, etc., but no one has yet considered bubble trajectories, fluid flow patterns and slag behaviour in the tundish, due to inert gas shrouding.

3.0 PHYSICAL MODELLING OF INERT GAS SHROUDING

3.1 Experimental setup

This section describes the details of the experimental setup. A **full scale** water model of a 12 tonne four strand delta shaped tundish was used for physically modelling the gas shrouding process. Liquid steel was replaced by its low temperature aqueous analogue (water) and compressed air was used to simulate the shroud gas (argon). A schematic representation of our full scale system is shown below in Figure 3.1.1

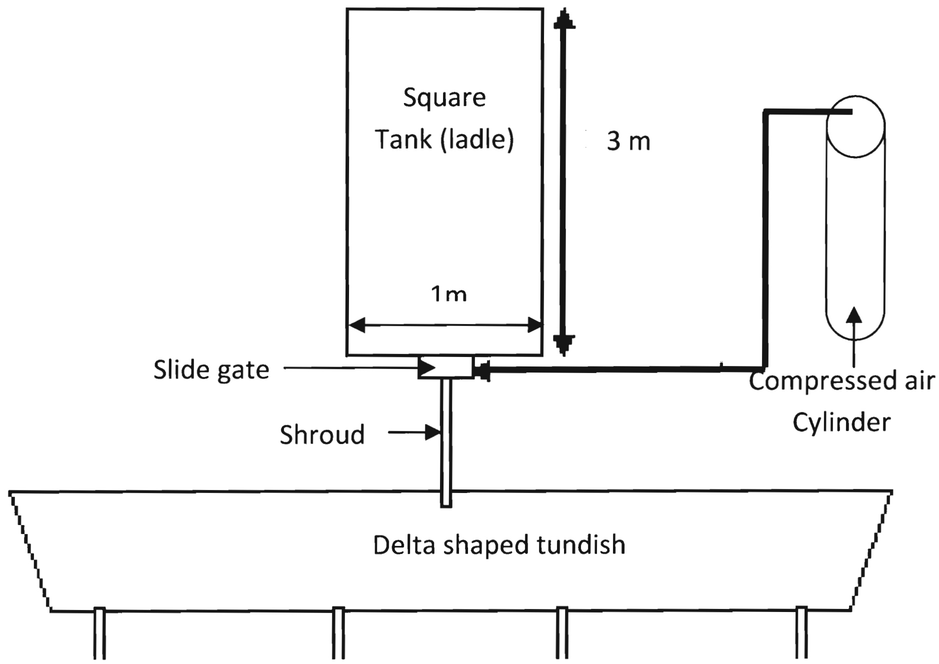

Figure-3.1.1schematic diagram of the full scale water model

The square tank above the tundish was used to simulate the three meter head pressure of liquid as in the real ladle and it helps to control the inflow rate of water into the water model tundish. The square tank is connected to the tundish by a slide gate nozzle i.e. the shroud. An actual photograph of the full scale plexi-glass system used at the MMPC, is shown in Figures 3.1.2 and 3.1.3. A flexible pipe was connected from a compressed air cylinder to just below the slide gate for gas injections.

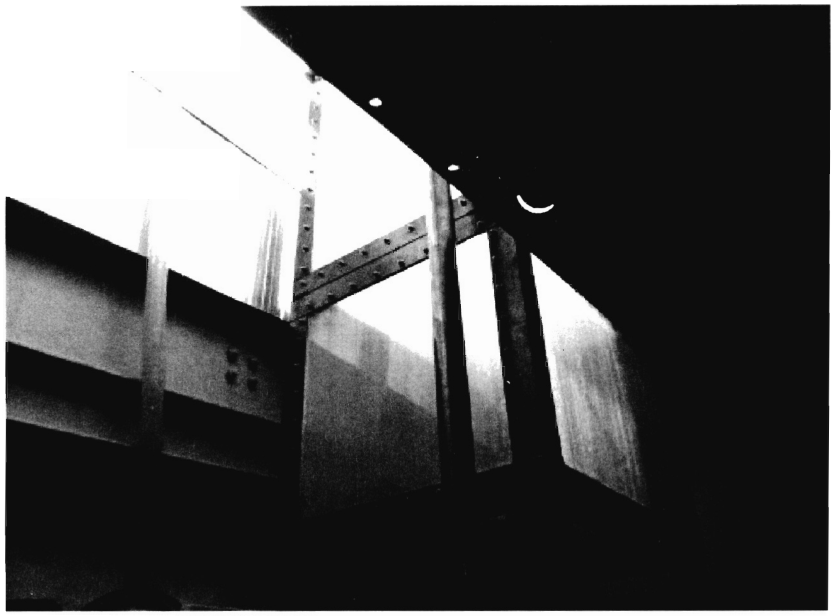

Figure-3.1.2 showing the square tank above the tundish simulating the actual ladle

Figure 3.1.3 showing the full scale plexi glass water model tundish

3.2 Experimental procedure

The tundish was first filled up with water from the square tank. A flow rate of 0.17 $m^3\ min^{-1}$ was maintained at the inflow to the tundish so as to achieve a steady level of 500 mm of water from its base. The flow rate of water was controlled with the help of digital flow meters fixed at the inlet (ladle shroud) and four outlet nozzles (SENs). The immersion depth of the 0.0572 m ladle shroud was 60 mm. Compressed air was injected from just below the slide gate through a 4mm diameter orifice at volumetric flow rates ranging between 2% and 10% of water entry flows. The flow rate of air was controlled with the help of a rotameter. The slag phase was simulated by using white coloured polyethylene beads which were uniformly poured over the free surface of water in the tundish (Figure-3.2.1). Neither flow modifiers nor flow control devices were used for any experiments described in this research programme.

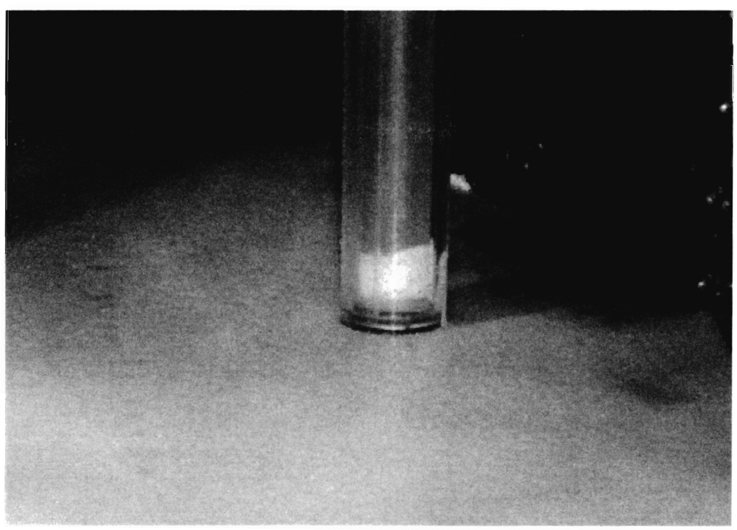

Figure-3.2.1 slag phase simulated by white polyethylene beads

As soon as compressed air was introduced, air bubbles formed and their movement within the tundish was monitored with the help of a video camera. Additionally the behaviour of the slag layer was simultaneously monitored. The movement of the slag layer was recorded. For tracer injection studies, a red dye was pumped in through the ladle shroud into the tundish and the colour of the water in the tundish was monitored with a camera at different instants of time. The dye injection was continued until a uniformly homogeneous colour was obtained throughout the tundish. The tracer injection studies gave an idea of the fluid motions and times required for complete mixing. Flow fields in the vicinity of the ladle shroud were examined by two dimensional Particle Image Velocimetry (2D PIV). A few fluorescent seeding particles (polyamide or hollow glass spheres) were added to the water within the tundish. The density of these tiny particles is generally equal to that of water and their separation velocities are almost nil. As such, they flow similarly as water. A dual pulse laser light plane was created which illuminated these fluorescent seeding particles. A CCD camera was placed perpendicular to the laser light sheet, which recorded the displacement of the seeding particles in between two frames. These images were processed with the help of software which performed cross correlation and ultimately generated the velocity vector field in the selected area of interest. As the flow within the tundish is predominantly turbulent, many images were taken (about 400) to mitigate the scatter caused by the stochastic nature of turbulence. These images were then processed and averaged to find average flow field velocity distributions. A schematic diagram of PIV is shown in Figure 3.2.2 and 3.2.3.

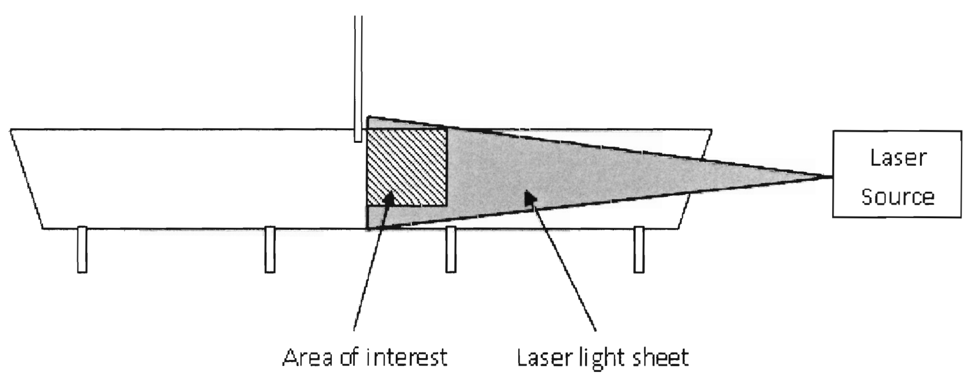

Figure-3.2.2 schematic diagram of 2D PIV measurements in the tundish

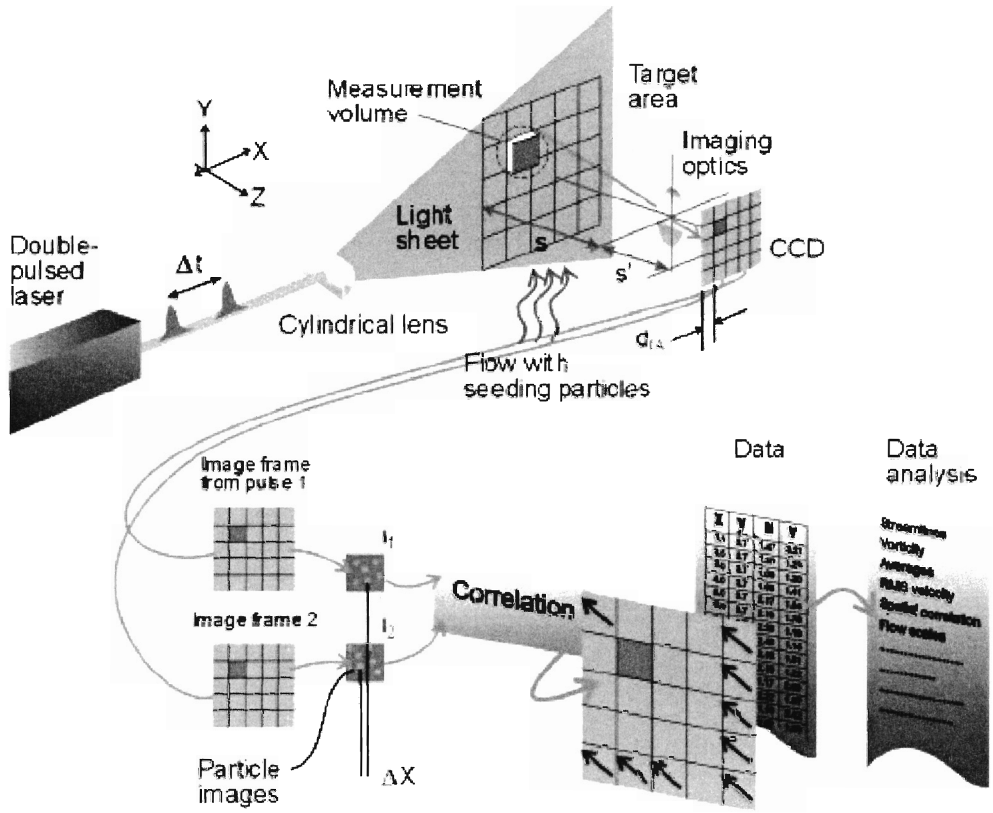

Figure-3.2.3 schematic diagram showing methodology of 2D PIV[80]

4.0 MATHEMATICAL MODELLING OF INERT GAS SHROUDING

4.1Theory

The mathematical model of two phase gas/liquid flows in the ladle shroud was based on the following two assumptions:

(1) The liquid in the shroud (water) is incompressible and Newtonian.
(2) The flow within the shroud is predominantly bubbly and discrete bubbles are formed which move down the shroud along with the down flowing water.

The standard k-ε model of Launder and Spalding[15] was used, coupled with the discrete phase model. The two way turbulence coupling was used to capture the effects of the discrete phase on the primary liquid phase. In the k-ε model, k is the kinetic energy of turbulence per unit mass and, ε is the rate of energy dissipation. Thus,

$$k = \frac{1}{2}\sum \overline{u_i^2} \qquad \text{[Eq: 4.1.1]}$$

So, in addition to the continuity and momentum equations, two extra equations for k and ε are solved.

$$\frac{Dk}{Dt} = \frac{\nu_t}{\sigma_k}\nabla^2 k + G_k - \varepsilon \qquad \text{[Eq: 4.1.2]}$$

$$\frac{D\varepsilon}{Dt} = \frac{\nu_t}{\sigma_\varepsilon}\nabla^2 \varepsilon + \frac{\varepsilon}{k}(C_1 G_k - C_2 \varepsilon) \qquad \text{[Eq: 4.1.3]}$$

Here G_k is the rate of production of k and is given by the following equation:

$$G_k = \nu_t\left[\frac{\partial v_i}{\partial x_j} + \frac{\partial v_j}{\partial x_i}\right]\frac{\partial v_i}{\partial x_j} \qquad \text{[Eq: 4.1.4]}$$

The turbulent and effective viscosity is calculated by the following equations[15]

$$\mu_t = \frac{C_\mu \rho k^2}{\varepsilon} \qquad \text{[Eq: 4.1.5]}$$

$$\mu_{eff} = \mu + \mu_t \qquad \text{[Eq: 4.1.6]}$$

The recommended values of the constants adopted in this study were C_1= 1.44, C_2= 1.92, C_μ= 0.09, σ_k = 1 and σ_ε=1.3 as proposed by Launder and Spalding[15]

In the discrete phase model, the particle trajectories are computed in a Lagrangian reference frame. The equations solved in addition to the basic conservation equations are as follows[52].

$$\frac{du_p}{dt} = F_D\left(u - u_p\right) + \frac{g_x(\rho_p - \rho)}{\rho_p} + F_x \qquad \text{[Eq: 4.1.7]}$$

The coupling between the continuous water phase and the discrete phase of air bubbles was done by defining the drag force (F_D) according to the following equation.

$$F_D = \frac{18\,\mu C_D Re}{24\,\rho_p d_p^2} \qquad \text{[Eq: 4.1.8]}$$

$$Re = \frac{\rho d_p |u_p - u|}{\mu} \qquad \text{[Eq: 4.1.9]}$$

$$C_D = a_1 + \frac{a_2}{Re} + \frac{a_3}{Re^2} \qquad \text{[Eq: 4.1.10]}$$

F_x in equation 4.1.7 is an additional acceleration term represents the "virtual mass" force, i.e. the force required to accelerate or decelerate a volume of fluid surrounding the particle[52].

In the two way turbulence coupling, as the trajectory of a particle is computed, a track of the momentum gained or lost by the particle stream that follows that trajectory is kept and these quantities can be incorporated in the subsequent continuous phase calculations. Thus, while the continuous phase always impacts the discrete phase, we can also incorporate the effect of the discrete phase trajectories on the continuum. This two-way coupling is accomplished by alternately solving the discrete and continuous phase equations, until the solutions in both phases have stopped changing.[81]

4.2 Procedure

The following steps were involved in the present mathematical modelling

- Drawing of the tundish (calculation domain) using basic CAD tools.
- Discretization of the whole domain into tiny cells(commonly called meshing).

- Exporting of the mesh to an appropriate CFD package.
- Setting up of material properties and boundary conditions.
- Setting up of solution parameters.
- Iterative solution of the discretized equations until convergence.
- Post processing and graphical representation.

The present calculations were carried out using the CFD FLUENT 6.3.26 package. The drawing of the system and meshing were performed using GAMBIT 2.4.6 and are shown in Figures 4.2.1 and 4.2.2.

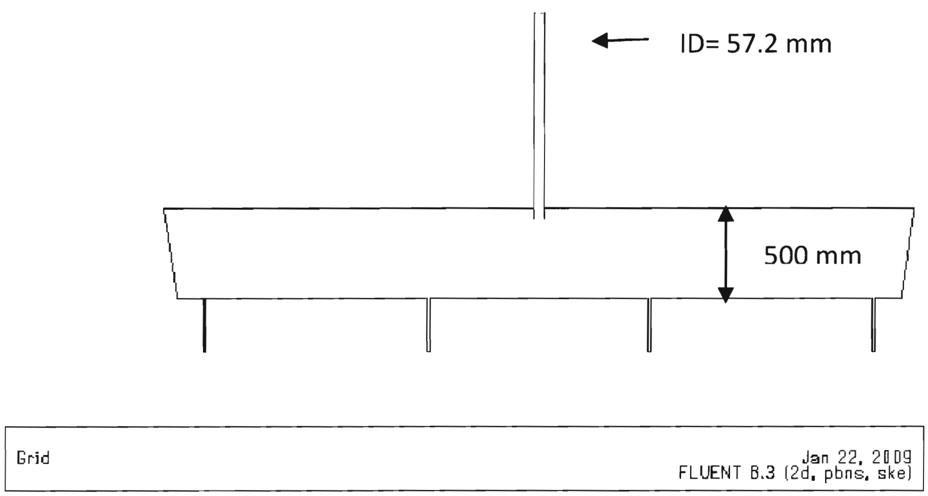

Figure-4.2.1 drawing of the tundish using GAMBIT 2.4.6

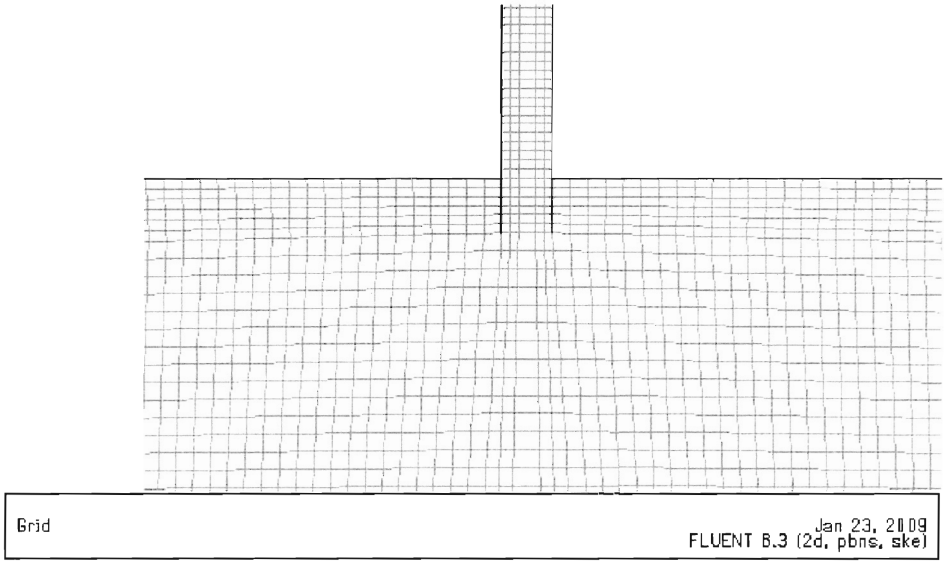

Figure-4.2.2 showing meshing of the tundish in GAMBIT 2.4.6

Calculations were performed in one half of the tundish by specifying a symmetry plane. This was done to save on computational time. All velocity components were set to zero at the walls by using the no- slip boundary condition. At the free surface of the liquid, the shear stress was set as zero. The primary fluid was taken to be water and the discrete phase material was set as air. A Quadrilateral type of mesh was used with finer grids in the vicinity of the ladle shroud.

In numerical modeling, the steady flow field solution was first obtained without any gas injection. After obtaining the steady state velocity field, gas injection was started under unsteady conditions with a time step size of 10^{-3}s. An average bubble diameter of 3.5mm for lower flow rates of 2%-4% and 5 mm for higher flow rates 6-10% (measured from physical experiments) was incorporated in the DPM.

During the initial steady state calculations we used the SIMPLE[25,26] algorithm along with the first order upwind scheme for momentum, K, and ε equations. Default values of the under relaxation factor were used i.e. unity for body forces, density and turbulent viscosity; 0.8 for the K, ε equations; 0.7 for the momentum equation. For pressure we used the standard scheme with an under relaxation of 0.3. After obtaining the steady state velocity field, when inert gas injections were started the under relaxation factors of K and ε were just changed to 0.5. This value was finalised after performing a lot of convergence tests.

After all the simulations were complete, the results were post processed to generate bubble tracks, velocity fields and turbulent kinetic energy contours. For all the simulations an Intel Core 2 Quad processor was used along with 8 gigabytes of RAM.

5.0 RESULTS AND DISCUSSION

5.1 Results of physical modelling

This section provides results of our physical modelling experiments. For convenience the section is divided into four sub sections.

5.1.1 Bubble trajectories

The bubble trajectories within the shroud and tundish were visualized with the help of video photography. They are shown in Figures 5.1.1.1 and 5.1.1.2.

Figure 5.1.1.1 air bubbles in the shroud.

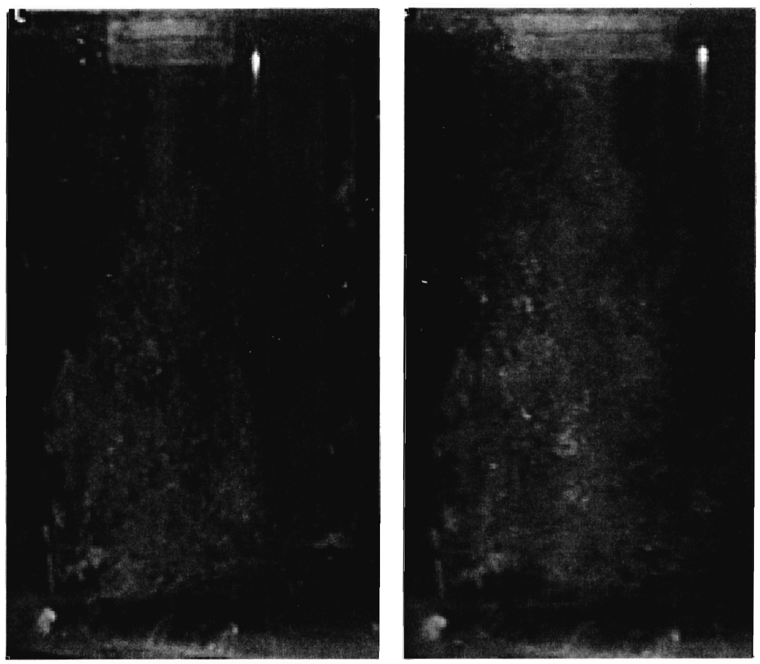

(a) (b)

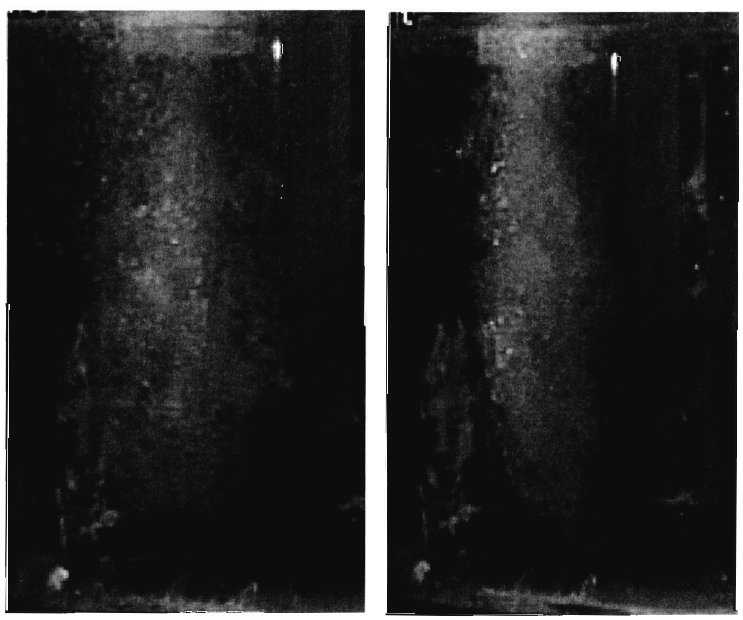

(c) (d)

Figure 5.1.1.2 showing bubble tracks captured by video photography
(a)2% (b)4% (c)6% (d)10% of gas/water entry flow rates

It is clear from Figure 5.1.1.2 that at lower flow rates of 2-4%, the bubble column reaching the bottom of the tundish. However, at higher flow rates, the bubble column does not touch the base of the tundish. Also at lower flow rates, it can be seen that the plumes are more dispersed and spread, as compared to higher gas flow rates where the plumes are dense and sharp. The average bubble size at lower flow rates of 2-4% was 3.5 mm where as at high flow rates the average bubble size was 5mm. These bubble sizes are quite large and hence each bubble has a significant buoyancy force and terminal rise velocity. Thus, the bubbles first travel down with the water jet from the shroud, reach the bottom of the tundish along with the down-flowing liquid. Then, due to their higher buoyancy, they rise straight up to the free surface of the liquid in the tundish.

5.1.2 Slag behaviour

The protective layer of slag used in the tundish was simulated using a 25mm layer of polyethylene beads. These were uniformly poured over the free surface of water in the tundish. Before injection of gas, the slag covers almost the entire surface of water, thereby assuring prevention against re-oxidation. This is shown in Figure 3.2.1. As soon as the injection of gas was started, the rising gas bubbles swept away the 'slag' and formed an exposed 'eye' around the shroud as shown in Figure 5.1.2.1. The size of this exposed eye keeps on increasing with increase in gas flow rate and finally when gas injection is stopped, the slag returns to its original state and the exposed eye is eliminated (Figure 5.1.2.1). This exposed eye around the shroud allows the steel to come into contact with ambient air and to be re-oxidised. Thus, high amount of gases in the shroud are not recommended. The reason for this type of slag movement is evident from the flow field studies discussed in the next section.

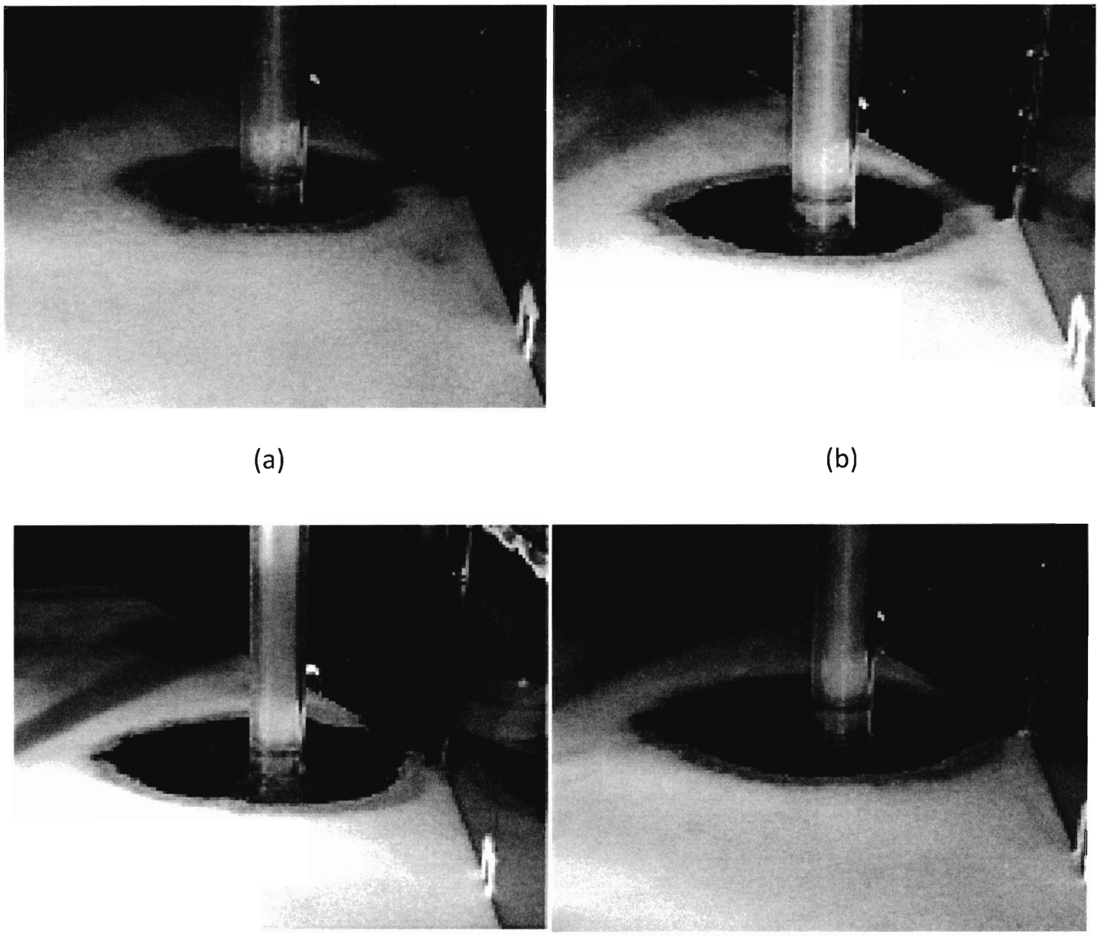

(a) (b) (c) (d)

Figure 5.1.2.1 showing the formation of an exposed "eye" at gas flow /water flow rate ratios of (a)2% (b)4% (c)6% (d)10%

5.1.3 Fluid flow patterns

Flow fields were visualized with the help of 2D Particle Image Velocimetry (PIV) scanning a plane near the shroud as shown schematically in Figure 5.1.3.1.

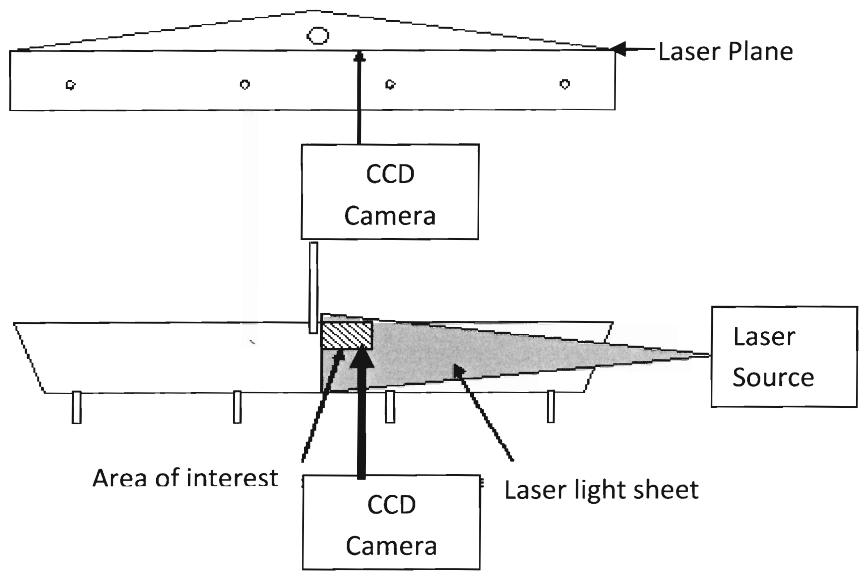

Figure 5.1.3.1 schematic diagram of PIV experiments and area of interest

As flow within the tundish is symmetrical, only one half of it was considered for the PIV studies. Before the start of gas injection into the shroud the velocity vectors near the shroud were pointing towards the shroud as shown in Figure 5.1.3.2. As a result the fluid in the tundish dragged the slag along with it in the same direction and covered itself around the shroud with no exposed eye. As soon as gas bubbling was started, it can be seen in Figure 5.1.3.3 that the reverse flows were formed in the regions adjacent to the shroud and thus the slag moved away from the shroud, creating the exposed eye. With increase in the amount of air flow rate, the reversed flows became even stronger, and so the area of the exposed eye kept on increasing.

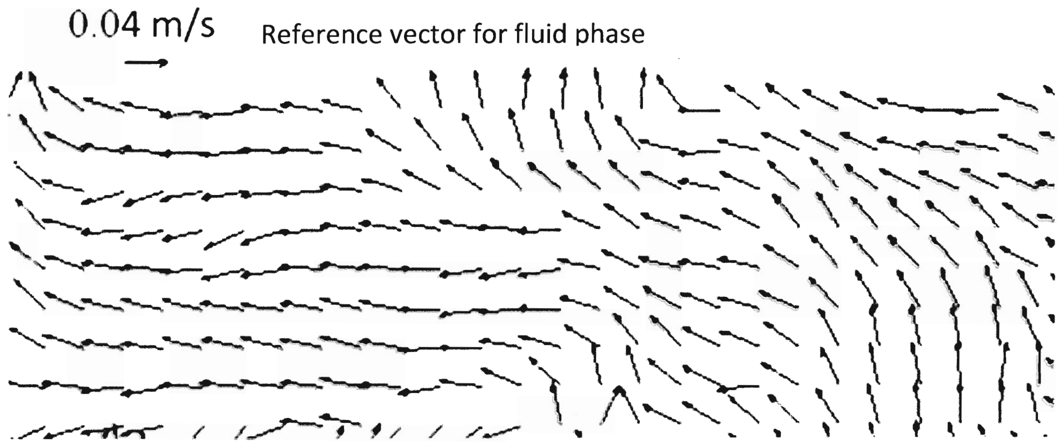

Figure 5.1.3.2 flow field before the start of gas injection

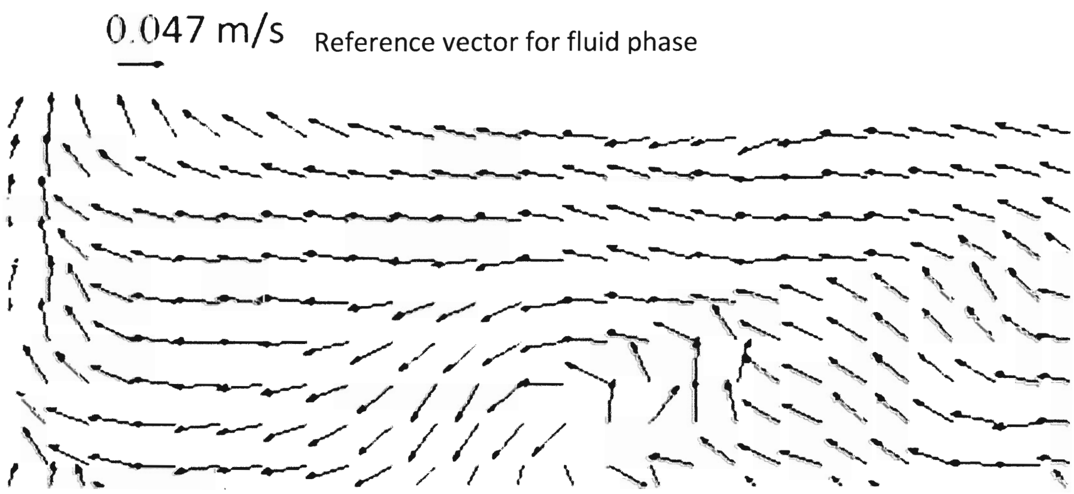

Figure 5.1.3.3 (a) flow field at volumetric gas flow/water flow ratio of 2%

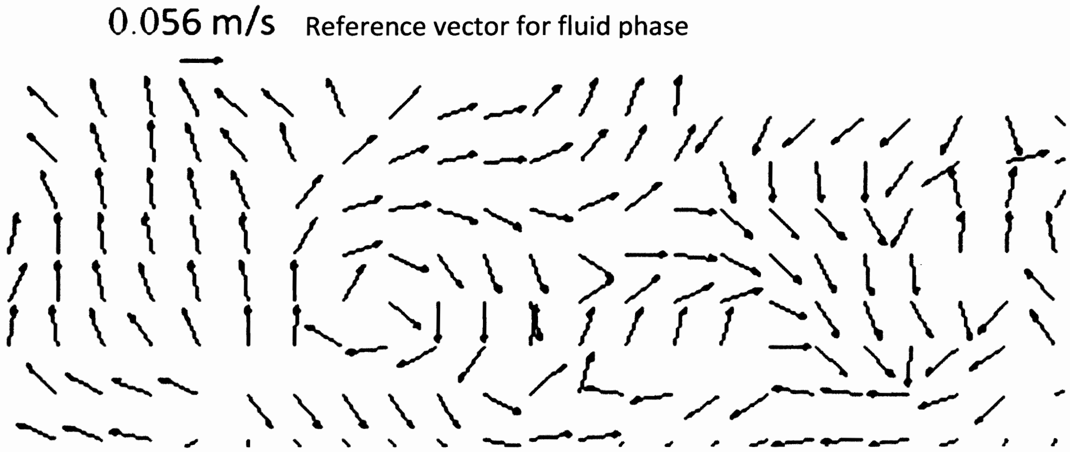

Figure 5.1.3.3 (b) flow field at volumetric gas flow/water flow ratio of 4%

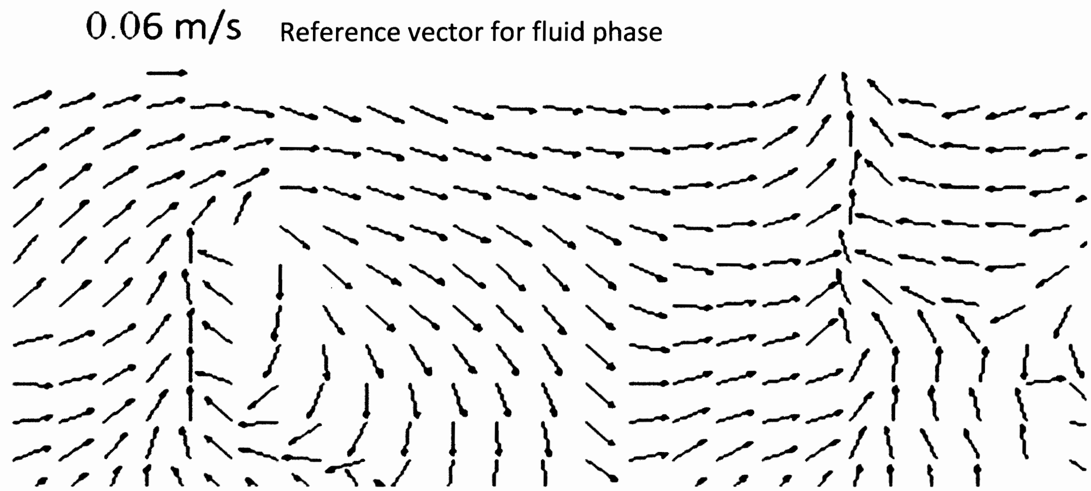

Figure 5.1.3.3 (c) flow field at volumetric gas flow/water flow ratio of 6%

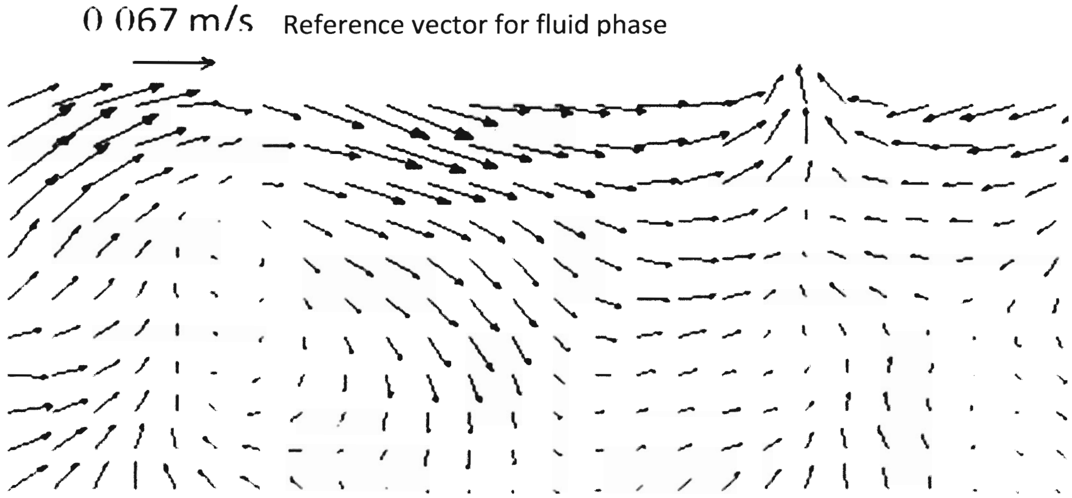

Figure 5.1.3.3 (d) flow field at volumetric gas flow/water flow ratio of 10%

5.1.4 Tracer Injection

Tracer injection studies were done to see the type of fluid motion and mixing behaviour inside the tundish. A red coloured, water soluble, dye (based on food colours) was used as the tracer. The mixing of the tracer in water was recorded at different instants of time. Figures 5.1.4.1 to 5.1.4.3 show the mixing behaviour of the tracer with time under different amounts of gas injection. As the flow in the tundish is symmetrical, only one half of the tundish was considered for monitoring the tracer mixing. From Figure 5.1.4.1 it is clear that the total time for complete mixing of the tracer in the tundish is ~140 seconds. Time for complete mixing was estimated by observing the colour of the fluid within the tundish. When the colour of the fluid in the whole tundish was uniformly red, it was concluded that complete mixing had taken place. Mixing in the first 20 seconds was very rapid and this is evident from Figures 5.1.4.1(a) and 5.1.4.1(b). Then the mixing slowed down and this is probably due to presence of dead volumes within the tundish, as seen in Figures 5.1.4.1(d) to 5.1.4.1(f).

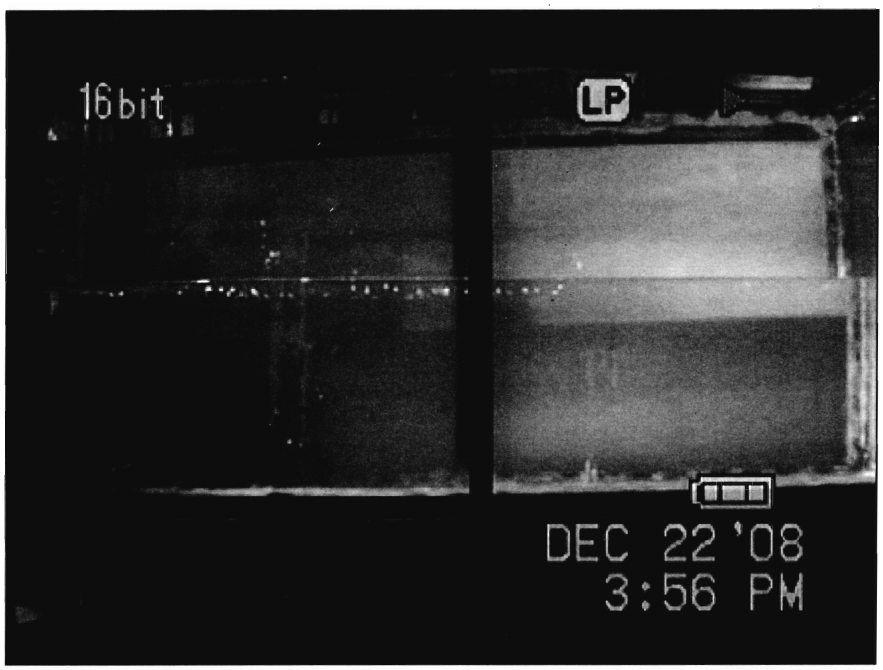

Figure 5.1.4.1(a) tracer injection at 0% shroud gas at time=0sec

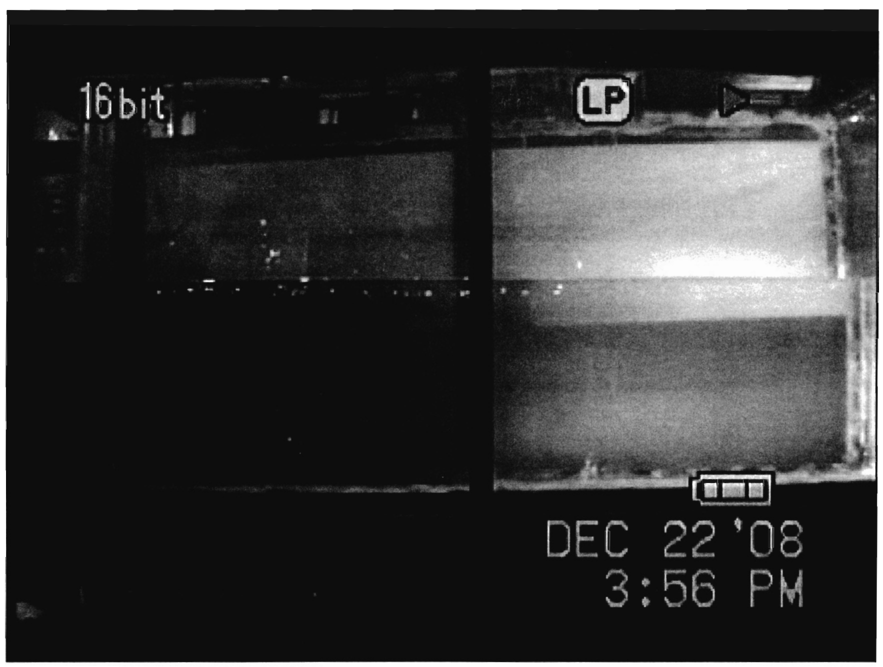

Figure 5.1.4.1(b) tracer injection at 0% shroud gas at time=20sec

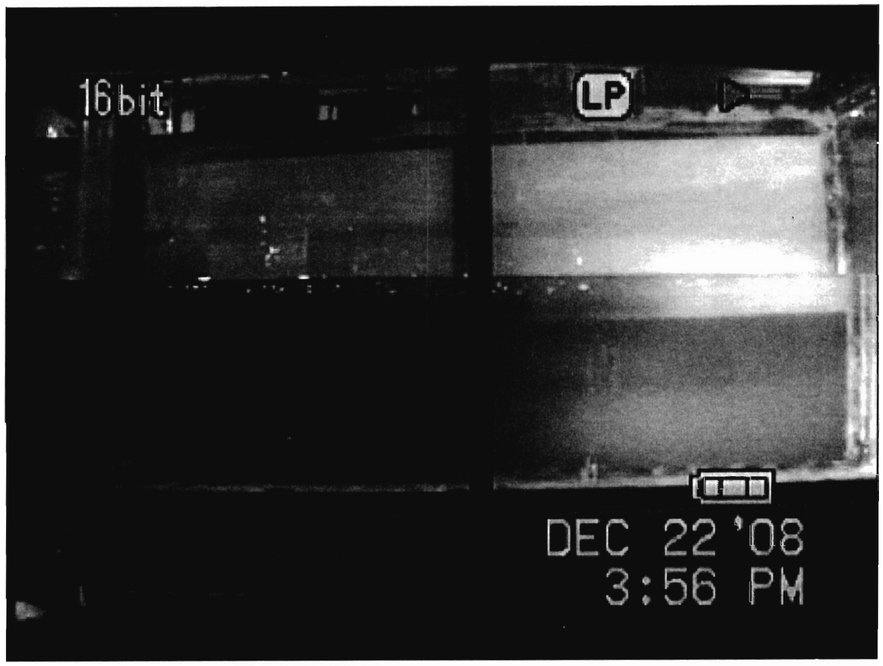

Figure 5.1.4.1(c) tracer injection at 0% shroud gas at time= 40sec

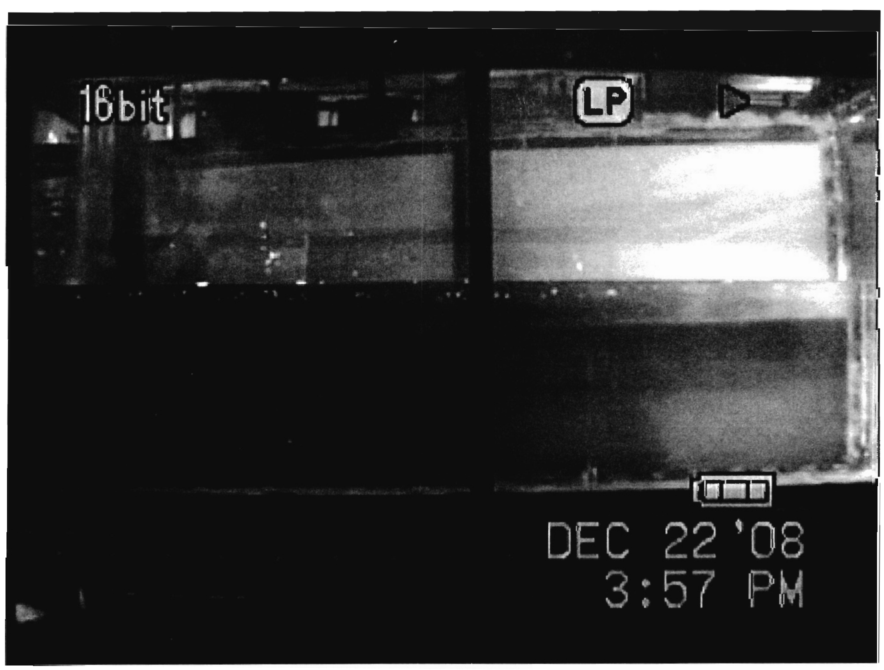

Figure 5.1.4.1(d) tracer injection at 0% shroud gas at time= 60sec

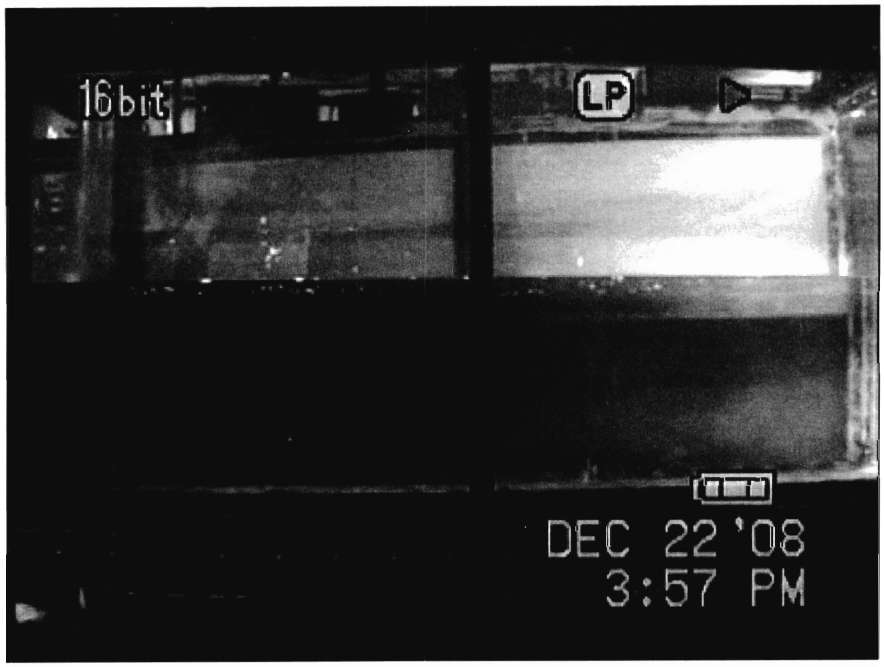

Figure 5.1.4.1(e) tracer injection at 0% shroud gas at time= 80sec

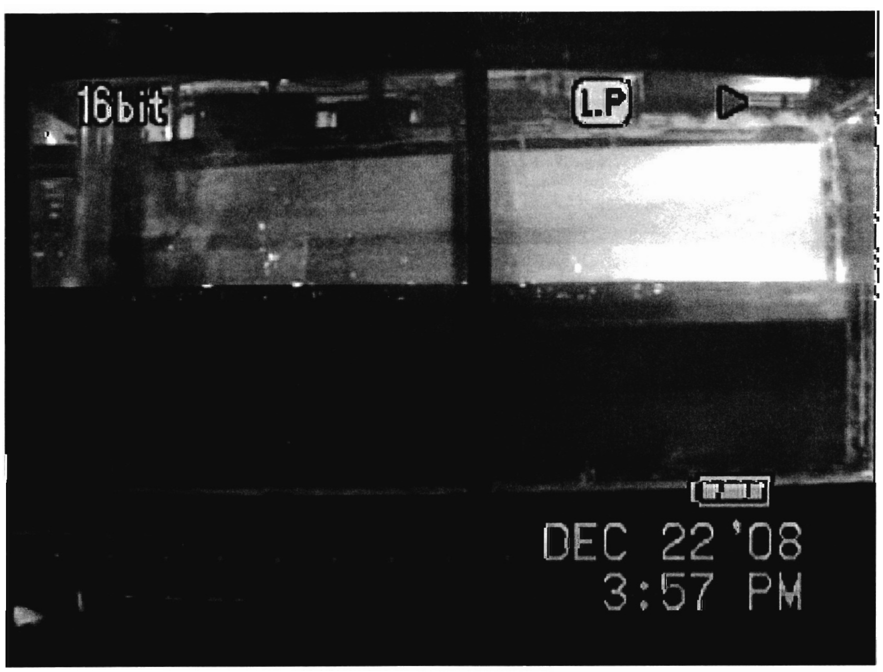

Figure 5.1.4.1(f) tracer injection at 0% shroud gas at time= 100sec

Figure 5.1.4.1(g) tracer injection at 0% shroud gas at time= 120sec

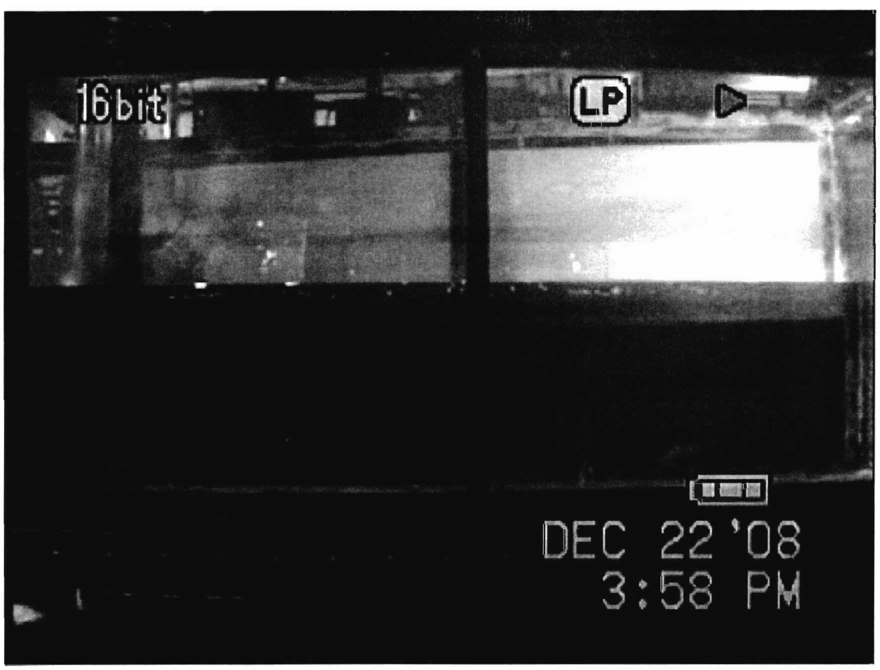

Figure 5.1.4.1(h) tracer injection at 0% shroud gas at time= 140sec

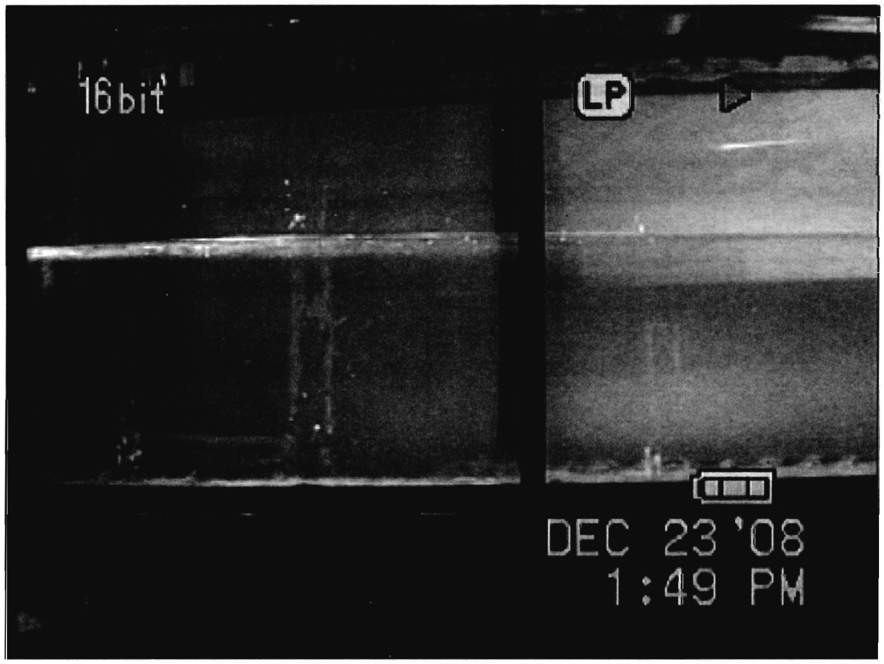

Figure 5.1.4.2(a) tracer injection at 2% shroud gas at time= 0sec

Figure 5.1.4.2(b) tracer injection at 2% shroud gas at time= 20sec

Figure 5.1.4.2(c) tracer injection at 2% shroud gas at time= 40sec

Figure 5.1.4.2(d) tracer injection at 2% shroud gas at time= 60sec

Figure 5.1.4.2(e) tracer injection at 2% shroud gas at time= 80sec

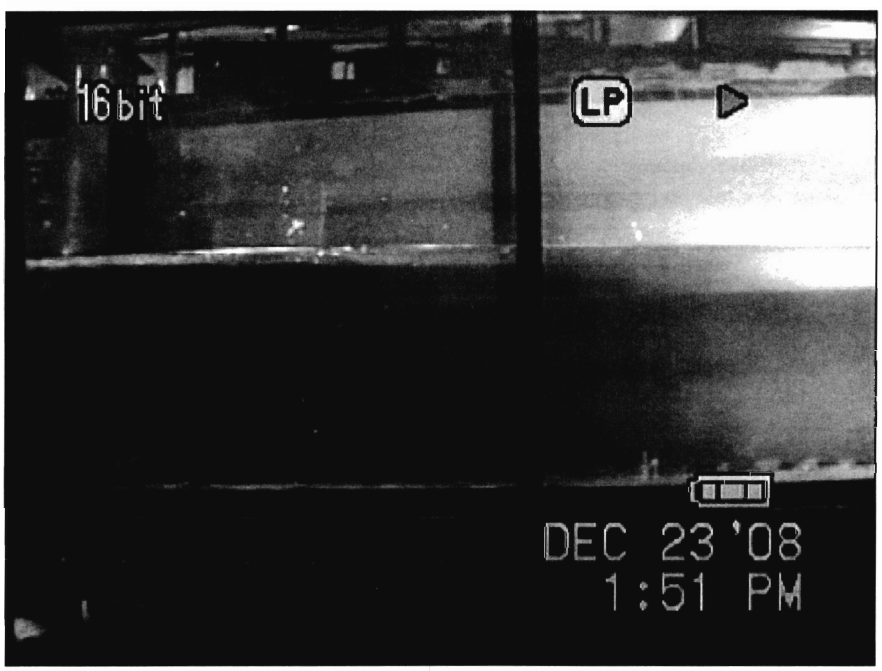

Figure 5.1.4.2(f) tracer injection at 2% shroud gas at time= 100sec

Figure 5.1.4.2(g) tracer injection at 2% shroud gas at time= 120sec

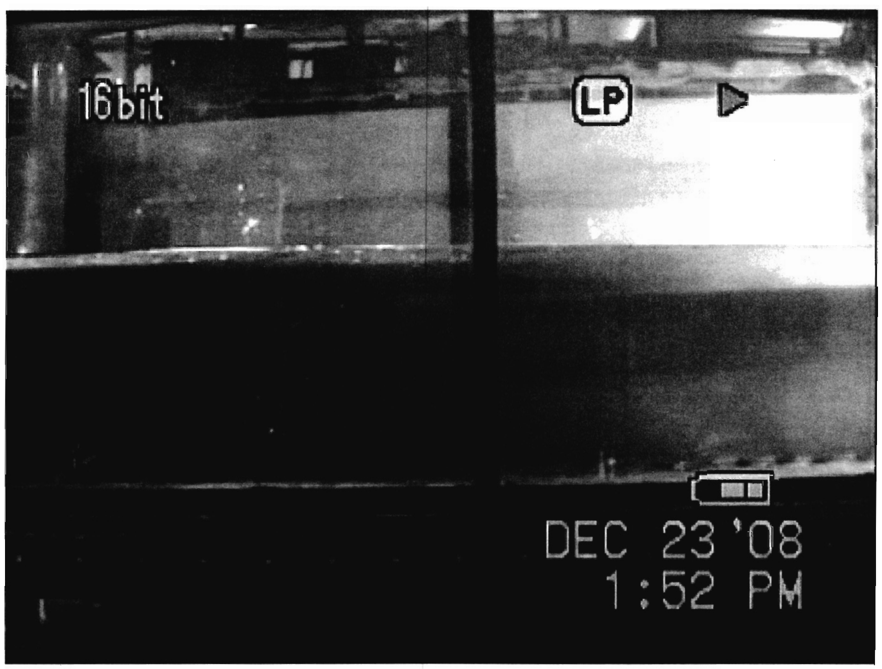

Figure 5.1.4.2(h) tracer injection at 2% shroud gas at time= 140sec

Figure 5.1.4.2(i) tracer injection at 2% shroud gas at time= 160sec

Figure 5.1.4.2(j) tracer injection at 2% shroud gas at time= 180sec

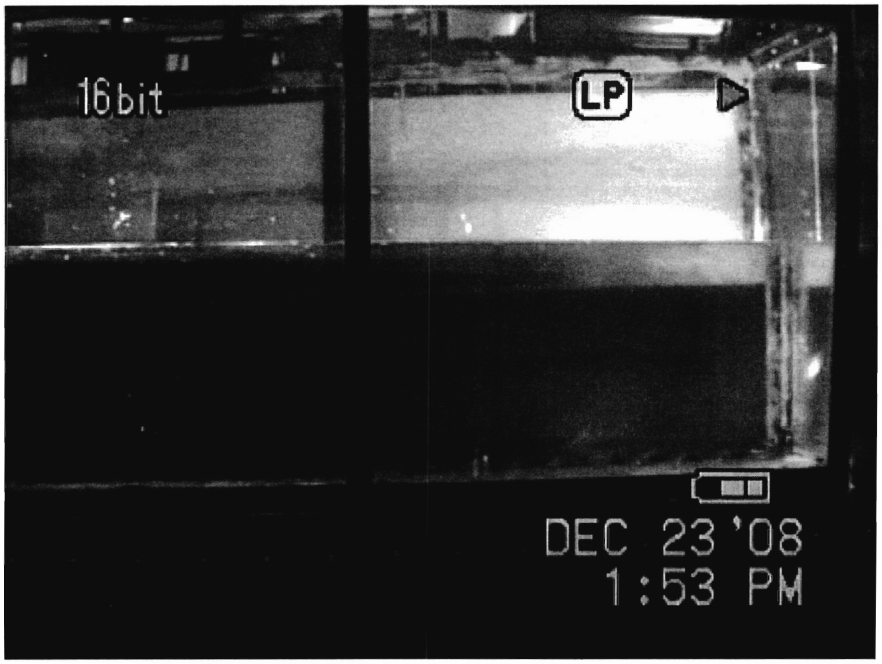

Figure 5.1.4.2(k) tracer injection at 2% shroud gas at time= 200sec

Figure 5.1.4.2(l) tracer injection at 2% shroud gas at time= 220sec

Figure 5.1.4.2(m) tracer injection at 2% shroud gas at time= 240sec

Figure 5.1.4.2(n) tracer injection at 2% shroud gas at time= 260sec

Figure 5.1.4.3(a) tracer injection at 6% shroud gas at time= 0sec

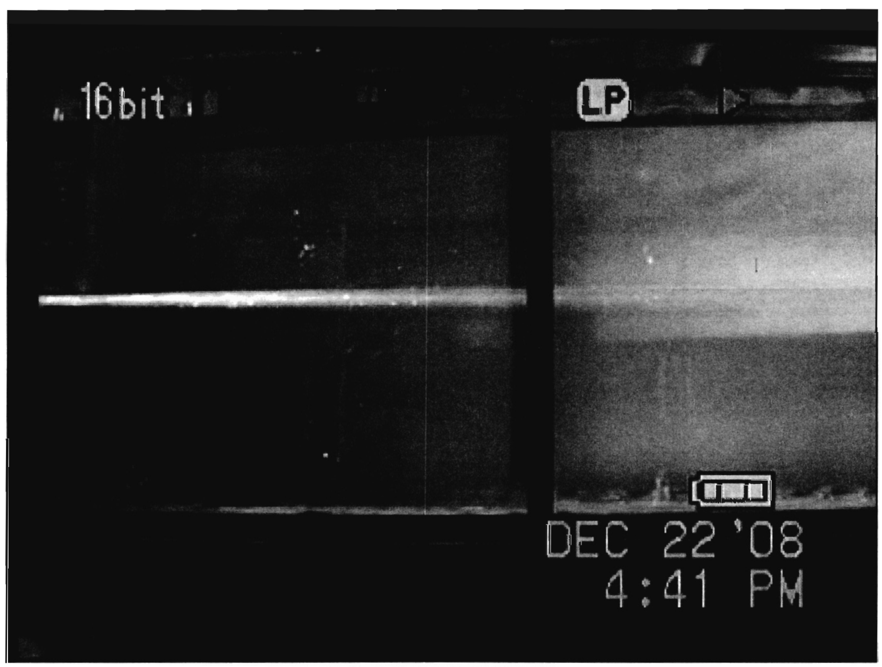

Figure 5.1.4.3(b) tracer injection at 6% shroud gas at time= 20sec

Figure 5.1.4.3(c) tracer injection at 6% shroud gas at time= 40sec

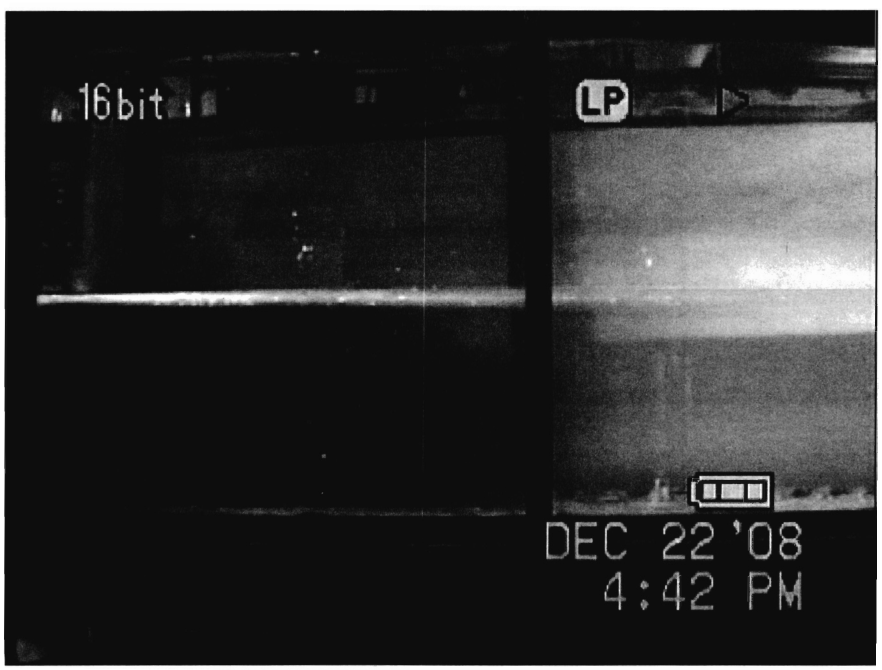

Figure 5.1.4.3(d) tracer injection at 6% shroud gas at time= 60sec

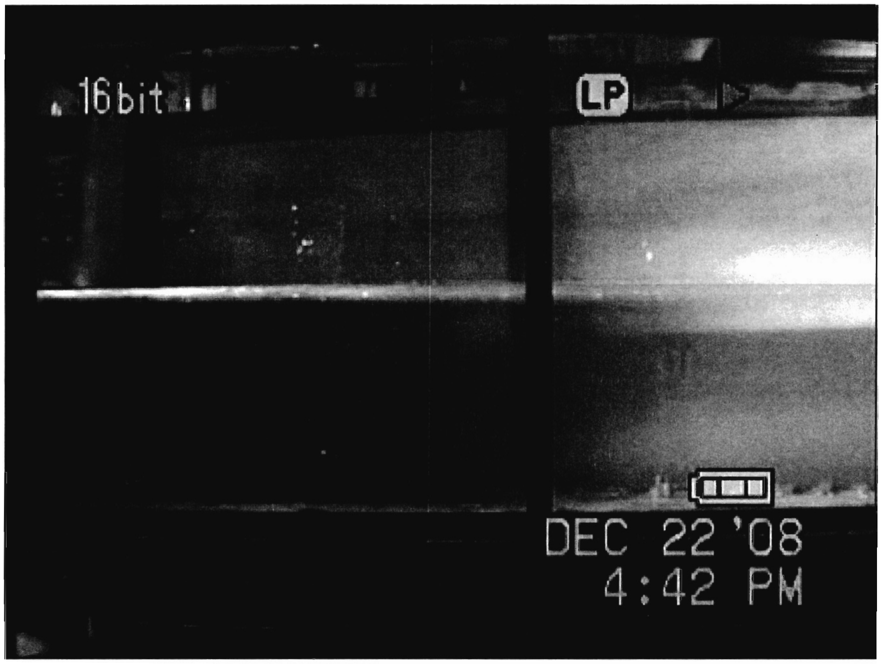

Figure 5.1.4.3(e) tracer injection at 6% shroud gas at time= 80sec

Figure 5.1.4.3(f) tracer injection at 6% shroud gas at time= 100sec

Figure 5.1.4.3(g) tracer injection at 6% shroud gas at time= 120sec

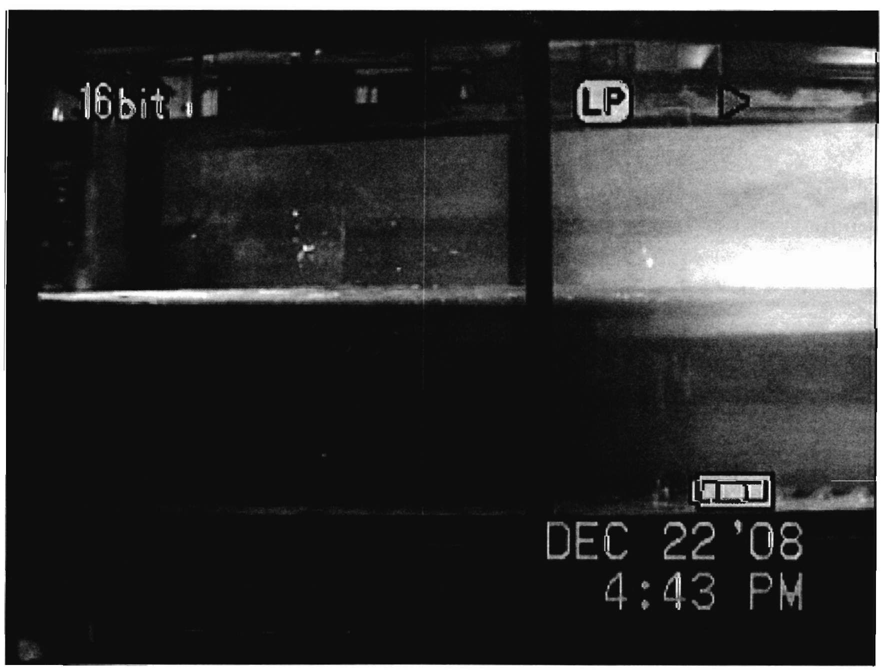

Figure 5.1.4.3(h) tracer injection at 6% shroud gas at time= 140sec

Figure 5.1.4.3(i) tracer injection at 6% shroud gas at time= 160sec

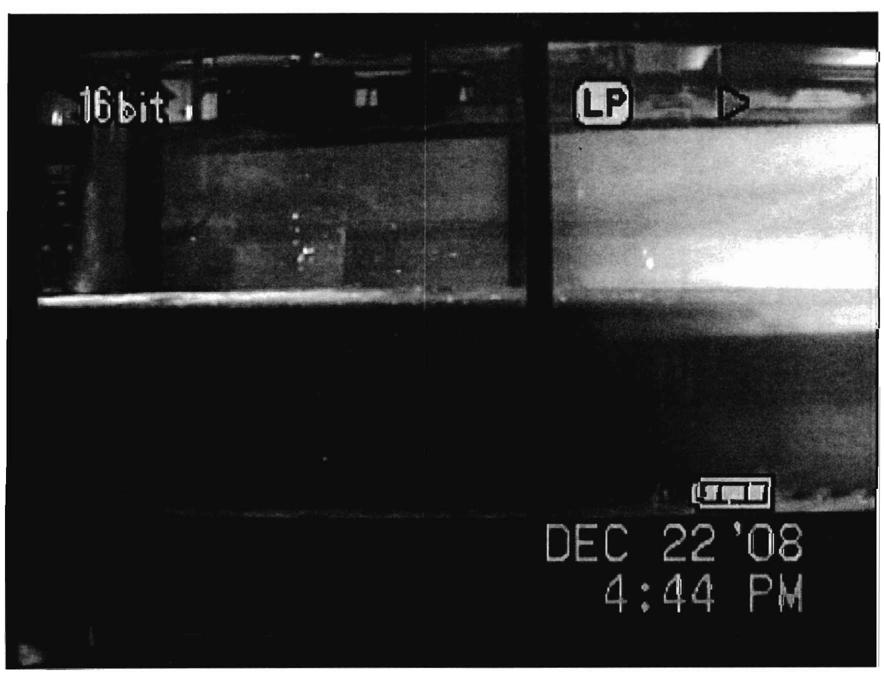

Figure 5.1.4.3(j) tracer injection at 6% shroud gas at time= 180sec

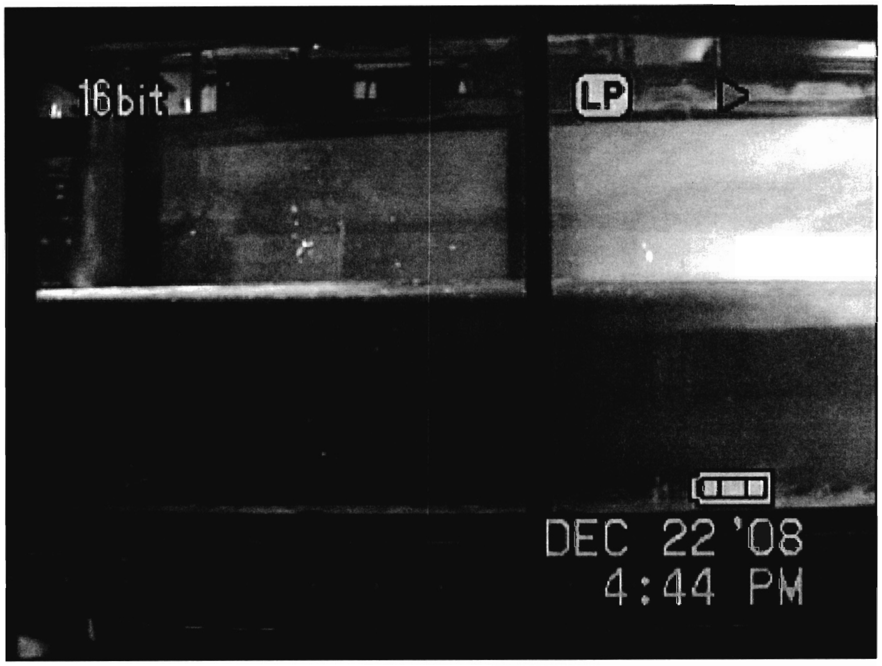

Figure 5.1.4.3(k) tracer injection at 6% shroud gas at time= 200sec

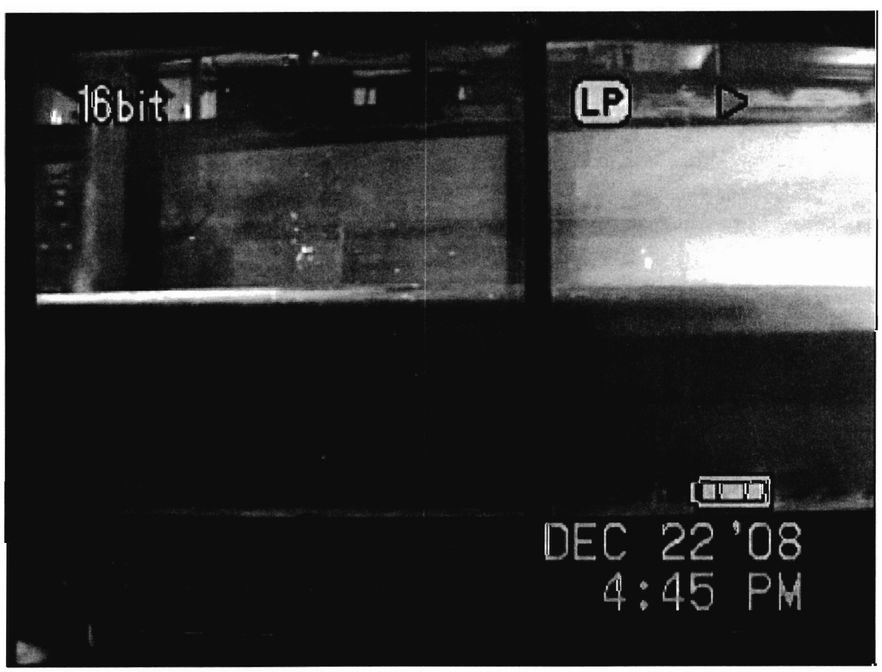

Figure 5.1.4.3(l) tracer injection at 6% shroud gas at time= 220sec

Figure 5.1.4.3(m) tracer injection at 6% shroud gas at time= 240sec

Figure 5.1.4.3(n) tracer injection at 6% shroud gas at time= 260sec

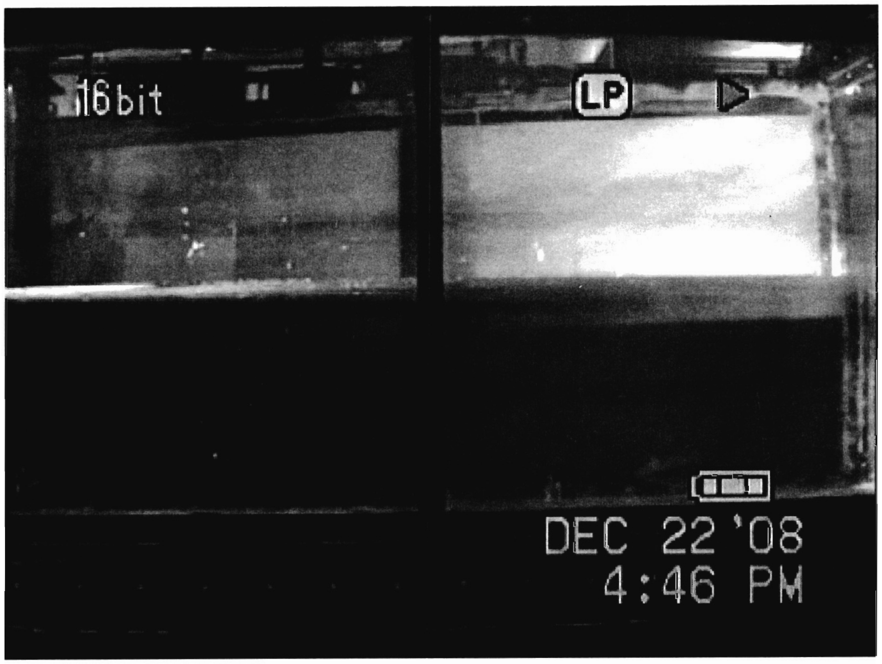

Figure 5.1.4.3(o) tracer injection at 6% shroud gas at time= 280sec

Figure 5.1.4.3(p) tracer injection at 6% shroud gas at time= 300sec

From Figures 5.1.4.2 and 5.1.4.3 it is clear that due to inert gas shrouding, the time for complete mixing of the tracer was significantly increased. For

2% gas injections, the time for complete mixing was 260 seconds and for 6% gas injections it was 300 seconds. Without any gas shrouding the time of mixing was only 140 seconds. Also if Figures 5.1.4.1, 5.1.4.2, and 5.1.4.3 are closely examined, it can be seen that in Figure 5.1.4.1(0% shroud gas), the mixing in the first 20 seconds is greater, as compared to Figures 5.1.4.2 (2% shroud gas), and 5.1.4.3 (6% shroud gas). The probable reason for this may be that the rising gas bubbles in the entry region prevent the tracer from moving in the forward direction and rather tries to arrest it in the bubbly zone. Thus, the mixing of the tracer in the tundish becomes slower with gas shrouding as compared to no gas injection. Also, the presence of dead volume towards the end of the tundish is evident from Figures 5.1.4.2(h to n) and 5.1.4.3 (j to p).

From the above discussions, it is believed that the injection of gas through the shroud perhaps increases the residence time of the tundish, but confirmatory tests should be done before reaching a final conclusion. The effect of inert gas shrouding on residence time of the tundish would be an interesting area of research and that is one of the next steps proposed for future work.

5.2 Results of mathematical modelling

This section provides results and discussion of the mathematical modelling of inert gas shrouding process. This section has also been divided into four sub- sections.

5.2.1 Bubble trajectories

From the 2D numerical model the bubble trajectories under transient conditions could be predicted quite efficiently. They are shown in Figure 5.2.1.1. It is clearly seen that the numerical predictions are in very good agreement with the physical experiments (Figure 5.1.1.2) .In Figures 5.2.1.1(a) and 5.2.1.1(b) i.e. at lower air flow rates the bubble plumes are more spread as compared to those in Figures 5.2.1.1(c) and 5.2.1.1(d).

Here also the bubbles first travel down the shroud up to the bottom of the tundish along with the down flowing liquid and then due to their high buoyancy rise straight back up to the free surface of the liquid in the tundish.

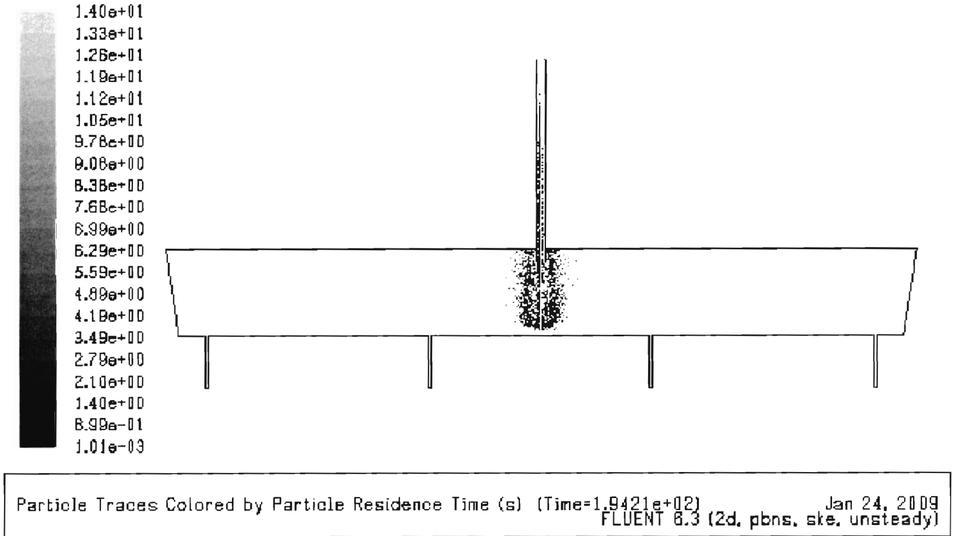

5.2.1.1(a) bubble trajectories at volumetric gas flow /water flow rate ratios of 2%

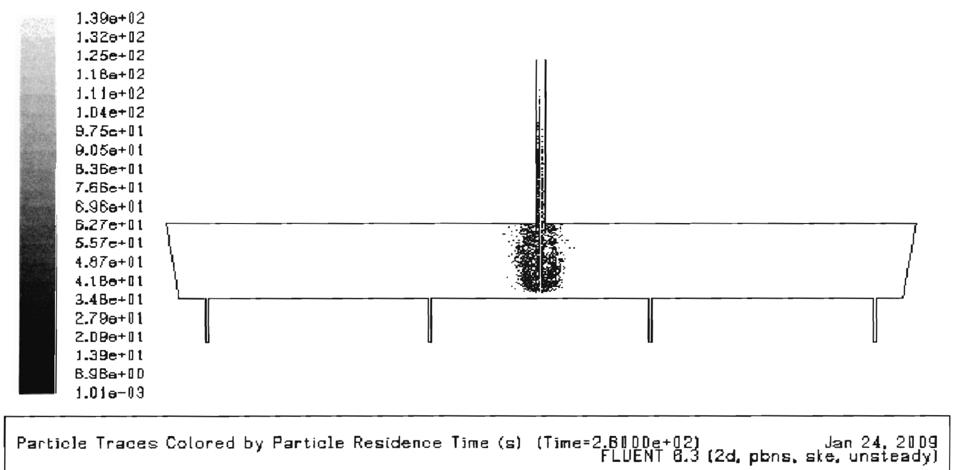

5.2.1.1(b) bubble trajectories at volumetric gas flow /water flow rate ratios of 4%

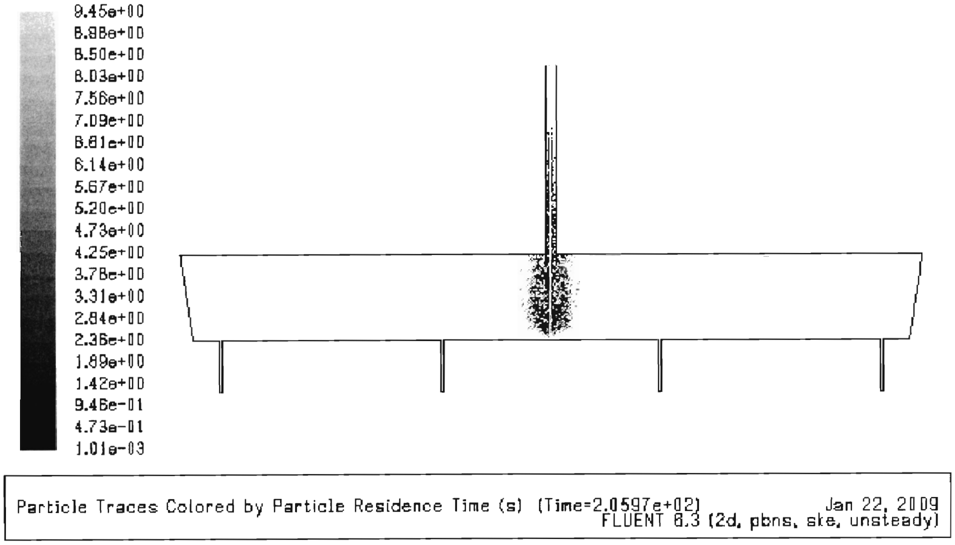

5.2.1.1(c) bubble trajectories at volumetric gas flow /water flow rate ratios of 6%

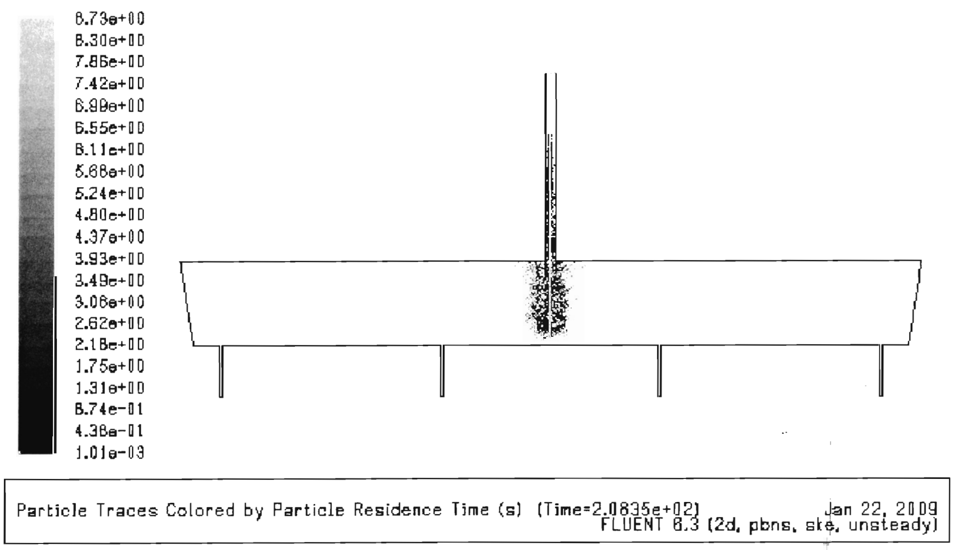

5.2.1.1(d) bubble trajectories at volumetric gas flow /water flow rate ratios of 10%

5.2.2 Flow fields and slag behaviour

The type of slag behaviour experienced in the physical model experiments can be clearly explained from the flow fields predicted by the 2D numerical model. Without any gas injection the flow field under transient conditions is as represented in Figure 5.2.2.1.

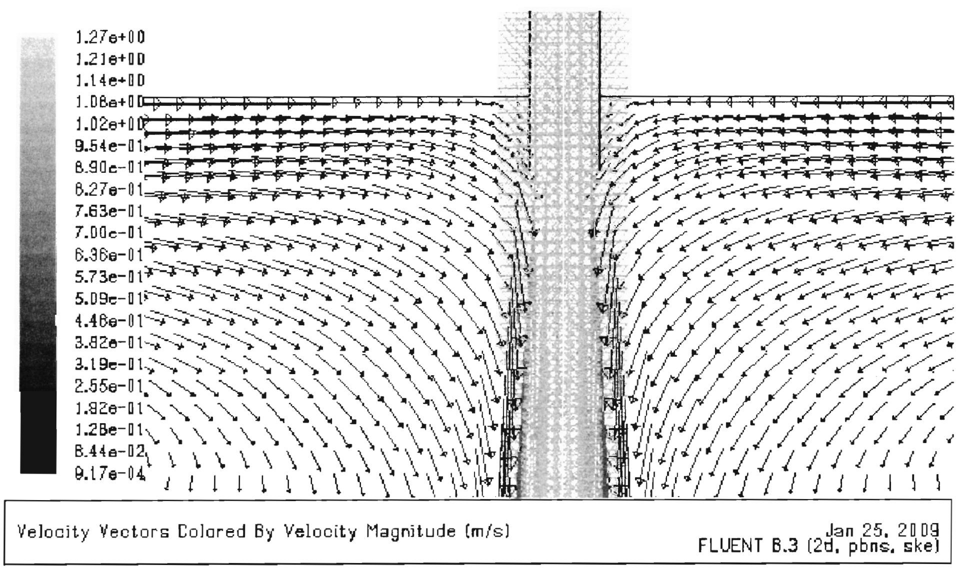

Figure 5.2.2.1 numerically predicted flow field without any shroud gas injection

The velocity vectors predicted under transient conditions coupled with gas injection are shown in Figure 5.2.2.2 (a to d). The rising gas bubbles caused these reversed flows and they become stronger at higher gas flow rates. As a result, the fluid in the tundish drags the slag away from the shroud and creates the exposed eye. Similar results are obtained in the water model PIV experiments.

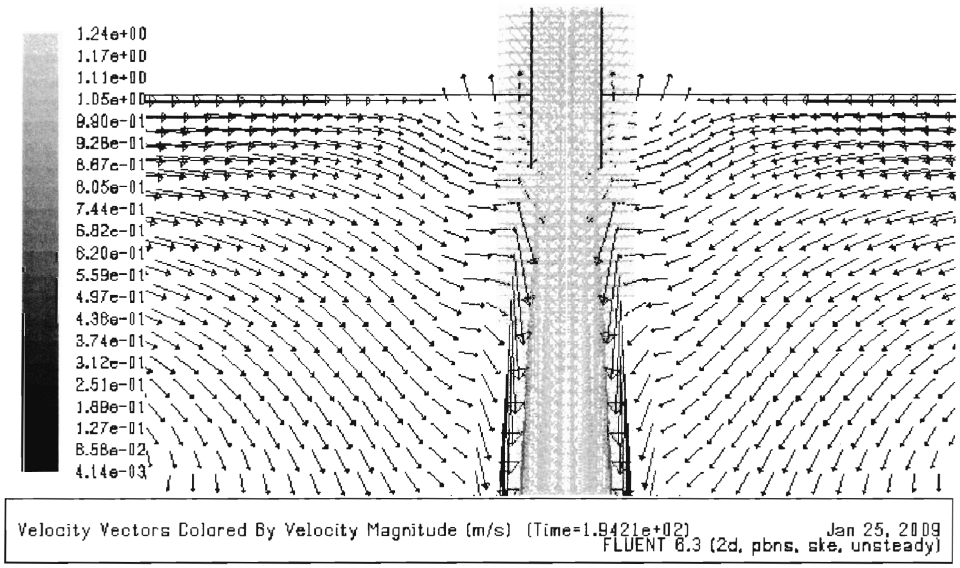

Figure 5.2.2.2(a) predicted flow field at gas flow /water flow rate ratios of 2%

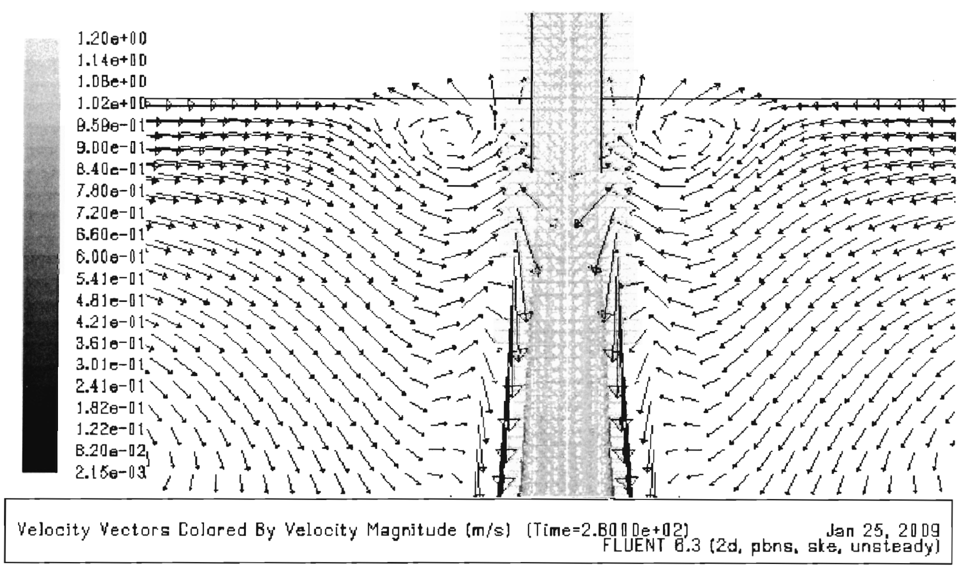

Figure 5.2.2.2(b) predicted flow field at gas flow /water flow rate ratios of 4%

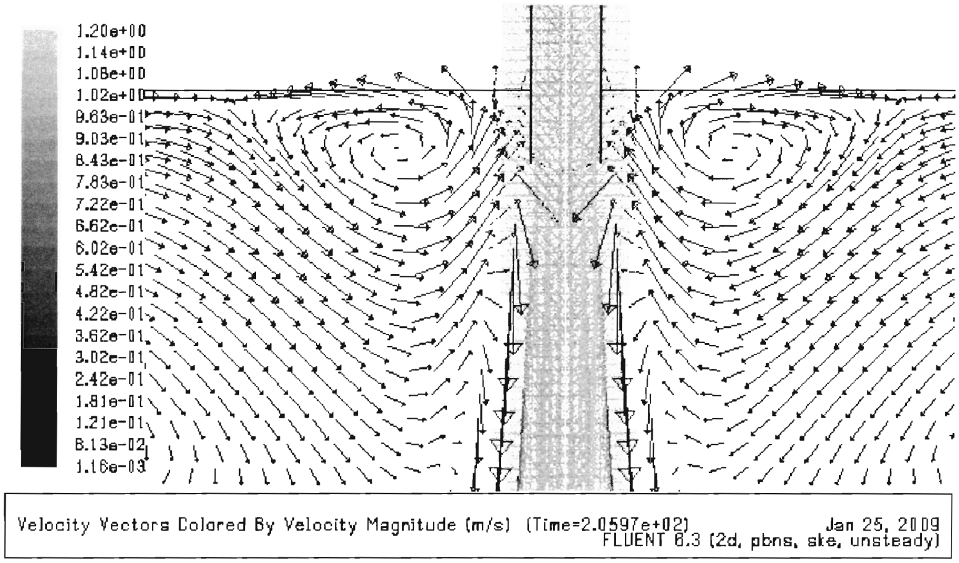

Figure 5.2.2.2(c) predicted flow field at gas flow /water flow rate ratios of 6%

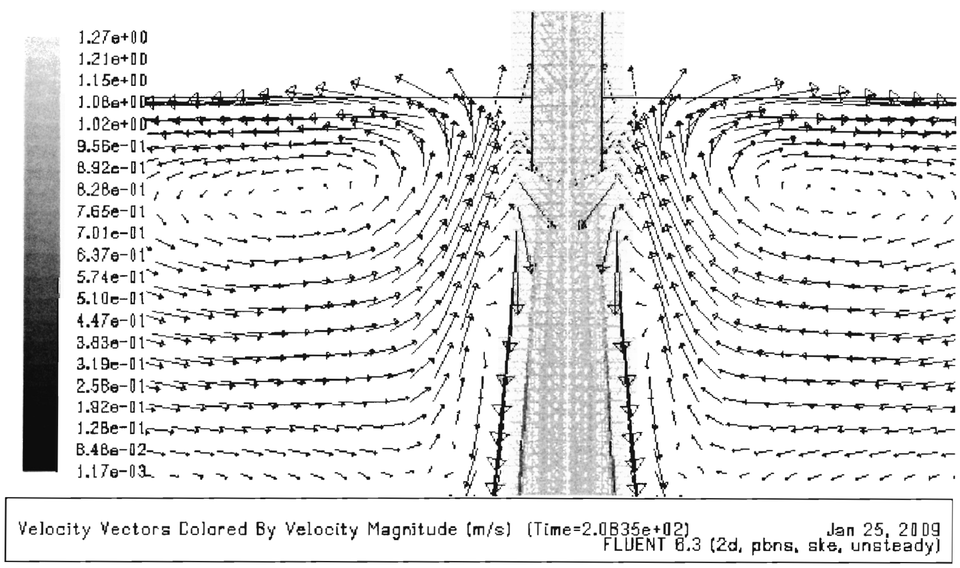

Figure 5.2.2.2(d) predicted flow field at gas flow /water flow rate ratios of 10%

However, the slight difference seen in actual and predicted flow patterns may be due to the fact that our numerical model is two dimensional where as the physical model is three dimensional. The plane of the laser light sheet could not be placed just beside the shroud because of physical obstructions and the delta shape of the full scale tundish. Also, in the two dimensional numerical model it is assumed that the ladle shroud and the outlets are in the same plane, which was not true in the physical model. But the velocity magnitudes obtained from the numerical model and PIV are almost similar, apart from minor differences. In both cases, the magnitude of the velocity vectors around the shroud is very low, in the range of 10^{-2} to 10^{-3} m s^{-1}. Therefore, we can conclude the model is validated with experimental results and the methodology involved in the development of the numerical model is correct. For future work, some modifications in mesh size and input parameters can be done to fine tune the model. Also, the development of a similar 3D model will be more accurate in predicting velocity fields. Another important thing to note is that a viscous layer of slag should be incorporated, in the model as a second phase, using multiphase modelling concepts. For this, the second phase (slag) should be tracked, to predict flow within the slag phase.

5.2.3 Turbulent Kinetic Energy (TKE) contours

TKE contours were generated for 2-10% gas injections in the shroud. These are shown in Figure 5.2.3.1. In the Figures, the more the colour is black the lesser is the TKE. Conversely, more the colour is white the greater is the TKE It is clearly seen that the as the amount of shroud gas is increased, the turbulent kinetic energy is dissipated more and more. This may be due to the fact that the rising gas bubbles take away the kinetic energy from the fluid and the bulk average TKE within the liquid is decreased with increasing amounts of shroud gas.

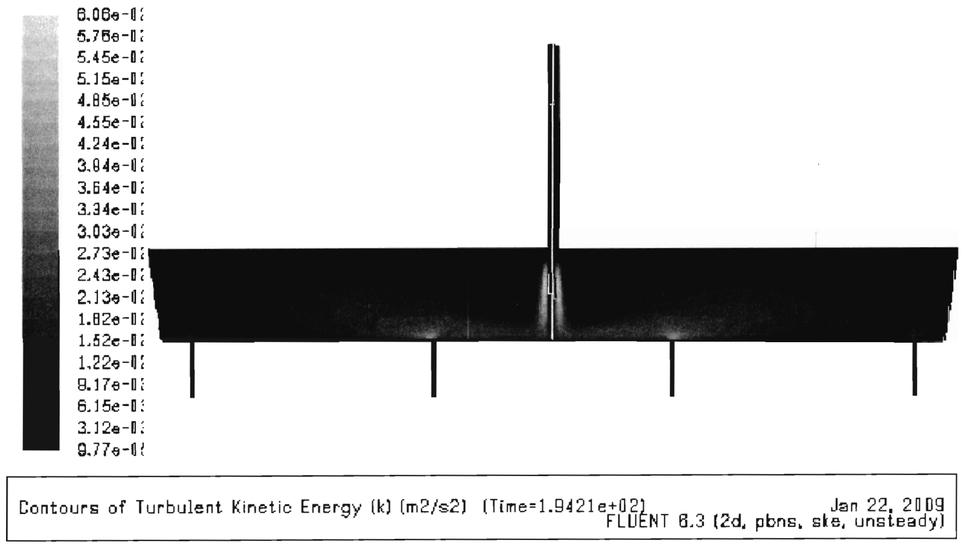

Figure 5.2.3.1 (a) contours of Turbulent Kinetic Energy (TKE) for gas flow/water flow ratios of 2%

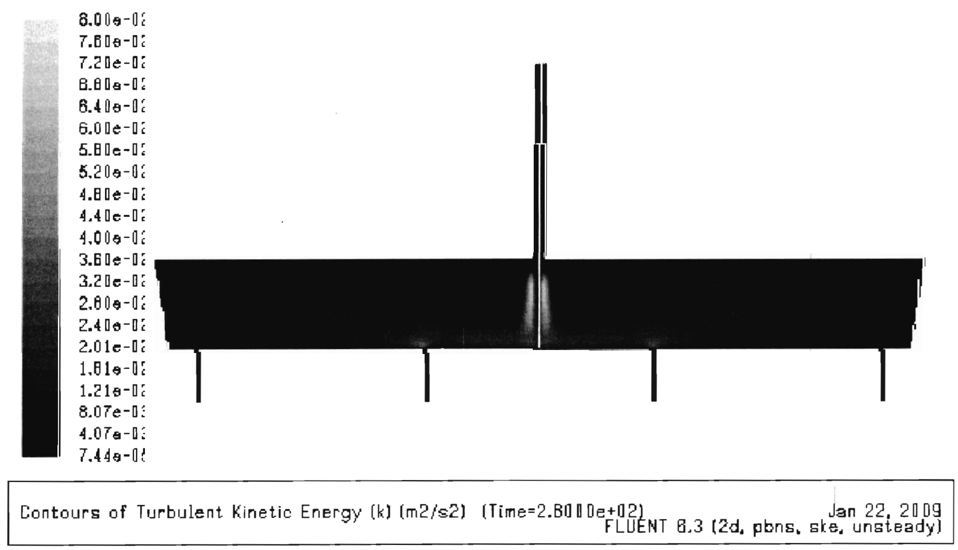

Figure 5.2.3.1 (b) contours of Turbulent Kinetic Energy (TKE) for gas flow/water flow ratios of 4%

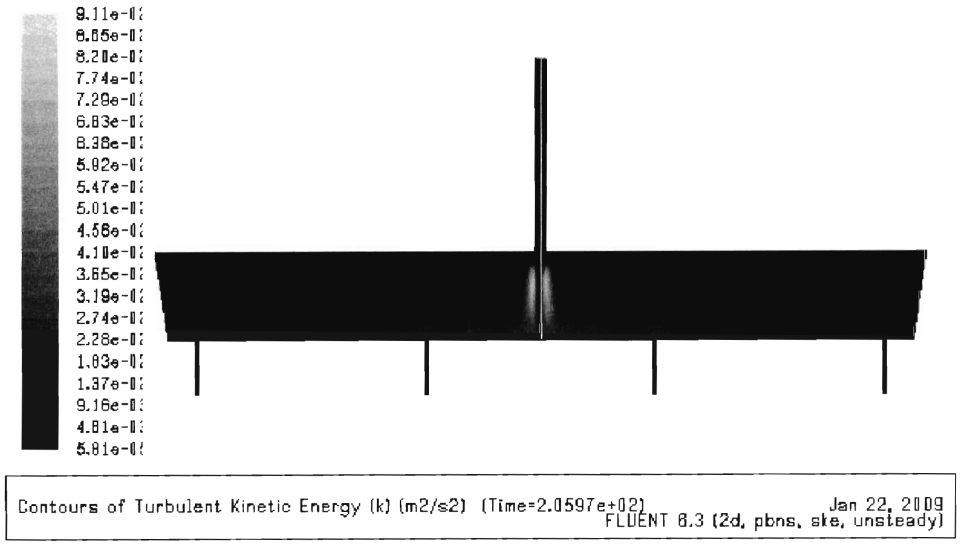

Figure 5.2.3.1 (c) contours of Turbulent Kinetic Energy (TKE) for gas flow/water flow ratios of 6%

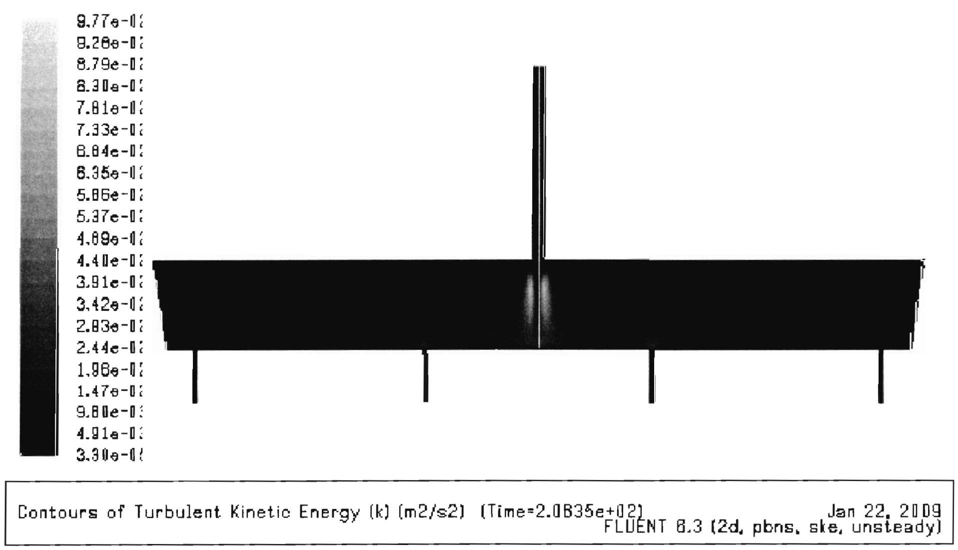

Figure 5.2.3.1 (d) contours of Turbulent Kinetic Energy (TKE) for gas flow/water flow ratios of 10%

5.2.4 Grid independency

After validation of our numerical model, the grid independency of our numerical model was checked. For all our previous simulations 3432 cells were generated in the whole calculation domain. Now, the grid size was reduced and 33305 cells were generated in the domain (Figure 5.2.4.1).

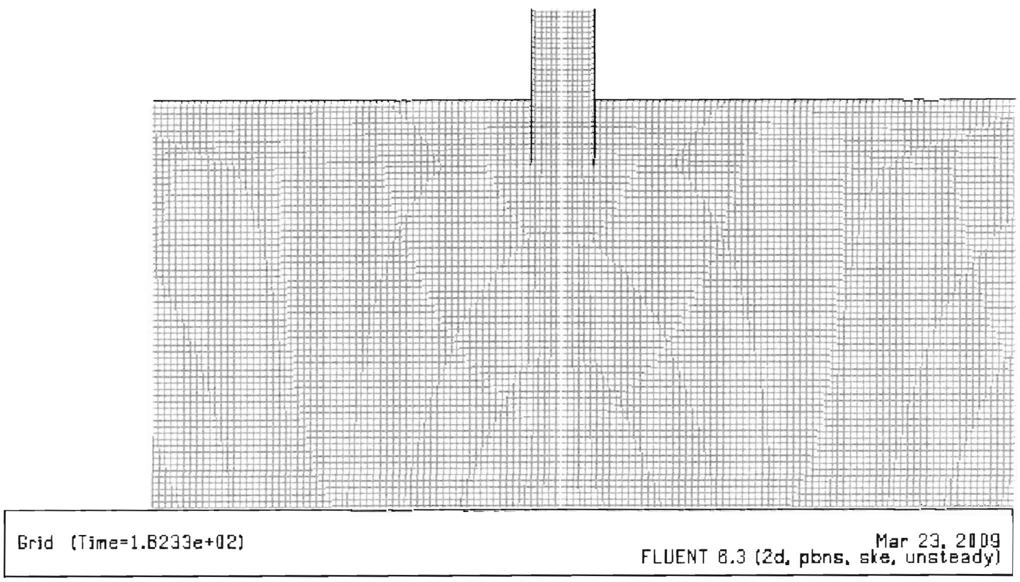

Figure 5.2.4.1 meshing of the tundish in GAMBIT with finer mesh (33305 cells) as compared to Figure 4.2.2 (3432 cells)

With finer grids we obtained similar flow fields to those computed previously (with 6% gas injection). This is shown in Figure 5.2.4.2. The grid size was then increased and only 979 cells were generated as shown in Figure 5.2.4.3. Now with these coarse grids, it was not possible to capture reversed flows generated by gas injection (Figure 5.2.4.4). Thus, it is clear that coarse grids are not suitable for capturing the effect of inert gas shrouding on flow fields within the tundish.

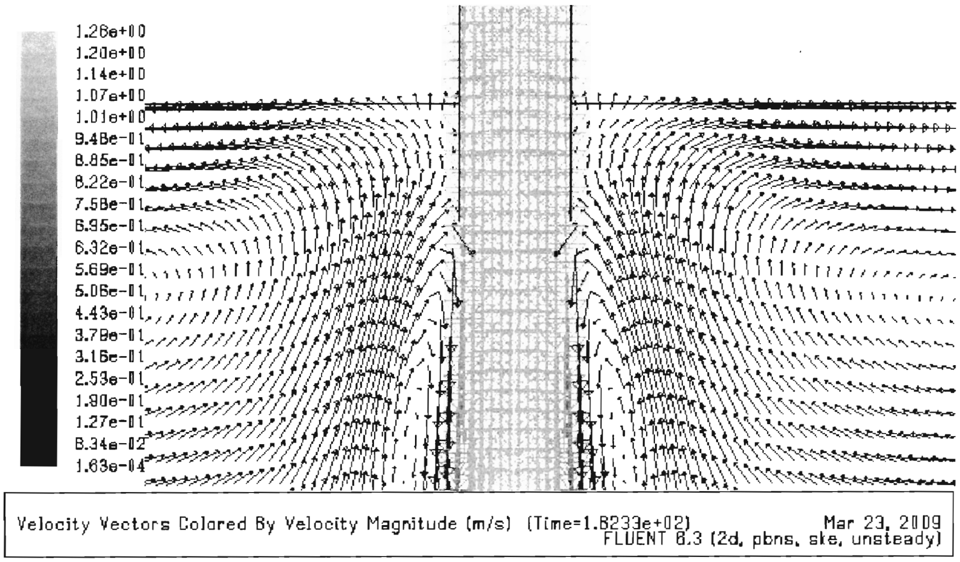

Figure 5.2.4.2 predicted velocity fields from the numerical model under transient conditions at gas flow /water flow rate ratio of 6% with finer mesh size

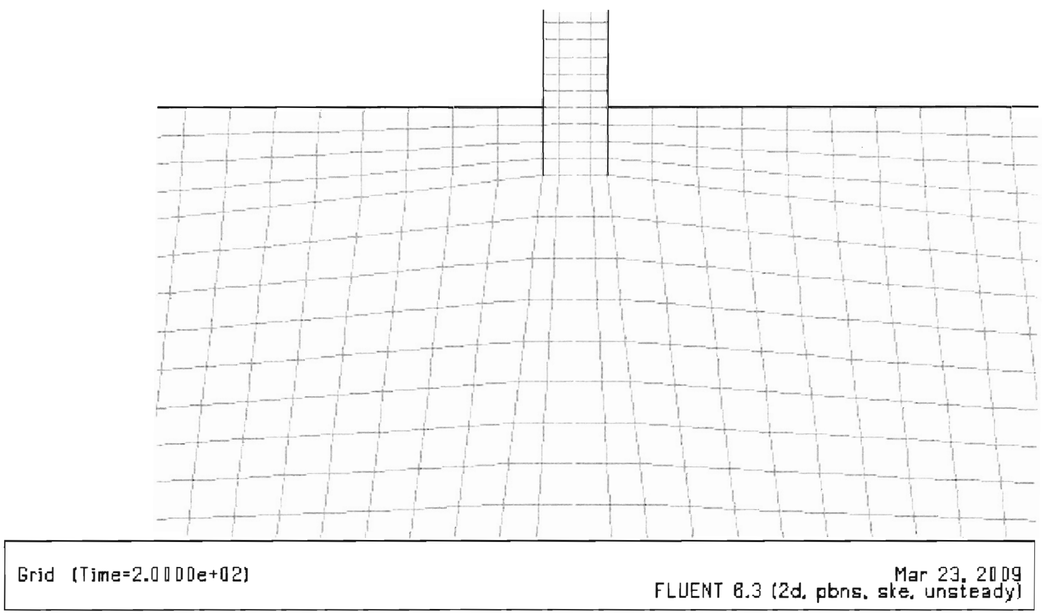

Figure 5.2.4.3 meshing of the tundish in GAMBIT with coarser mesh (979 cells) as compared to Figure 4.2.2 (3432 cells)

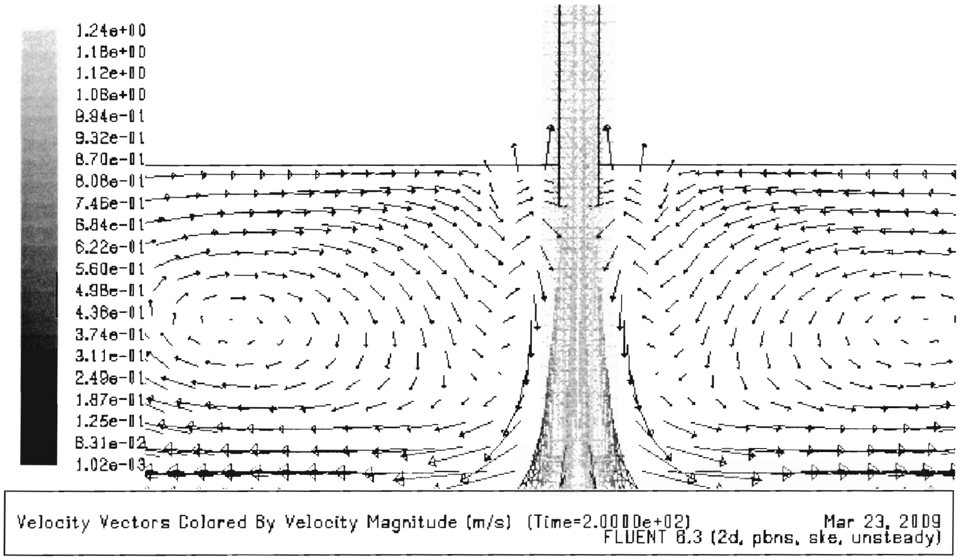

Figure 5.2.4.4 predicted velocity fields from the numerical model under transient conditions at gas flow /water flow rate ratio of 6% with coarser mesh size

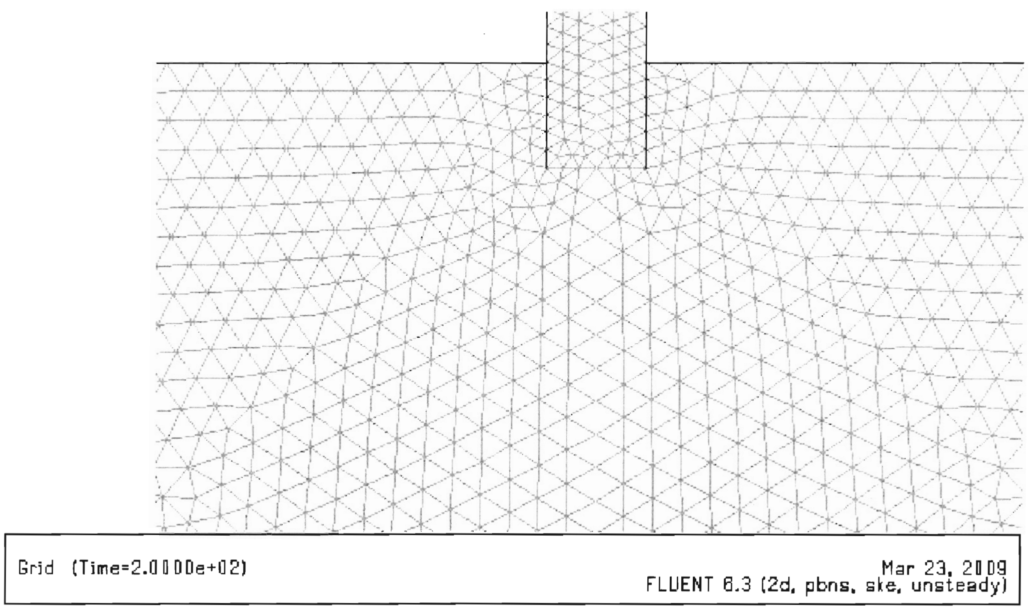

Figure 5.2.4.5 meshing of the tundish in GAMBIT with triangular grids (7160 cells)

Another interesting simulation was done by changing the grid shape. Previously a Quad type of mesh was used. Now it was changed into triangular type of mesh with 7160 cells (Figure 5.2.4.5). Here also the reversed flows were captured as shown in Figure 5.2.4.6, but certain irregularities were observed in the vector field.

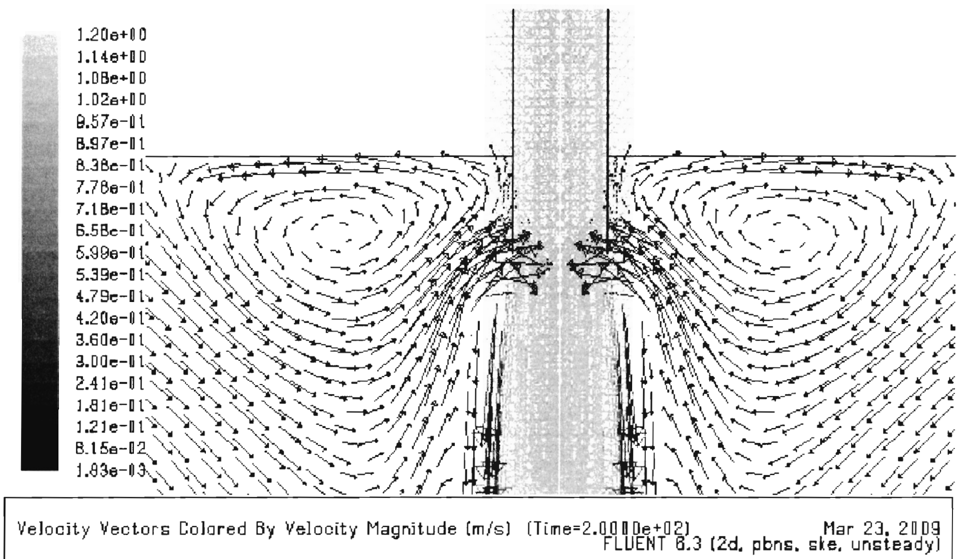

Figure 5.2.4.6 predicted velocity fields from the numerical model under transient conditions at gas flow /water flow rate ratio of 6% with triangular grids.

Thus, it can be seen quadrilateral type of mesh with a finer grid size would be the best for these types of simulations. They are effective in capturing reversed flows around the shroud and also in generating proper particle tracks for the discrete phase. Certainly physical models are indispensible for keeping CFD predictions well grounded.

5.3 Determination of critical bubble size

From the previous sections, it is clear that the numerical model predictions are in good agreement with physical experiment results. From our physical and mathematical studies it is clear that the bubbles generated so far are large and hence have significant buoyancy forces relative to inertial forces. So they rise straight up to the free surface of liquid in the tundish and form a column of rising gas bubbles and disrupt the protective slag layer. It was thought that with similar gas flow rates if micro-bubbles can be produced rather than macro-bubbles then it will be of additional advantage. It was thought that micro-bubbles, having less buoyancy force, would spread uniformly throughout the tundish and will help in removal of many of the fine inclusions(<40μm) and perhaps super clean steel can be produced. With this in mind, in the numerical model, the bubble size was reduced step by step and the predicted trajectories were monitored. As soon as it was seen that the bubbles spread throughout the whole of the tundish, it was concluded that the critical bubble size had been obtained for these specific flow parameters. From our numerical model, the critical bubble size was predicted to be 250 micro meters. The results are shown in Figures 5.3.1, 5.3.2 and 5.3.3. In Figure 5.3.3 it is seen that with micro bubbles of air at 6% of water entry flows, no reverse flows are formed, and no re-oxidation of steel is likely.. However, these are just numerical predictions, and the results should be verified by physical modelling experiments. Also it is required to devise a strategy to form argon micro bubbles in the real tundish with liquid steel in it. Thus, this is a exciting new area of research and will be one of the next for my Doctoral program.

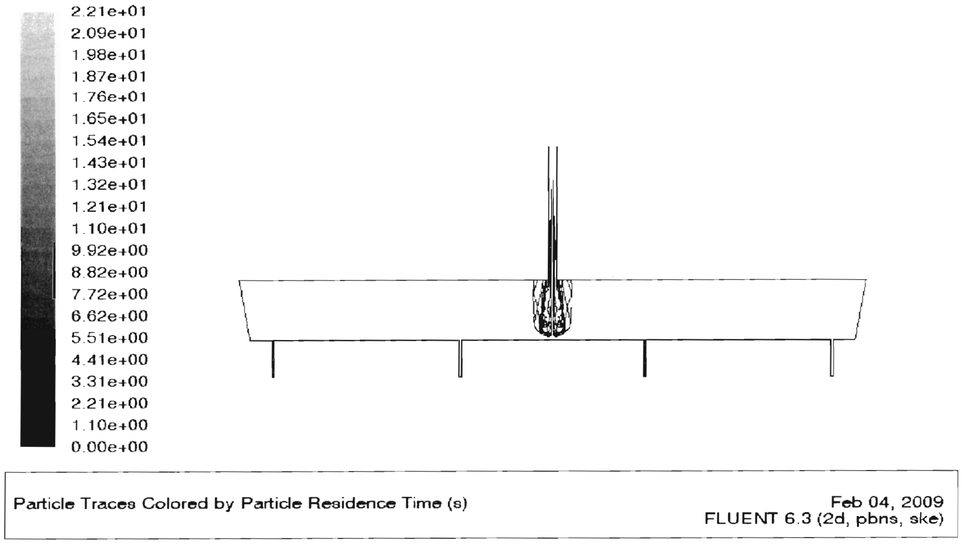

Figure 5.3.1(a) numerically predicted bubble tracks with bubble size of 5mm

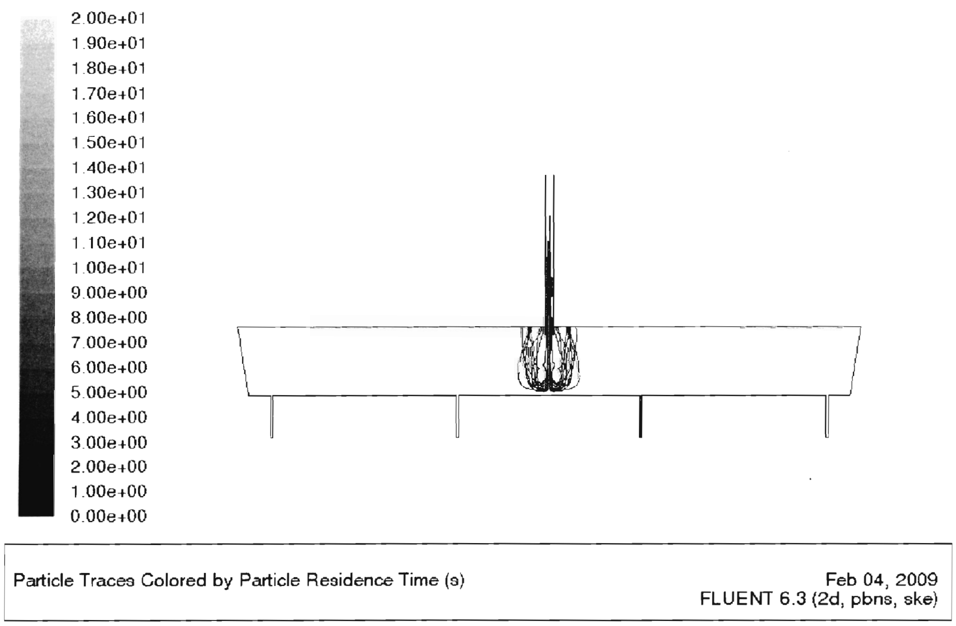

Figure 5.3.1(b) numerically predicted bubble tracks with bubble size of 3mm

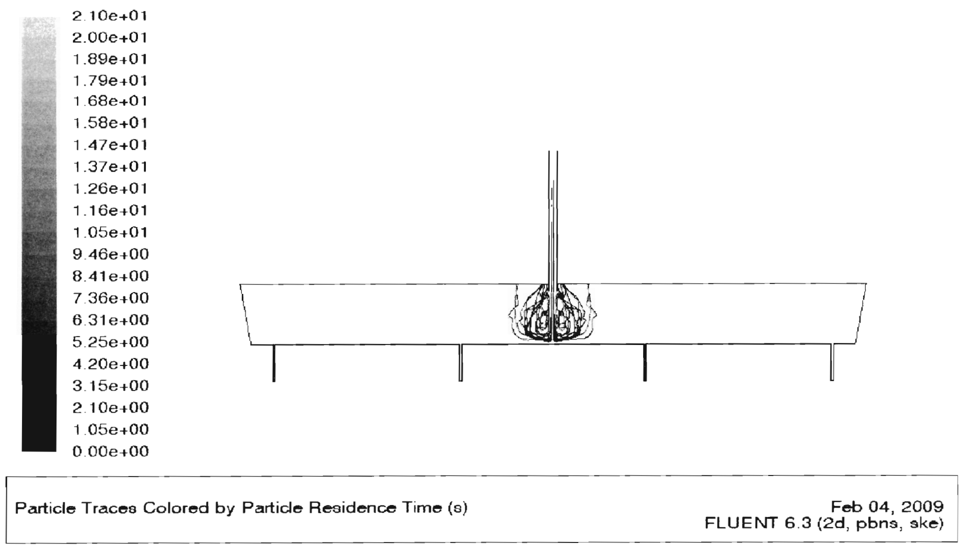

Figure 5.3.1(c) numerically predicted bubble tracks with bubble size of 2mm

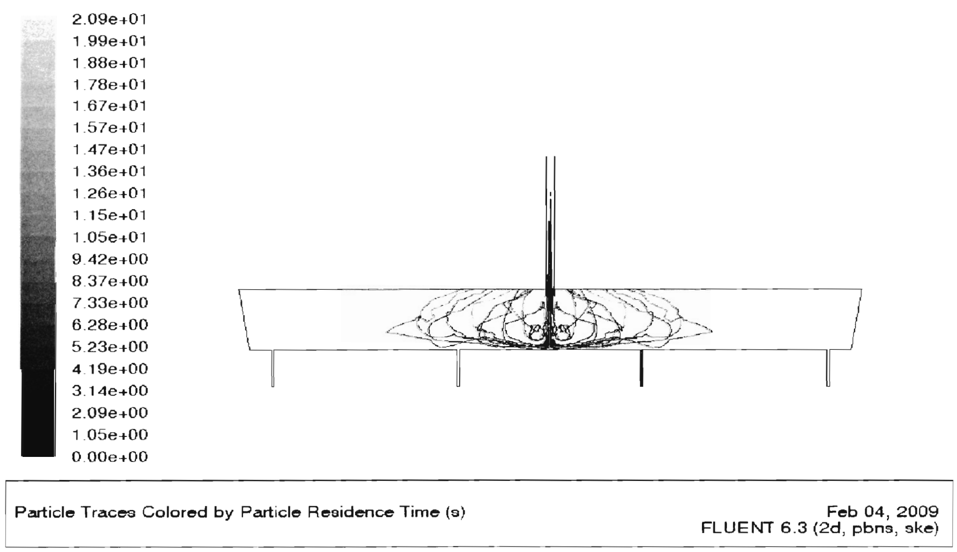

Figure 5.3.1(d) numerically predicted bubble tracks with bubble size of 1mm

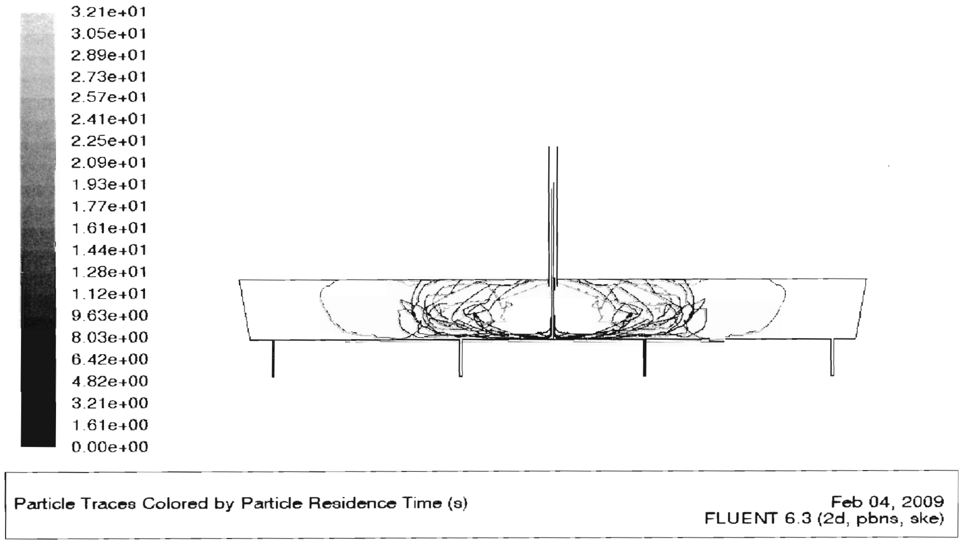

Figure 5.3.1(e) numerically predicted bubble tracks with bubble size of 0.5mm

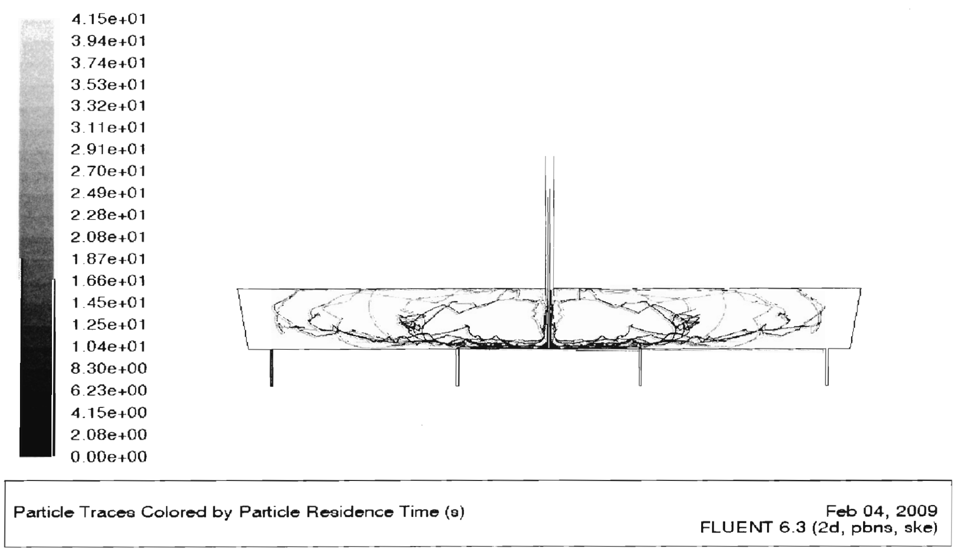

Figure 5.3.1(f) numerically predicted bubble tracks with bubble size of 0.25mm

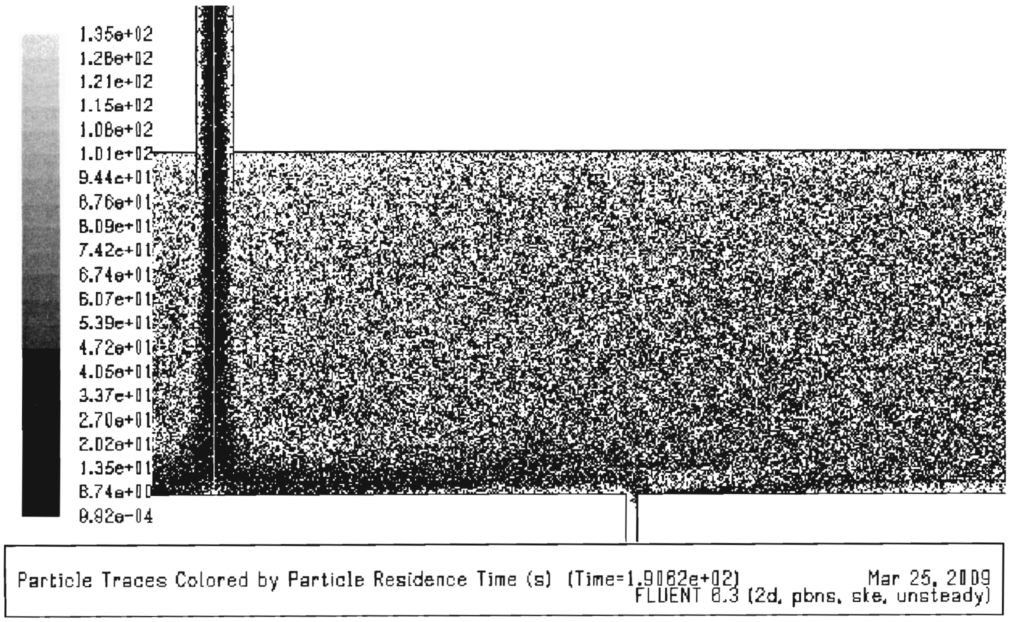

Figure 5.3.2 bubbles of 250 micro meters spreading uniformly in the whole tundish

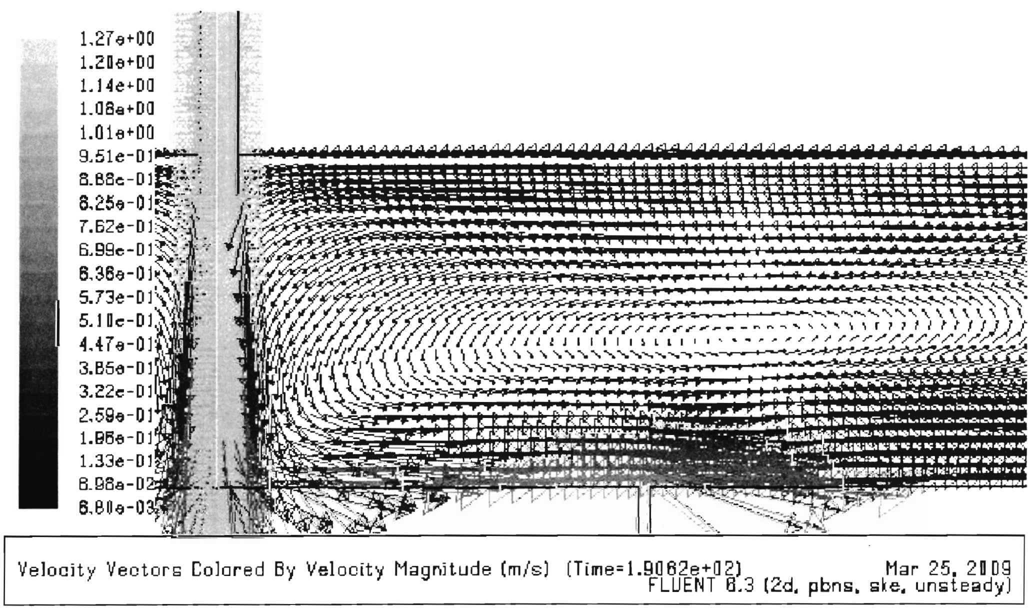

Figure 5.3.3 numerically predicted flow fields with micro bubbles (250 micro meters) at 6% gas injection in the shroud

6.0 CONCLUSIONS & RECOMMENDATIONS FOR FUTURE WORK

The entrained air bubbles formed under present experimental conditions within the ladle shroud had large diameters. As such, they had enough buoyancy forces to rise straight back up to the free surface of the water in the tundish. These rising gas bubbles created reversed flows which swept away the protective slag and created an exposed 'eye'. With increases in gas flow rate through the shroud, the reversed flows became stronger and hence the area of the exposed eye increased. So too much shroud gas is not recommended.

The 2D PIV equipment proved to be an effective tool for capturing the reversed flows in the vicinity of the shroud the tundish. Use of proper seeding particles is necessary for obtaining satisfactory results.

Tracer injection studies showed that gas injection through the shroud slows down mixing within the tundish as compared to that with no gas injection. Tracer studies also revealed the presence of dead volumes towards the ends of the tundish.

The predictions of the numerical models were in good agreement with physical (experimental) results. The flow fields generated by the 2D numerical model for entrained gas bubbles, were similar in nature to those measured by 2D PIV experiments. However, the magnitudes of the predicted velocity vectors were not exactly equal to those obtained from PIV measurements but they were in the same range of 10^{-2} to 10^{-3} m s^{-1}. This is due to the fact that the numerical model is two dimensional whereas the physical model is three dimensional. Fine tuning of the present 2D numerical model may improve the results. So the development of a 3D numerical model is better and represents a next step. Also, a viscous layer of slag should be incorporated as a second phase in the model, so that the second phase can be tracked to get predicted slag behaviour.

The numerical model has effectively predicted a critical bubble size which can result in the uniform spread of bubbles throughout the tundish, which may greatly help in the removal of fine inclusions. This numerical prediction needs to be validated with physical model experiments and represents an ongoing area for research. The formation of argon micro bubbles in the real tundish remains a challenge but serious thought has been given to it, and proof of concept must first be demonstrated.

As practical conditions in the industry are non-isothermal, the development and implementation of a non-isothermal model is almost mandatory, or at least highly encouraged. The results should be closely compared with isothermal flow fields for a wide range of flow control devices.

7.0 REFERENCES

[1]. Mazumdar, D., Guthrie, R.I.L., *The Physical and Mathematical Modeling of Continuous Casting Tundish Systems,* ISIJ International, (1999) 39(6), pp 524-547.

[2] Guthrie, R.I.L., and Isac, M., *The Process Metallurgy of Ladle-Tundish-Mould Operations for Continuously Casting Slabs, Blooms and Billets,* Iron and Steel Making, (2003), pp 27- 32

[3] Guthrie, R.I.L., *Engineering in Process Metallurgy,* Oxford University Press, (1992).

[4] Tanaka, S., PhD Thesis, McGill University ,Montreal, Canada, 1989

[5] Krishnapisharody, K., and Irons, G., *Studies of Slag Droplet Formation in Ladle Metallurgy: Part I. Physical Modeling,* ICS 2008,pp-367-374

[6] Damle.C and Sahai.Y , *A Criterion for Water Modeling of Non-isothermal Melt Flows in Continuous Casting Tundishes,* ISIJ international, (1996) 36(6), pp 681-689

[7] Sahai, Y., and Emi, T., *Tundish Technology for Clean Steel Production*, World Scientific Publication Co. Pte. Ltd. (2008)

[8] Ghosh, A., *Secondary Steel Making, Principles and Applications,* CRC Press (2001)

[9] Lopez-Ramirez, S., Barreto, J De J., Vite-Martinez, P., Serrano, J A Romero, Duran-Valencia, C., *Physical and Mathematical Determination of the Influence of Input Temperature Changes on the Molten Steel Flow Characteristics in Slab Tundishes,* Metallurgical and Materials Transactions B, (2004) 35B(5), pp 957-966

[10] Vargas-Zamora, A., Morales, R. D., Diaz-Cruz, M., Palafox-Ramos, J., Garcia, D. L., *Heat and Mass Transfer of a Convective-Stratified Flow in a Trough Type Tundish,* International Journal of Heat and Mass Transfer, (2003), 46(16); pp 3029-3039.

[11] Craig, K. J., De Kock, D. J., Makgata. K. W., De Wet, G. J., *Design Optimization of a Single-Strand Continuous Caster Tundish Using Residence Time Distribution Data*, ISIJ International, (2001) 41(10), pp 1194-1200.

---

[12] Solhed, H., Jonsson, L., Jonsson. P., *A Theoretical and Experimental Study of Continuous-Casting Tundishes Focusing on Slag-Steel Interaction,* Metallurgical and Materials Transactions B, (2002) 33B(2), pp 173-185.

[13] Solhed, H., Jonsson, L., *An Investigation of Slag Floatation and Entrapment in a Continuous-Casting Tundish Using Fluid-FlowSimulations, Sampling and Physical Metallurgy,* Scandinavian Journal of Metallurgy, (2003) 32(1), pp 15-32.

[14] Debroy, T., and Sychterz, J.A., *Numerical Calculation of Fluid Flow in a Continuous Casting Tundish,* Metallurgical and Materials Transactions B,(1985)16B, pp 497-504.

[15] Launder, B.E., and Splading, D. B., *Lectures in Mathematical Models of Turbulence,* Academic Press, NY, 1972

[16] Yakhot, V., and Orszag, S. A.,*Renormalization Group Analysis of Turbulence. I. Basic Theory,* J. Sci. Comput., (1986).

[17] Shih, T.-H., Liou, W.W., Shabbir, A., Yang, Z. and Zhu, J., *A New k-ε Eddy Viscosity Model for High Reynolds Number Turbulent Flows -Model Development and Validation,* NASA TM 106721,(1994)

[18] Schwarze, R., Obermeier, F., Hantusch,J., Franke, A., Janke, D., *Mathematical Modelling of Flows and Discrete Phase Behaviour in a V-Shaped Tundish,* Steel Research, (2001) 72(5+6), pp 215-220.

[19] Schwarze, R., Obermeier, F., Janke, D., *Numerical Simulation of Fluid Flow and Disperse Phase Behaviour in Continuous Casting Tundishes,* Modelling and Simulation in Materials Science and Engineering, (2001), 9(4); pp 279-287

[20] Qinfu, H., Zongshu, Z., Comparison Between Standard and Renormalization Group *k-ε* models in numerical simulation of Swirling Flow Tundish, ISIJ International, (2005) 45(3), pp 325-330.

[21] Jha, P. K., Ranjan,R., Mondal, S. S. and Dash, S. K., *Mixing in a Tundish and a Choice of Turbulence Model for its Prediction,* International journal of Numerical Methods for Heat and Fluid Flow, (2003) 13(8), pp 964 – 996

[22] Ilegbusi, O. J., *Application of Two Fluid Model of Turbulence to Tundish Problems,* ISIJ International, (1994) 34(9), 732-738.

[23] Jha, P .K., Dash, S. K., Effect of Outlet Positions and Various Turbulence Models on Mixing in a Single and Multi Strand Tundish, International Journal of Numerical Methods for Heat & Fluid Flow, (2002) 12(5), pp 560-584.

[24] Robert, A., Mazumdar, D., *Physical and Mathematical Modelling of Flow and Residence Time Distributions in Different Tundish Designs,* Steel Research, (2001) 72(3); pp 97-105

[25] Patankar, S. V., and Spalding, D. B., *A Calculation Procedure for Heat, mass and Momentum Transfer in Three Dimensional Flows,* International Journal of Heat and Mass Transfer, (1972) 15, 1787-1806

[26] Versteeg, H. K and Malalasekera, W., *An Introduction to Computational Fluid Dynamics: The Finite Volume Method*, McGraw-Hill, Loughborough University, (1995)

[27] Fan, C-M., Hwang, W-S., *Mathematical Modeling of Fluid Flow Phenomena During Tundish Filling and Subsequent Initial Casting Operation in Steel Continuous Casting Process,* ISIJ International, (2000) 40(11), pp 1105-1114.

[28] Odenthal, H-J., Pfeifer, H., Klaas, M., *Physical and Mathematical Modeling of Tundish Flows Using Digital Particle Image Velocimetry and CFD-Methods,* Steel Research, (2000) 71(6+7), pp 210-219.

[29] Sheng , D.Y., and Jonsson, L., *Two-Fluid Simulation on the Mixed Convection Flow Pattern in a Non-isothermal Water Model of Continuous Casting Tundish,* Metallurgical and Materials Transactions B, (2000) 31B (4), pp 867-875.

[30] Ahn, J. H., Lee, Jung-Eui, Yoon, J. K., *Analysis of mixed grade transition in continuous thin slab casting with EMBR ,* International Conference on Processing Materials for Properties, Proceedings, 2nd, San Francisco, CA, United States, (2000), pp577-581.

[31].Sinha, S.K, Godiwalla, K.M, Shaw, D.K., and Sivaramakrishnan, C.S., Scandinavian Journal of Metallurgy, (2001) 30, Pg 103-107

[32] Sahai.Y, *Modelling of Melt Flow in Continuous Casting Tundishes*, The Brimacombe Memorial Symposium, Vancouver, BC, Canada, (2000) pp 631-641

[33] Ferro, S.P., Principe, R.J., and Goldschmit, M.B., *A New Approach to the Analysis of Vessel Residence Time Distribution Curves,* Metallurgical and Materials Transactions B, (2001) 32B, pp1185 - 1193

[34] Gardin, P., Brunet, M., Domgin, J.F., and Pericelous, K., *An Experimental and Numerical CFD Study of Turbulence in a Tundish Container,* Applied Mathematical Modelling, (2002) 26, pp323-336

[35] Jha, P.K. and Dash, S.K., International Journal of Numerical Methods for Heat and Fluid Flow, (2004) 14(8), pp 953-979

[36] Pardesi, R., Basak, S., Singh, A.K., Basu, B., Mahashabde ,V., Roy, S.K., and Kumar, S., *Mathematical Modeling of the Tundish of a Single-Strand Slab Caster,* ISIJ International, (2004) 44 (9) , pp 1534-1540.

[37] Kumar A., Koria S.C., and Mazumdar D., *An Assessment of Fluid Flow Modelling and Residence Time Distribution Phenomena in Steelmaking Tundish Systems,* ISIJ International, (2004) 44 (8), pp 1334 - 1341.

[38] Zamora, A.V., Morales, R.D., Diaz-Cruz, M., Palafox-Ramos, J., and Barreto, J .DE J., Metallurgical and Materials Transactions B, (2004) 35B, pp247

[39] Ramos-Banderas, A., Sanchez-Perez, R., Morales, R.D. Palafox-Ramos, J., Demedices-Gracia, L., and M. Diaz-Cruz, Metallurgical and Materials Transactions B, (2004) 35B, pp449

[40] Tripathi, A. and Ajmani, S.K, *Numerical Investigation of Fluid Flow Phenomenon in a Curved Shape Tundish of Billet Caster* ,ISIJ International, 2005 45(11) , pp 1616-1625

[41] Cho, M.J. and Kim, I.C., *Simple Tundish Mixing Model of Continuous Casting during a Grade Transition,* ISIJ International, (2006) 46(10), pp 1416-1420

[42] Huang, X., and Thomas, B.G., Metallurgical and Materials Transactions B, (1996) 27B,pp 617

[43] Alkishriwi, N., Meinke, M., and Schroder, W., Aerodynamics Institute, RWTH Aachen, Germany

[44] Davila, O., Morales, R.D., and Gracia-Demedices, L., Metallurgical and Materials Transactions B, (2006) 37B, pp71

[45] Sankanarayan, R., and Guthrie, R.I.L, Ironmaking and Steelmaking, (2002) 29, pp 147-153

[46] Sankanarayan, R., and Guthrie, R.I.L, ISS Steelmaking Conf., (1992) 75, pp. 655-664

[47] Vayrynen, P. Vapalahti, S., Louhenkilpi, S., Clark, M. and Wagner, T. STEEL SIM 2007, Austria

[48] Zorzut, M., Vecchiet, F. Kapaj, N., and Paderno, A.,BHM, 152. Jg.(2007), Heft 11

[49] Alizadeh, M., Edris, H., and Shafyei, A.,Journal of Iron and Steel Research, International. 2008, 15(2), pp7-13, 22

[50] Hamill, I., Lucas, T., *Computational Fluid Dynamics Modelling of Tundishes and Continuous Casting Moulds,* Fluid Flow Phenomena in Metals Processing, TMS Annual Meeting, San Diego, (1999), pp279-286.

[51] Joo, S., and Guthrie, R.I.L. Canadian Metallurgical Quarterly, Vol 30, (1991), pp261

[52] Hulstrung, J., Zeimes, M., Au, A., Oppermann, W., and Redusch, G., *Optimization of Tundish Design to Increase the Product Quality By Means of Numerical Fluid Dynamics,* Steel Research, (2005) 76(1), pp 59-63

[53] Solorio-DIAZ G., Morales, R. D., Palafox-Ramos, J., Ramos-Banderas, A., *Modeling the Effects of A Swirling Flow on Temperature Stratification of Liquid Steel and Floatation of Inclusions in a Tundish,* ISIJ International, (2005), 45(8), 1129-1137

[54] Zhang, L., Taniguchi, S., Cai, K., *Fluid Flow and Inclusion Removal in Continuous Casting Tundish ,* Metallurgical and Materials Transactions B, (2000) 31B(2), pp 253-266

[55] Javurek, M., Kaufmann, B., Zuba, G., Gittler, P., *Some New Aspects on inclusion Separation in Tundishes,* Steel Research, (2002) 73(5); pp 186-193

[56] B.G.Thomas and Hua Bai, 18th Process technology Division Conference Proceedings, Vol 18. Iron and Steel Society, Warrendale, PA, 2001, pp 895-912

[57] Rogler, J. P., Heaslip, L. J., Mehrvar, M., Inclusion Removal in a Tundish By Gas Bubbling, Canadian Metallurgical Quarterly, (2004) 43(3), pp 407-415

[58] Nguyen, A.V. , Ralston, J., and Schulze. H.J., Int. J. Miner. Process.,1998 ,vol. 53, pp. 225-249

---

[59] Kuklev, A.V., et al. Metallurgist, Vol 48, Nos. 3-4,2004

[60] Rogler, J. P., Heaslip, L. J., Mehrvar, M., *Physical Modelling of Inclusion Removal in a Tundish by gas Bubbling,* Canadian Metallurgical Quarterly, (2005) 44(3),pp 357-368

[61] Lopez-Ramirez, S., Morales, R.D., and Romero Serrano, J.A., *Numerical Simulation of the Effects of Buoyancy Forces and Flow Control Devices on Fluid Flow and H|eat Transfer Phenomena of Liquid Steel in a Tundish,* Numerical Heat Transfer, Part A, (2000) 37(1) , pp 69-86

[62] Odenthal, H.J., Bolling, R., Pfeifer, H., Holzhauser, J.F., Wahlers, F.J. *Mechanism of fluid flow in a continuous casting tundish with different turbo-stoppers,* Steel Research, (2001) 72(11+12), pp 466-476.

[63] Morales, R.D., Diaz-Cruz, M., Palafox-Ramos, J., Ramirez, S.L., Barreto Sandoval, J.De J., Steel Research, 72(2001), No.1,pp 11-16

[64] Bao, Y., Jang, W., Xu, B., Zhang, H., Journal of University Science and Technology, Beijing, (2002) 9(1), pp 13

[65] Palafox-Ramos, J., Barreto, J. De J., Lopez-Ramirez, S., Morales, R. D., *Melt Flow Optimization Using Turbulence Inhibitors in Large Volume Tundishes,* Ironmaking and Steelmaking, (2001) 28(2), pp 101-109

[66] Morales, R. D., Lopez-Ramirez, S., Palafox-Ramos, J., Zacharias, D., *Mathematical simulation of effects of flow control devices and buoyancy forces on molten steel flow and evolution of output temperatures in tundish,* Ironmaking and Steelmaking, (2001) 28(1), pp 33 - 43

[67] K.H.Tacke and J.C.Ludwig: Steel Research , 1987, 58, 262-270

[68] Sinha, A.K., PhD Thesis, The Ohio State University, USA (1990)

[69] H.Nakajima, F.Sebo, S.Tanaka, L.Dumitru, D.J.Harris and R.I.L.Guthrie: Steelmaking Conference Proceedings, ISS-AIME, 1986, 69, 705-716.

[70] Solorio-Diaz, G., Morales, R. D., Palafax-Ramos, J., Garcia-Demedices, L., Ramos-Banderas, A., *Analysis of Fluid Flow Turbulence in Tundishes Fed by a Swirling Ladle Shroud,* ISIJ International, (2004) 44(6), pp 1024-1032

[71] .Solorio-DIAZ G, Morales R D, Palafox-Ramos J, Ramos-Banderas A, *Modeling the Effects of a Swirling Flow on Temperature Stratification of*

Liquid Steel and Floatation of Inclusions in a Tundish, ISIJ International, 2005, 45(8), pp 1129-1137

[72] Kim, H.B., Master of Engineering Thesis, McGill University, Montreal, Canada

[73] Bai, H., and Thomas, B.G., *Effects of Clogging, Argon Injection, and Continuous Casting Conditions on Flow and Air aspiration in Submerged Entry Nozzles,* Metallurgical and Materials Transactions B, (2001) 32B, pp707- 722

[74] Evans, G.M., Rigby, G.D., Honeyands, T.A., He, Q.L., *Gas Dispersion ThroughPorous Nozzles into Down-Flowing Liquids,* Chemical Engineering Science, (1999) 54, pp 4861-4867

[75] Bai, H., and Thomas, B.G., *Turbulent Flow of Liquid Steel and Argon Bubbles in Slide-Gate Tundish Nozzles: Part I. Model Development and Validation,* Metallurgical and Materials Transactions B, (2001) 32B, pp 253 - 267

[76] Bai, H., and Thomas, B.G., *Turbulent Flow of Liquid Steel and Argon Bubbles in Slide-Gate Tundish Nozzles: Part II. Effect of Operation Conditions and Nozzle Design,* Metallurgical and Materials Transactions B, (2001) 32B, pp 269 - 284.

[77] CFX4.2 Users Manual, AEA Technology, Pittsburgh,PA, 1997.

[78] Li Tao WANG, Qiao Ying ZHANG, Chen Hong DENG and Zheng Bang Li, *Mathematical Model for Removal of Inclusion in Molten Steel by Injecting Gas at Ladle Shroud,* ISIJ International, (2005) 45(8), pp. 1138-1144

[79] Koria, S.C., and Srivastava, S.C., *Residence Time Distribution of Steel Melt Due to Argon Shrouded Stream Pouring in a Tundish,* Steel Research, (1999), 70(6) , pp. 221- 226

[80] http://www.dantecdynamics.com/Default.aspx?ID=820, Dantec Dynamics website

[81] FLUENT 6.3.26 User Guide, section 22.9.2, ANSYS, USA